Tomas Bata University in Zlín

Faculty of Technology

Doctoral Thesis

Rheological Characterization of Polymer Solutions with Respect to Quality of Electrospinning Process

Reologická charakterizace polymerních roztoků
s ohledem na kvalitu elektrostatického zvlákňování

Petra Peer

June 2015

Zlín, Czech Republic

Doctoral study programme: P 2808 Chemistry and Materials Technology

2808V006 Technology of Macromolecular Substances

Supervisor: Assoc. Prof. Petr Filip

Consultant: Assoc. Prof. Vladimír Pavlínek

CONTENTS

ABSTRACT

Nowadays, nanofibrous layers are intensively studied for their unique properties and potential applications. For instance medical applications like tissue engineering use fibres as a carrier of the cells. The advantage of the nanofibrous layers is a high specific surface area together with high porosity and fibre diameters reaching at most hundreds of nanometres. There are many production processes of nanofibres to which we can include an electrostatic spinning from polymer solutions or melts. If a polymer solution is exposed to external high voltage evoking electrostatic forces, the fibres are emitted from the surface layer of polymer solution and finally collected in drawing state.

Rheological characterization of polymer solutions represents a crucial factor influencing electrostatic spinning and thus morphology of nanofibres. Flow behaviour of polymer solutions is influenced by polymer, solvent, concentration of solution, additives and mechanical stress or temperature, to mention a few.

Large amount of the modern methods exists for the characterisation of the rheological properties of fluid including those enabling measurements under an electric field.

Primary attention in this work is paid to an influence of an electric field on rheological characteristics of polymer solutions. In the first part, the devices enabling measurements in presence of electric field are compared. The second part is devoted to the influence of electric field on shear viscosity of polymer solutions, to the stability of polymer solutions in time and to the influence of polymer solutions preparation on rheological characteristics in connection with a process of electrospinning.

Keywords: Electrospinning • Nanofibrous layer • Polymer solution • Rheology • Electrorheology • Shear viscosity

ABSTRAKT

V dnešní době je výroba nanovlákenných vrstev velmi žádoucí pro své unikátní vlastnosti a jejich potenciální aplikace. Například v lékařství tkáňové inženýrství využívá vlákna jako nosiče buněk. Předností takové nanovlákenné vrstvy je její vysoký specifický povrch spolu s vysokou pórézností a průměry vláken dosahujících maximálně stovek nanometrů. Pro výrobu nanovláken existuje řada výrobních procesů, mezi které se řadí i elektrostatické zvlákňování z polymerních roztoků či tavenin. Při něm je polymerní roztok vystaven vnějšímu vysokému napětí a vlivem elektrostatických sil je z povrchové vrstvy roztoku emitováno vlákno, které se přenese ke sběrnému kolektoru dloužením.

Reologické chování polymerních roztoků je významným faktorem ovlivňujícím elektrostatické zvlákňování i morfologii vznikajících nanovláken. Tokové chování polymerních roztoků je podmíněno např. druhem užitého polymeru či rozpouštědla, koncentrací roztoku, aditivy a dále mechanickým namáháním či teplotou.

Pro charakterizaci tokových vlastností tekutin existuje řada moderních technologií včetně těch, umožňujících měření reologických vlastností v elektrickém poli.

Prvořadá pozornost je tudíž v této práci věnována vlivu elektrického pole na reologii polymerních roztoků. V první části práce jsou porovnávána zařízení na měření reologických charakteristik v elektrickém poli. Druhá část práce se pak zabývá vlivem elektrostatického pole na viskozitu polymerního roztoku, stabilitou polymerního roztoku v čase a vlivem přípravy polymerního roztoku na reologické vlastnosti v souvislosti s elektrostatickým zvlákňováním.

Klíčová slova: Elektrostatické zvlákňování • Nanovlákenná vrstva • Polymerní roztok • Tokové vlastnosti • Elektroreologie • Smyková viskozita

LIST OF PAPERS

PAPER I

PEER, P., STĚNIČKA, M., FILIP, P., PAVLÍNEK, V. Comparison of electrorheological measurements based on different methods of electric field generation. *Applied Rheology.* 2014, vol. 24, 42875 (4 pp.).

PAPER II

PEER, P., STĚNIČKA, M., PAVLÍNEK, V., FILIP, P., KUŘITKA, I., BRUS, J. An electrorheological investigation of PVB solutions in connection with their electrospinning qualities. *Polymer Testing.* 2014, vol. 39, pp.115-121.

PAPER III

PEER, P., STĚNIČKA, M., PAVLÍNEK, V., FILIP, P. The storage stability of polyvinylbutyral solutions from an electrospinnability standpoint. *Polymer Degradation and Stability.* 2014, vol. 105, pp. 134-139.

PAPER IV

PEER, P., STĚNIČKA, M., SEDLAČÍK, M., FILIP, P., PAVLÍNEK, V. Magnetorheological behaviour and electrospinning of PEO suspensions with magnetic nanoparticles. *Journal of Intelligent Material Systems and Structures.* (submitted)

PAPER V

FILIP, P., ŠVRČINOVÁ, P. Measurement of elongational viscosity of polymer melts using SER Universal Testing Platform. *Applied Rheology.* 2012, vol. 22, 14776 (5 pp.).

THEORETICAL BACKGROUND

1. Electrostatic spinning

There are a few technological processes how to produce nanofibres [1]:

- **drawing**: nanofibres are fabricated with the help of a micropipette dipped into a droplet of material used. The micropipette is then withdrawn from the liquid thus forming a nanofibre. The pulled fibres are deposited on the surface by touching it with the end of the micropipette.

- **template synthesis**: usage of a template with the pores of nanoscale diameter. Pressed polymer solution after passage through the porous membrane solidifies and the diameters of nanofibres are generated by the dimensions of pores.

- **phase separation**: production of nanofibres consists of 5 steps: polymer dissolution in a solvent; gelation; solvent extraction after separation of phases due to their physical incompatibility; freezing; and freeze-drying.

- **self-assembly**: build-up of nanoscale fibres using smaller molecules as basic building blocks using the intermolecular forces as a main mechanism.

- **electrospinning**: this process creates nanofibres through an electrically charged viscoelastic jet of polymer solution or polymer melt.

History of the electrospinning process is not as straightforward as it could be expected for such a cost-effective method. The origin can be related to the year 1628 when William Gilbert observed that a spherical water droplet was pulled into a conical shape if a charged piece of amber was held above it. Further serious research dates back to the beginning of the last century when electrically formed droplet formation was studied [2]. The process of electrostatically produced polymer fibres was invented by Formhals [3] in 1934. His patent more or less coincides in time with the invention of nylon to which the prior attention

7

was paid. The works in open literature improving and modifying the original apparatus developed by Formhals appeared not earlier than in the mid60s'. The milestone in the academic research is represented by a series of studies by Taylor (e.g. [4]) published in the period 1964-1969. He derived the equilibrium conditions that occur when a conducting fluid droplet is exposed to an electric field. The resulting shape is a cone with an apex angle of 98.6° now known as the Taylor cone. The participating forces have their origin in gravity, surface tension, and electrical stresses. Depending on the status of equilibrium there are three possible results: no ejection, or the cone ejects droplets, or the cone ejects a liquid jet. An extensive attention to electrospinning started in the 90s' of the last century. Nowadays, the electrospinning process has still received a great deal of attention, see e.g. [5-10].

1.1. Electrospinning Process

Electrospinning process whose simple sketch is depicted in Fig.1 consists schematically of a pipette holding the polymer solution, two electrodes, a DC voltage supply in the kV range (tens of kV), and a grounded collector. The critical voltage causes the pendant droplet to deform into a conical structure called Taylor cone and the jet erupts from tip of the spinneret. As the jet accelerates toward the grounded collector, the solvent evaporates while the elasticity of polymer solution prevents the jet breaking up (Rayleigh instability). Beyond the stable region, the jet is subject to a bending instability and further elongation that result in fibre formation on the collector. Different type of collector can be used, including a stationary plate, rotating mandrel [11], solvent bath [12] (e.g. water), etc., due to various orientation of fibre in the layer. Diverse fibre morphologies have been produced, such as beaded [13], circular, ribbon [14-15], porous [16-18] and core-shell fibres [19-21].
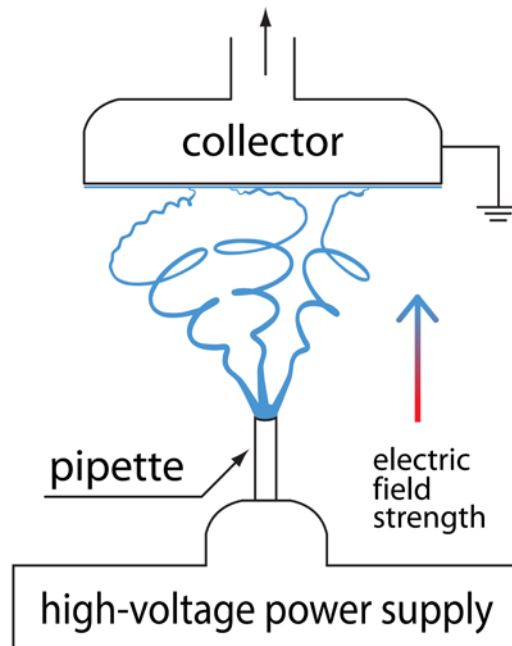
Figure 1. Sketch of an electrospinning apparatus [22].

Electrospinning can be characterised as a low-cost procedure with the possibility to be relatively simply arranged in the laboratory conditions. In addition needle-free Nanospider™ technology is designed by Jirsak et al. [23] for effective industry production of nanofibrous layers. In contrast to the technological processes introduced above the electrospinning can produce long continuous nanofibres.

The process itself composes of four distinct regions:

1. *The tip of a source of material to be electrospun (Taylor cone)*

The Taylor cone (its geometry) is a result of balance between the surface tension stress and electric normal stress. The tangential electric field accelerates charge carriers in the liquid. This accelerates the surrounding liquid toward the counter electrode. Viscosity of the material used substantially determines whether the cones eject a spray (electrospraying) or liquid jet (electrospinning), see Ganan-Calvo and Barrero [24]. The above mentioned apex of the Taylor

cone (98.6º) was discussed in Yarin et al. [25]. They received both theoretically and experimentally the apex 67º.

2. *The single viscoelastic jet*

Fibre consistency is subject mainly to surface tension, charge density, and viscosity [13]. Influence of surface tension consists in minimisation of a specific surface area (tendency to form spheres (beads)). This behaviour contradicts to the effect of electrical charge with tendency to increase the surface area what results in making thinner jets. Increasing viscosity of polymer solutions participates not only in undesired bead formation but even in increasing bead sizes.

3. *The jet instability*

The length along which the viscoelastic jet is stable subjects to the characteristics of individual polymer solution and electrical configuration. Surface tension is responsible for axisymmetric Rayleigh instability (at lower electric fields) that is characterised by dripping corresponding to small droplets being emitted from the capillary. Axisymmetric conducting instability results from the competition between the surface charges with the surface tension of the moving fibre (for detailed analysis see [26-27]). For a description of viscoelastic jet behaviour in so-called splay region it was necessary to use a high-speed camera [28-29]. This technique in contrast to a naked-eye observation negated the idea of bifurcating jets. It demonstrated that the jet whips so fast that it looks like multiple jets but in reality only one jet is present. Bending instability (resulting from an application of higher electric field and dependent on the conductivity of the solution) is the first stage of non-axisymmetric whipping instability responsible for the small diameters of nanofibres. This is a result of the complex relationship between surface tension, viscosity, the acceleration of jets surface charges, and internal charges by the external electric field, to which

the jet is exposed during the increased spiralling and looping path length. It is possible to conclude that the whipping instability predominates at high field strengths and flow rates, while the axisymmetric instability and Rayleigh instability predominate at lower flow rates and electric field strengths. However, for formation of nanofibres and their final quality and morphology of the splay region seems to be crucial. The problem is that there is a series of quantities participating non-negligibly in the whole process, and hence general analysis evokes a series of hitherto unsolved problems.

4. *The collector*

The collector, completing the electric circuit from the tip of a pipette, represents the final region where the jet and all instabilities are stopped and the fibres are collected. The collector consists of an electrode of opposite charge for the fibres to be accelerated to. Intensive study has been devoted to the geometry of electrodes, their orientation, material they are made of, etc.

Typical operating conditions: internal diameter of the capillary-end is usually 0.7-1 mm, flow rates of 2-10 ml/h are commonly employed at a potential drop of 5-40 kV and distances of 10-30 cm between the capillary-end and collector.

1.2. Parameters influencing electrospinning process

Many recent studies [30-33] have focused on three basic groups of factors participating in realisation and affecting the quality of nanofibrous webs. These include the solution parameters (surface tension, conductivity, dielectric constant, viscosity, concentration, solvent volatility, molecular weight, molecular weight distribution, topology of the polymer (branched, linear etc.)), process parameters (feed rate, applied electric field in kV, electric current in

mA, distance between the tip of a pipette or other supplier of polymer solution and a collector in cm, orifice diameter, motion of target screen), and process variables (charge distribution, centreline displacement, axial velocity, temperature, humidity, pressure).

According to Sill et al. [34] general relationships between processing and solution parameters can be summarized in the following Table 1.

Table 1. Effects of electrospinning parameters on fibre morphology [34]

PARAMETER	EFFECT ON FIBER MORPHOLOGY
Applied voltage ↑	Fiber diameter ↓ initially, then ↑
Flow rate ↑	Fiber diameter ↑ (beaded morphologies occur if the flow rate is too high)
Distance tip-to-collector ↑	Fiber diameter ↓ (beaded morphologies occur if the distance tip-to-collector is too short)
Viscosity ↑	Fiber diameter ↑
Solution conductivity ↑	Fiber diameter ↓ (broad diameter distribution)
Solvent volatility ↑	Fibres exhibit pores

1.3. Application of nanofibre layers

The utilization of nanofibres determines the material used therefore nanofibres made from natural polymers, polymer blends, nanoparticle-loaded polymers and ceramic precursors have been produced. A highly porous web and

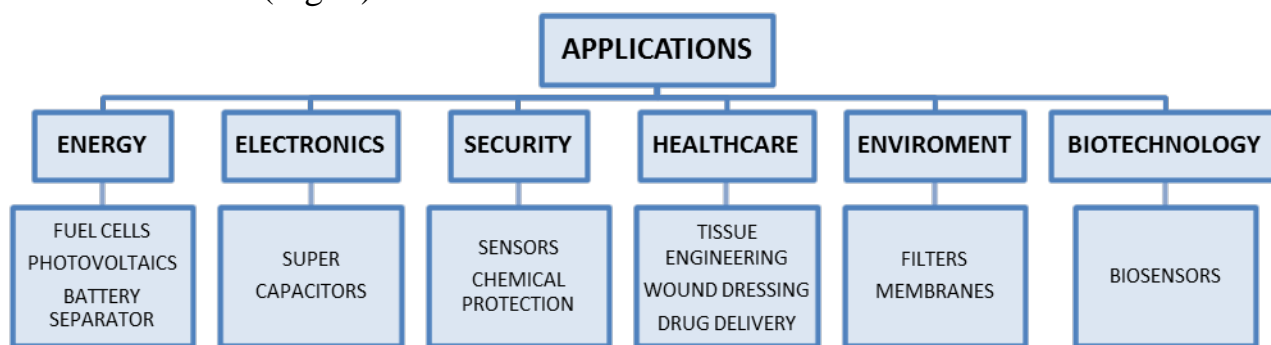large surface-to-volume ratio of nanofibres have found applications in many different areas (Fig. 2).

Figure 2. Potential applications of electrospun fibres [7, 41]

Several reviews [35-40] summarize the most recent potential applications of nanofibres in tissue engineering and drug delivery. The applications of electrospinning relating to energy and environmental areas have been also extensively discussed in literature [41-45].

2. Rheology of polymer solutions

Rheological characterization of polymer solutions relates to the key factors indicating expected quality of electrospinnability. Not only viscosity measurements (both shear η and elongational η_E viscosities), but also oscillatory measurements relating elastic (storage modulus G') and viscous (loss modulus G'') components describe flow behaviour of the studied solutions.

2.1. Shear and elongation flow

In many technical processes especially in fibre spinning, fluids are subject to complex flow fields incorporating strong shear and extensional components. Shear flow is a type of deformation based on the principle of sliding of neighbouring layers relative to each other and the tangential stress determines

behaviour of a material. Uniaxial elongation differs geometrically from deformation in shear flow where only normal stresses are applied [46].

The resistance to shear/elongation flow is expresses like shear/elongation viscosity, and it is determined as a ratio of shear/normal stress to the gradient of velocity [47].

$$\eta = \frac{\tau}{\dot{\gamma}} \;\; ; \qquad \eta_{\mathrm{E}} = \frac{\tau_{\mathrm{N}}}{\dot{\varepsilon}}$$

η ; η_{E} shear; elongational viscosity

τ ; τ_{N} shear; normal stress

$\dot{\gamma}$; $\dot{\varepsilon}$ shear; extension rate (gradient of velocity)

For Newtonian liquids (dilute polymer solution), their elongational viscosity equals $3\eta_0$. The equality $\eta_{\mathrm{E}} = 3\eta_0$ is called the Trouton law and the value η_{E} is called the Trouton viscosity [48].

2.2.   Important factors influencing viscosity

The viscosity of polymer depends on average molecular weight, molecular-weight distribution, temperature, stress (shear, normal), and hydrostatic pressure. Despite the large amount of literature, the rheology of polymer solutions is more complex than that of polymer melts, because two more parameters are involved: the nature and the concentration of the solvent. The nomenclature of solution viscosity, their symbols and defining equations are shown in Table 2.

Table 2. Nomenclature of solution viscosity [59]

NAME	SYMBOL AND DEFINING EQUATION
Relative viscosity	$\eta_{rel} = \dfrac{\eta}{\eta_s}$
Specific viscosity	$\eta_{spec} = \eta_{rel} - 1 = \dfrac{\eta - \eta_s}{\eta_s}$
Reduced viscosity	$\eta_{red} = \dfrac{\eta_{spec}}{c}$
Inherent viscosity	$\eta_{inh} = \dfrac{\ln \eta_{rel}}{c}$
Intrinsic viscosity	$[\eta] = \left(\dfrac{\eta_{spec}}{c}\right)_{c \to 0} = \left(\dfrac{\ln \eta_{rel}}{c}\right)_{c \to 0}$

Polymer

The polymer molecule is consisted of the repeating short units up to long linear or branched polymer chain. The solution rheological properties are function of both polymer molecular weight and concentration [49]. Viscosity is directly proportional to molecular weight, M, up to the critical molecular weight, M_c, where dependence of zero shear viscosity changes from M^1 to $M^{3.4}$ and the entanglements of chains are considerable. Both zero shear and elongational viscosities are a function of the number of chain entanglements. The molecular weight of the polymer may have also significant effect on electrical conductivity, dielectric strength and on surface tension in the solution.

Concentration of polymer chains in solution is classified into three concentration regimes: dilute, semidilute and concentrated [50, 51], see Fig. 3. In dilute solution, the polymer chains are separated from each other. The critical chain overlap concentration, c^*, is the crossover concentration between the dilute and semidilute concentration regimes. In semidilute regime two states

exist: unentangled, it is a concentration when macromolecular chains start cover $c^*[\eta] \sim 1$, and entangled semidilute, where the critical entanglement concentration, c_e, begins. At the higher concentration, c^{**}, the solution enters to a concentrated regime in which the polymer chains do not have a sufficient space to move. The nanofibers can be obtained using a solution with sufficient chain overlapping and entanglements.
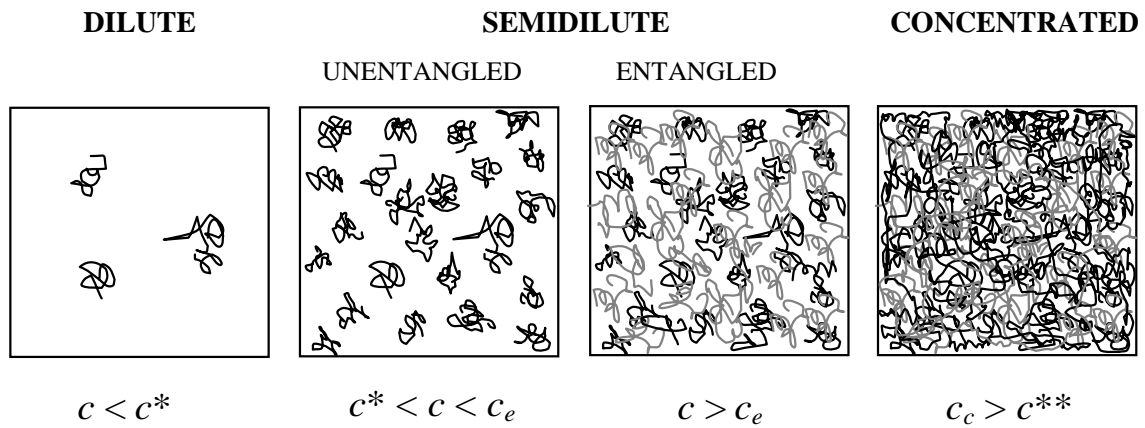
DILUTE	**SEMIDILUTE**		**CONCENTRATED**
	UNENTANGLED	ENTANGLED	

$$c < c^* \qquad c^* < c < c_e \qquad c > c_e \qquad c_c > c^{**}$$

Figure 3. Representation of three concentration regimes for solutions of linear polymer: dilute, semidilute and concentrated [50, 51].

In the literature, there is extensively documented that the changes in polymer concentration vary solution viscosity and simultaneously the process of electrospinning. Due to increasing concentration of polymer solution there were created uniform and bead-free fibres but the mean fibre diameter also increases, as shown in Fig. 4. Many researchers have concentrated on the formation of electrospun fibres in the different concentration regimes [51-54] and on the effect of polymer molecular weight [55-58] on the fibre structure.
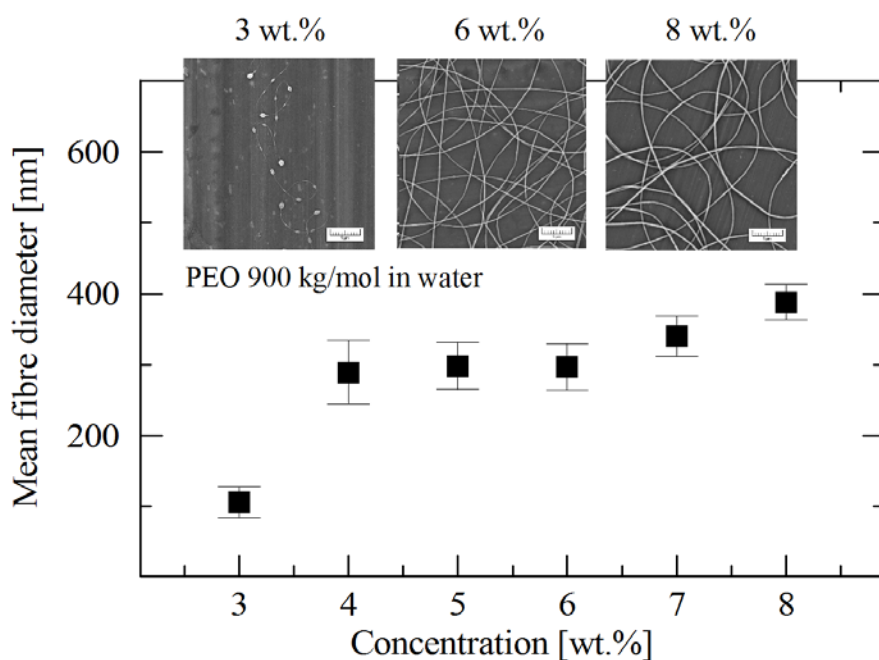
Figure 4. Mean fibre diameter dependence on the concentration
of poly(ethylene oxide) aqueous solution

Solvent

The chemical structure and also physical state of polymer is important for its solubility properties. The solubility of a given polymer in a given solvent is favoured if the solubility parameters of polymer and solvent are similar or equal [59]. The solubility parameter is defined as the square root of the cohesive energy and this parameter is widely used for correlating polymer solvent interactions. For the prediction of polymer solubility in various solvents there are often used Hansen solubility parameters (HSP) [60] representing energy from dispersion bonds, polar bonds, and hydrogen bonds between molecules. These three parameters can be evaluated by using atomic group contribution methods: Small, Hoy, van Krevelen–Hoftyzer, Askadskii and Breitkreutz methods [61]. Then the solubility profiles of the polymer in selected solvents can be visualized using a spherical representation, see Fig. 5.

The radius of the sphere, R (radius of interaction), indicates the maximum difference in affinity for which a good interaction takes place. The HSPs of the

17

good solvents are located closer to a centre of the sphere, the poorer ones approach the radius, and non-solvents are located outside of the sphere.
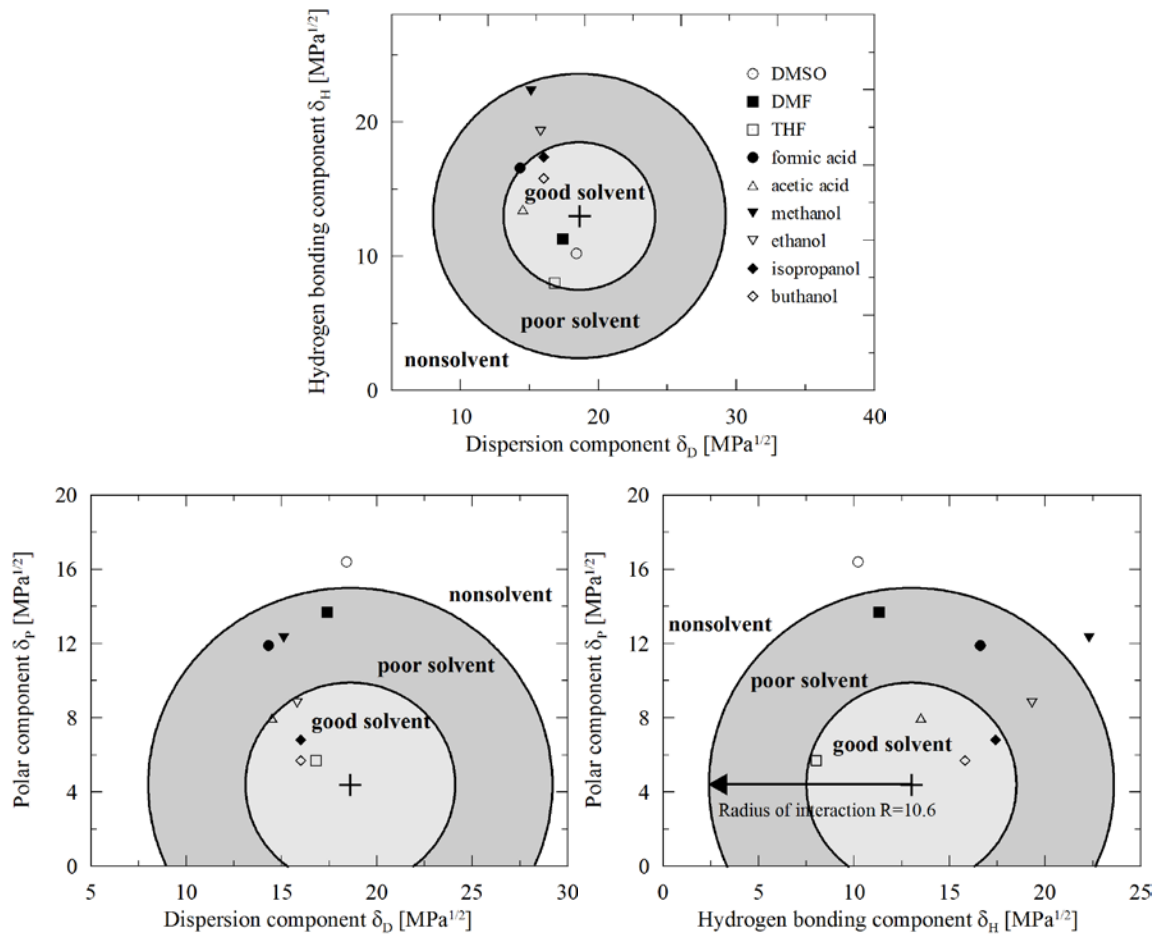

Figure 5. Hansen solubility parameters for polyvinylbutyral and solvents

The solvent effect on the polymer coil is more important in a dilute solution. A good solvent has higher affinity to the polymer coil and causes its expansion; on the contrary poor solvent favours contraction and aggregation of polymer coils. In a semi-dilute concentration region solvent effect can be weakened by chain entanglements [62]; nevertheless it may be expected some aggregation of chains and changes in the rheology of polymer solution and consequently the complications in process.

Solvent effects on the formation of nanofibres were studied by several researchers [54, 63-66]. Luo [63] suggested that the lower solubility can be

better suited for creation good electrospinnable solutions than solvents of high solubility. Nanofibrous webs from PVB dissolved in different quality of solvents are shown in Fig. 6; further examples of spinnable polymers and their poor solvents are in Tab. 3. In addition, nanofibres with highly porous morphology can be obtained by applying solvent/non-solvent mixtures [63, 67-70].
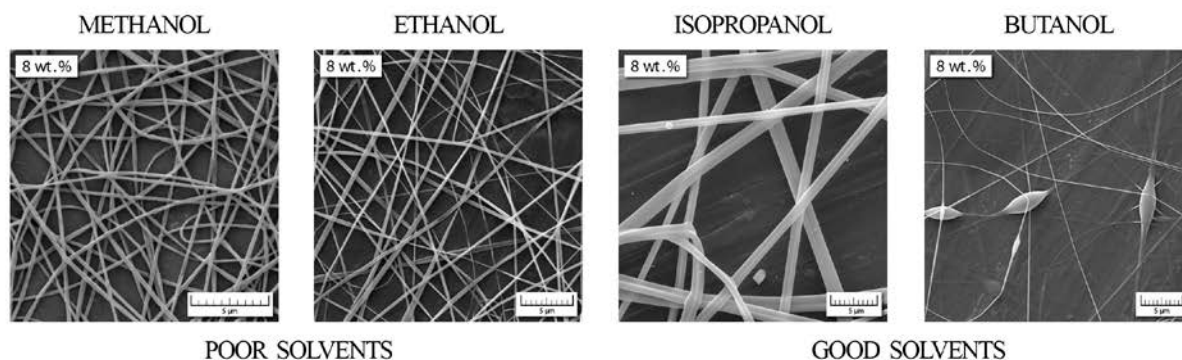

Figure 6. Nanofibrous web from PVB and various solvents [66]

Table 3. Further spinnable polymers in poor solvents

Polymer	Poor solvent	Spinnability, Fibres	Literature
PEO	water	Very good, 200 nm	Son et al. [54]
PVB	methanol	Very good, 250 nm	Peer et al. [66], Lubasova et al. [67]
PS	DMF	Very good, 500 nm	Wannatong et al. [64], Jaruswannapoom et al. [65]
PMSQ	Methanol Acetone	Short fibres, 400 nm Very good, 2 μm	Luo et al. [63]
PMMA	DMF	Very good, 500 nm	Gupta et al [51], Wang et al. [71]

2.3. Electrorheology

The shear viscosity of some materials is subject to the presence or absence of an electric field. This dependence is significantly exhibited by so-called electrorheological materials, for which an increase in shear viscosity under the presence of an electric field does not represent mere multiples but several orders.

The common factors influencing electrorheological measurements are amplified by the mode of generation of an electric field [72] and the geometrical arrangement measuring system [73]: a parallel-plate or a concentric cylinders system as shown in Fig. 7. More details about factors affecting ER effect are available from the literature [74-80].
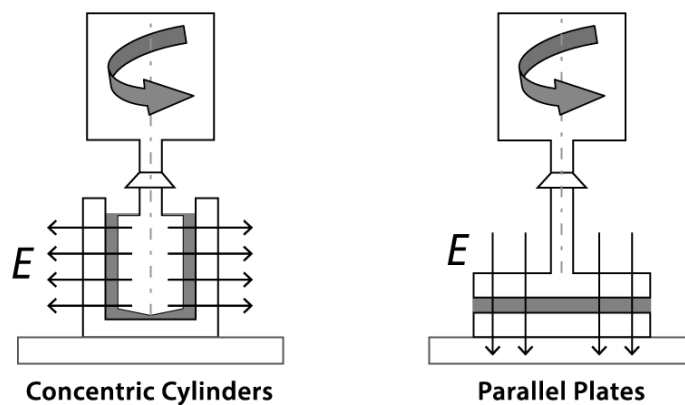

Figure 7. Radial and plan-parallel orientation of an electric field generated in the individual geometries [73]

AIMS OF THE DOCTORAL STUDY

The aim of this work is divided into two parts: experimental techniques and analysis of parameters participating in the process of electrospinning. First part of the presented work deals with the comparison of different experimental techniques for measuring viscosity in electric field. The measurements using two rotational rheometers (Physica MCR 501 (Anton Paar, Austria) and Bohlin Gemini CVOR 150 (Malvern Instruments, United Kingdom)) equipped with electrocells generating an electric field in two different ways were analysed. Furthermore, the technique for the measurement of the elongational viscosity of polymer melt was examined.

Second part of the work concentrates on the parameters participating in the electrostatic spinning whose appearance in the literature is scarce:

- The mutual relation between rheological characteristics measured in the absence and in the presence of an electric field to which the viscoelastic jets are exposed during the process of electrospinning.

- The storage stability of applied polymer solutions and its impact on the quality of electrospun webs.

- Magnetorheology of polymer solution with magnetic nanoparticles and spinnability of this nanofluid.

SUMMARY OF THE PAPERS

In the following, the highlights of enclosed original papers are introduced. This chapter is divided into several parts corresponding to the main aims of the thesis.

3. Effect of electric field

The effect of generation of an electric field was analysed in PAPER I [72] and a geometrical arrangement of the measuring system in [73]. The rotational rheometers, a Physica MCR 501 (Anton Paar) equipped with the electrorheological cell and a Bohlin Gemini CVOR 150 (Malvern Instruments) modified for electrorheological experiments generate an electric field in two completely different ways. Each of the two generations has a specific influence on electrorheological measurements. The experimental data were obtained and compared for a suspension of polyaniline powders mixed (10 wt.%) in silicone oil. For a concentric-cylinders arrangement, it was shown that the data are fully comparable for both rheometers. However, for a parallel-plate arrangement, the data using the Physica MCR 501 provide higher values in comparison with both the corresponding plate-plate data obtained with the Bohlin Gemini CVOR 150 and with the mutually comparable concentric cylinders data.

Very important is also a mutual relation between rheological characteristics measured in absence and presence of an electric field to which the viscoelastic jets are exposed during the process of electrospinning in PAPER II [66]. When exposed to an external electric field, PVB solutions with either poor or good solvents respond in different ways. It was shown that the complex viscosity ratio η_E^*/ η_0^* (where η_E^* and η_0^* represent complex viscosities of a solution in the presence and absence of an external electric field, respectively) can serve as an indicator as to whether a chosen material is a potential candidate for an acceptable electrospinning process [66]. As shown in Fig. 8 the PVB solutions

with the good solvents exhibit no increase in complex viscosity in the presence of the electric field in contrast to the striking enhancement for the poor solvents. It was shown that an increase in the complex viscosity ratio correlates with the good electrospinnability of PVB solutions.
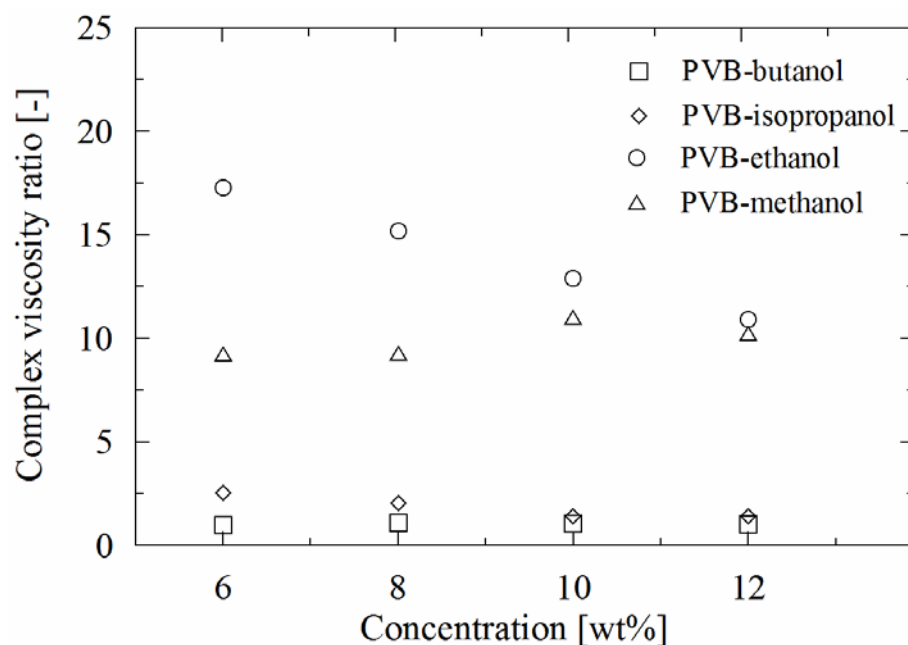

Figure 8. Complex viscosity ratio as a function of concentration for all PVB solutions [66]

4. Effect of ageing

The storage stability of applied polymer solutions and its impact on the quality of electrospun webs are described in PAPER III [22]. The nanofibrous webs created by electrospinning from PVB dissolved in poor solvents (methanol and ethanol) were compared within a period of almost 7 months. During this time, the PVB solutions were kept under constant storage conditions (at 20°C in the dark box). Using rheological and conductivity measurement, SEM, FTIR, and DSC, it was revealed that the storage period for the solution used had almost

no effect on the quality of electrospun fibres, see Fig. 9. This result is a very positive from the practical point of view.
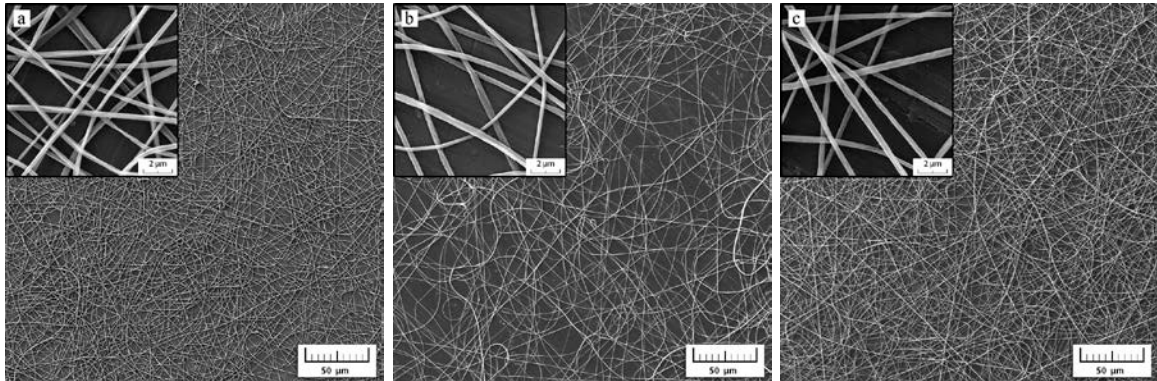

Figure 9. SEM images of nanofibrous webs from PVB in methanol electrospun from a) 1 day; b) 113 day; c) 197 day-old solution samples [22]

5. Magnetorheology of polymer solution

The object of aim in PAPER IV [81] is the comparison of the magnetorheological behaviour and sedimentation stability of the nanofluid and the classical magnetorheological fluid. In this case nanofluid means the magnetic nanoparticles synthesized under microwave assisted radiation incorporated in the PEO aqueous solution. In the contrast to classical MR fluids, the presence of PEO in suspension improved the sedimentation stability. This ensures homogeneous distribution of magnetic particles in the nanofluid, and consequently even distribution of these particles in electrospun mats. The magnetic properties of nanofibrous web were validated by EDX-XRF measurement.

6. Measurement of elongational viscosity

During the electrospinning process the polymer viscoelastic jet is subject to high extension rates under which the polymer chains are stretched and oriented.

At a final stage, a solvent-free polymer fibre is drawn and deposited on the grounded template. The knowledge of the elongational viscosity is required to achieve a sufficient viscoelastic stress for fibre formation. PAPER V [82] examined a widely used technique for the measurements of the extensional viscosity of polymer melts. The measurements were carried out using a SER Universal Testing Platform from the Xpansion Instruments; the model SER-HV-P01 was applied to an Anton Paar MCR501 rotational rheometer host system with the convection heated measuring chamber CTD450 equipped with a camera system. The widths and the thicknesses of the samples were chosen in the broad range. It was found invariantness of the sample dimensions with respect to the obtained transient elongational viscosities, see Fig. 10.
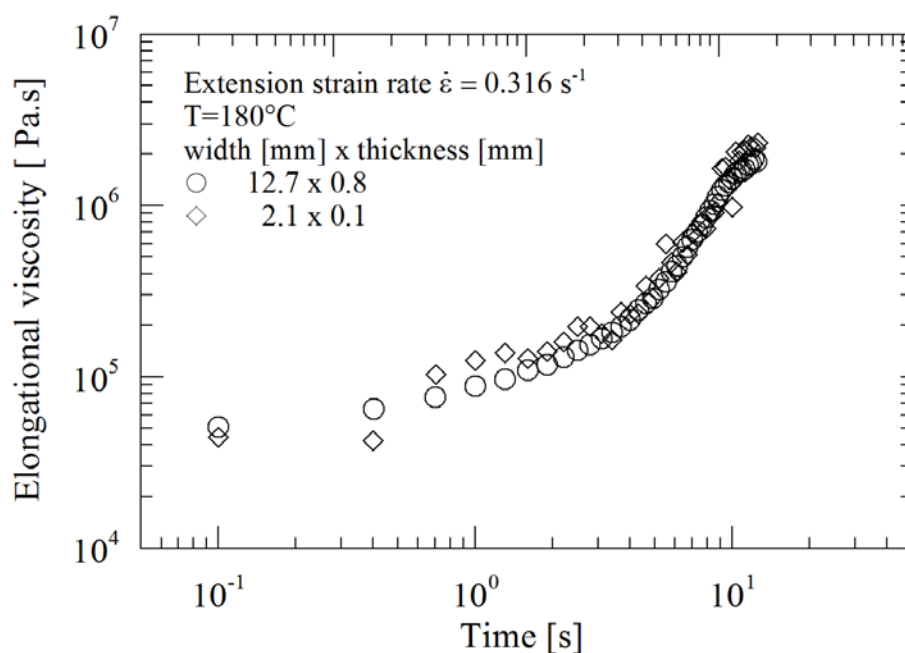

Figure 10. Comparison of uniaxial elongational viscosity measured
with two distinctive dimensions of the samples at temperature of 180°C [82]

THE THESIS CONTRIBUTION TO SCIENCE AND PRACTICE

Electrorheological characterization of polymer solutions indicates usefulness of the chosen materials for possible electrospinnability. Newly derived criteria can substantially reduce time and save money in the process of evaluation of new materials from the viewpoint of potential good or poor electrospinnability.

ACKNOWLEDGEMENT

LIST OF SYMBOLS AND ACRONYMS

c	[wt.%]	concentration
c_e	[wt.%]	entanglement concentration
c^*	[wt.%]	critical chain overlap concentration
c^{**}	[wt.%]	the highest concentration
E	[kV/mm]	electric field strength
G'	[Pa]	storage modulus
G''	[Pa]	loss modulus
M	[g/mol]	molecular weight of polymer
M_C	[g/mol]	critical molecular weight of polymer
δ	[MPa$^{1/2}$]	parameter solubility
δ_P	[MPa$^{1/2}$]	polar component of parameter solubility
δ_D	[MPa$^{1/2}$]	dispersion component of parameter solubility
δ_H	[MPa$^{1/2}$]	hydrogen bonding component of parameter solubility
$\dot{\varepsilon}$	[s^{-1}]	extension rate
$\dot{\gamma}$	[s^{-1}]	shear rate
η	[Pa s]	shear viscosity
η_E	[Pa s]	elongational viscosity
η^*_0	[Pa s]	complex viscosity in absence of electric field
η^*_E	[Pa s]	complex viscosity in presence of electric field
η_{inh}	[m^3/kg]	inherent viscosity
η_{red}	[m^3/kg]	reduced viscosity
η_{spec}	[Pa s]	specific viscosity
η_{rel}	[-]	relative viscosity
$[\eta]$	[m^3/kg]	intrinsic viscosity

τ	[Pa]	shear stress
τ_N	[Pa]	normal stress

DMF N,N-dimethylformamide

DMSO   dimethylsulphoxide

EDX-XRF   energy dispersive X-ray fluorescence spectroscopy

ER   electrorheological

HSP   Hansen solubility parameters

PEO   poly(ethylene oxide)

PMSQ   polymethylsilsesquioxane

PMMA   poly(methyl methacrylate)

PVB   polyvinyl butyral

PS   polystyrene

THF   tetrahydrofuran

REFERENCES

[1] RAMAKRISHNA, S., FUJIHARA, K., TEO, W.E., LIM, T.C., MA, Z. *An Introduction to Electrospinning and Nanofibres*. World Scientific Publishing Co., Singapore 2005.

[2] ZELENY, J. The electrical discharge from liquid points, and a hydrostatic method of measuring the electric intensity at thin surfaces. *Physics Review*. 1914, vol. 3, pp. 69-91.

[3] FORMHALS, A. Process and apparatus for preparing artificial threads. 1934, U.S. Patent 1,975,504.

[4] TAYLOR, G.I. Electrically driven jets. *Proc. Royal Soc. London A*. 1969, vol. 313, no. 1515, pp. 453-475.

[5] BHARDWAJ, N., KUNDU, S.C. Electrospinning: A fascinating fiber fabrication technique. *Biotechnology Advances*. 2010, vol. 28, no. 3, pp. 325-347.

[6] RUTLEDGE, G.C., FRIDRIKH, S.V. Formation of fibers by electrospinning. *Advanced Drug Delivery Reviews*. 2007, vol. 59, no. 14, pp. 1384-1391

[7] RAMAKRISHNA, S., FUJIHARA, K., TEO, W.E., YONG, T., MA, Z., RAMASESHAN, R. Electrospun nanofibers: solving global issues. *Materials Today*. 2006, vol. 9, no. 3, pp. 40-50.

[8] TEO, W.E., RAMAKRISHNA, S. A review on electrospinning design and nanofibre assemblies. *Nanotechnology*. 2006, vol. 17, no. 14, pp. 89-106.

[9] LI, D., XIA, Y. Electrospinning of nanofibers: Reinventing the wheel? *Advanced Materials*. 2004, vol. 16, no. 14, pp. 1151-1170.

[10] HUANG Z.M., ZHANG, Y.Z., KOTAKI, M., RAMAKRISHNA, S. A review on polymer nanofibers by electrospinning and their applications in nanocomposites. *Composites Science and Technology*. 2003, vol. 63, no. 15, pp. 2223-2253.

[11] BAZBOUZ, M.B., STYLIOS G.K. Aligment and optimization of Nylon 6 nanofibers by electrospinning. *Journal of Applied Polymer Science*. 2008, vol. 107, no. 5, pp. 3023-3032.

[12] YOKOYAMA, Y., HATTORI, S., YOSHIKAWA, C., YASUDA, Y., KOYAMA, H., TAKATO, T., KOBAYASHI, H. Novel wet electrospinning system for fabrication of spongiform nanofiber 3-dimensional fabric. *Materials Letters*. 2009, vol. 63, no. 9-10, pp. 754-756.

[13] FONG, H., CHUN, I., RENEKER, D.H. Beaded nanofibers formed during electrospinning. *Polymer*. 1999, vol. 40, no. 16, pp. 4585-4592.

[14] DU, Q., HARDING, D.R., YANG, H. Helical peanut-shaped poly(vinyl pyrrolidone) ribbons generated by electrospinning. *Polymer.* 2013, vol. 54, no. 25, pp. 6752-6759.

[15] KOOMBHONGSE, S., LIU, W., RENEKER, D.H. Flat polymer ribbons and other shapes by electrospinning. *Journal of Polymer Science Part B: Polymer Physics.* 2001, vol. 39, no. 21, pp. 2598-2606.

[16] BAE, H.S., HAIDER, A., SELIM, K.M.K., KANG, I.K., KIM, E.J., KANG, I.K. Fabrication of highly porous PMMA electrospun fibers and their application in the removal of phenol and iodine. *Journal of Polymer Research.* 2013, vol. 20, no.158, pp. 7.

[17] LU, P., XIA, Y. Maneuvering the internal porosity and surface morphology of electrospun polystyrene yarns by controlling the solvent and relative humidity. *Langmuir.* 2013, vol. 29, no. 23, pp. 7070-7078.

[18] BOGNITZKI, M., CZADO, W., FRESE, T., SCHAPER, A., HELLWIG, M., STEINHART, M., GREINER, A., WENDORFF, J.H. Nanostructured fibers via electrospinning. *Advanced Materials.* 2001, vol. 13, no. 1, pp. 70-72.

[19] FORWARD, K.M., FLORES, A., RUTLEDGE, G.C. Production of core/shell fibers by electrospinning from a free surface. *Chemical Engineering Science.* 2013, vol. 104, pp. 250-259.

[20] ZHUO, H.T., HU, J.L., CHEN, S.J. Coaxial electrospun polyurethane core-shell nanofibers for shape memory and antibacterial nanomaterials. *eExpress Polymer Letters.* 2011, vol. 5, no. 2, pp. 182-187.

[21] ZHANG, J.F., YANG, D.Z., XU, F., ZHANG, Z.P., YIN, R.X., NIE, J. Electrospun core-shell structure nanofibers from homogeneous solution of Poly(ethylene oxide)/Chitosan. *Macromolecules.* 2009, vol. 42, no. 14, pp. 5278-5284.

[22] PEER, P., STĚNIČKA, M., PAVLÍNEK, V., FILIP, P. The storage stability of polyvinylbutyral solutions from an electrospinnability standpoint. *Polymer Degradation and Stability.* 2014, vol. 105, pp. 134-139.

[23] JIRSÁK, O., SANETERNÍK, F., LUKÁŠ, D., KOTEK, V., MARTINOVÁ, L., CHALOUPEK, J. *A method of nanofibers production from polymer solution using electrostatic spinning and a device for carrying out the method.* 2005, CZ Patent, 294274 (B6), WO 2005024101

[24] CANAN-CALVO, A.M., BARRERO, A. Current and droplet size in the electro-spraying of liquid scaling laws. *Journal of Aerosol Science.* 1997, vol. 28, no. 2, pp. 249-275.

[25] YARIN, A.L., KOOMBHONGSE, S., RENEKER, D.H. Bending instability in electrospinning of nanofibers. *Journal of Applied Physics.* 2001, vol. 89, no. 5, pp. 3018-3026.

[26] SHIN, Y.M., HOHMAN, M.M., BRENNER, M.P., RUTLEDGE, G.C. Experimental characterization of electrospinning: the electrically forced jet and instabilities. *Polymer.* 2001, vol. 42, no. 25, pp. 9955-9967.

[27] HOHMAN, M.M., SHIN, Y.M., RUTLEDGE, G.C., BRENNER, M.P. Electrospinning and electrically forced jets. II. Applications. *Physics of Fluids.* 2001, vol. 13, no. 8, pp. 2221-2236.

[28] RENEKER, D.H., YARIN, A.L., FONG, H., KOOMBHONGSE, S. Bending instability of electrically charged jets of polymer solutions in electrospinning. *Journal of Applied Physics.* 2000, vol. 87, no. 9, pp. 4531-4547.

[29] SHIN, Y.M., HOHMAN, M.M., BRENNER, M.P., RUTLEDGE, G.C. Electrospinning: A whipping fluid jet generates submicron polymer fibers. *Applied Physics Letters.* 2001, vol. 78, no. 8, pp. 1149-1151.

[30] DEITZEL, J.M., KLEINMEYER, J., HARRIS, D., BECK TAN, N.C. The effect of processing variables on the morphology of electrospun nanofibers and textiles. *Polymer.* 2001, vol. 42, no. 1, pp. 261-272.

[31] ZHONG, X., KIM, K., FANG, D., RAN, S., HSIAO, B.S., CHU, B. Structure and process relationship of electrospun bioabsorbable nanofiber membranes. *Polymer.* 2002, vol. 43, no. 16, pp. 4403-4412.

[32] THERON, S.A., YARIN, A.L. Experimental investigation of the governing parameters in the electrospinning of polymer solutions. *Polymer.* 2004, vol. 45, no. 6, pp. 2017-2030.

[33] TAN, S.H., INAI, R., KOTAKI, M., RAMAKRISHNA, S. Systematic parameter study for ultra-fine fiber fabrication via electrospinning process. *Polymer.* 2005, vol. 46, no. 16, pp. 6128-6134.

[34] SILL, T.J., VON RECUM, H.A. Electrospinning: Applications in drug delivery and tissue engineering. *Biomaterials.* 2008, vol. 29, no. 13, pp. 1989-2006.

[35] AGARWAL, S., WENDORFF, J.H., GREINER, A. Use of electrospinning technique for biomedical applications. *Polymer.* 2008, vol. 49, no. 26, pp. 5603-5621.

[36] GOH, Y.F., SHAKIR, I., HUSSAIN, R. Electrospun fibers for tissue engineering, drug delivery, and wound dressing. *Journal of Materials Science.* 2013, vol. 48, no. 8, pp. 3027-3054.

[37] SARACINO, G.A.A., CIGOGNINI, D., SILVA, D., CAPRINI, A., GELAIN, F. Nanomaterials design and tests for neural tissue engineering. *Chemical Society Reviews.* 2013, vol. 42, no. 1, pp. 225-262.

[38] WANG, C., WANG, M. Electrospun multifunctional tissue engineering scaffolds. *Frontiers of Material Science*. 2014, vol. 8, no. 1, pp. 3-19.

[39] SON, Y.J., KIM, W.J., YOO, H.S. Therapeutic applications of electrospun nanofibers for drug delivery systems. *Archives of Pharmacal Research.* 2014, vol. 37, no. 1, pp. 69-78.

[40] SHARMA, R., SINGH, H., JOSHI, M., SHARMA, A., GARG, T., GOYAL, A.K., RATH, G. Recent advances in polymeric electrospun nanofibers for drug delivery. *Critical Reviews in Therapeutic Drug Carrier Systems.* 2014, vol. 31, no. 3, pp. 187-217.

[41] THAVASI, V., SINGH, G., RAMAKRISHNA, S. Electrospun nanofibers in energy and environmental applications. *Energy Environmental Science.* 2008, vol. 1, no. 2, pp. 205-221.

[42] DONG, Z., KENNEDY, S.J., WU, Y. Electrospinning materials for energy-related applications and devices. *Journal of Power Sources.* 2011, vol. 196, no. 11, pp. 4886-4904.

[43] CAVALIERE, S., SUBIANTO, S., SAVYCH, I., JONES, D.J., ROZIERE, J. Electrospinning: designed architectures for energy conversion and storage devices. *Energy Environmental Science.* 2011, vol. 4, no. 12, pp. 4761-4785.

[44] HOMAEIGOHAR, S., ELBAHRI, M. Nanocomposite electrospun nanofiber membranes for environmental remediation. *Materials.* 2014, vol. 7, no. 2, pp. 1017-1045.

[45] MIAO, J., MIYAUCHI, M., SIMMONS, T.J., DORDICK, J.S., LINHART, R.J. Electrospinning of nanomaterials and applications in electronic components and devices. *Journal of Nanoscience and Nanotechnology.* 2010, vol. 10, no. 9, pp. 5507-5519.

[46] MACOSKO, C.W. *Rheology. Principles, measurements and applications.* 1st ed. New York: VCH Publishers, 1994. 568 pp. ISBN 1-56081-579-5

[47] MEZGER, T.G. *The rheology handbook*. 2nd ed. Hannover: William Andrew Publishing, 2006. 252 pp. ISBN 0815515294

[48] MALKIN, A.Y., ISAYEV, A.I. *Rheology: Concepts, methods, and applications*. 1st ed. Toronto: ChemTec Publishing, 2006. 553 pp. ISBN 1-895198-33-X

[49] FERRY, J.D. *Viscoelastic properties of polymers*. 3rd ed. New York: John Wiley and Sons, INC. 1980. 672 pp. ISBN 9780471048947

[50] TERAOKA, I. *Polymer solutions: An introduction to physical properties.* 1st ed. New York: John Wiley and Sons, INC., 2002. 338 pp. ISBN 978-0-471-38929-3

[51] GUPTA, P., ELSKIN, C.L, LONG, T.E., WILKES, G.L. Electrospinning of linear homopolymers of poly(methyl methacrylate): exploring relationships between fiber formation, viscosity, molecular weight and concentration in a good solvent. *Polymer.* 2005, vol. 46, no. 13, pp. 4799-4810.

[52] KOSKI, A., YIM, K., SHIVKUMAR, S. Effect of molecular weight on fibrous PVA produced by electrospinning. *Material Letters.* 2004, vol. 58, no. 3-4, pp. 493-497.

[53] McKEE, M.G., ELKINS, C.L., LONG, T.E. Influence of self-complementary hydrogen bonding on solution rheology/electrospinning relations. *Polymer.* 2004, vol. 45, no. 26, pp. 8705-8715.

[54] SON, W.K., YOUK, J.H., LEE, T.S., PARK, W.H. The effect of solution properties and polyelectrolyte on electrospinning of ultrafine poly(ethylene oxide) fibers. *Polymer.* 2004, vol. 45, no. 9, pp. 2959-2966.

[55] LEE, J.S., CHOI, K.H., GHIM, H.D., KIM, S.S., CHUN, D.H., KIM, H.Y., LYOO, W.S. Role of molecular weight of atactic poly(vinyl alcohol) (PVA) in the structure and properties of PVA nanofabric prepared by electrospinning. *Journal of Applied Polymer Science.* 2004, vol. 93, no. 2, pp. 1638-1646.

[56] TAO, J., SHIVKUMAR, S. Molecular weight dependent structural regimes during the electrospinning. *Materials Letters.* 2007, vol. 61, no. 11-12, pp. 2325-2328.

[57] NIE, H., HE, A., WU, W., ZHENG, J., XU, S., LI, J., HAN, C.C. Effect of poly(ethylene oxide) with different molecular weights on the electrospinnability of sodium alginate. *Polymer.* 2009, vol. 50, no. 20, pp. 4926-4934.

[58] HOMAYONI, H., RAVANDI, S.A.H., VALIZADEH, M. Influence of the molecular weight of chitosan on the spinnability of chitosan/poly(vinyl alcohol) blend nanofibers. *Journal of Applied Polymer Science.* 2009, vol. 113, no. 4, pp. 2507-2513.

[59] VAN KREVELEN, D.W., TE NIJENHUIS, K. *Properties of polymer: their correlation with chemical structure; their numerical estimation and prediction from additive group contributions* 4th ed. Elsevier Science, Amsterdam 2009, 1004 pp. ISBN 978008-0548197

[60] HANSEN, C.M. *Hansen Solubility Parameters: A User`s Handbook* 2nd ed. CRC Press, Taylor & Francis Group, USA 2007, 519 pp. ISBN

[61] OZDEMIR, C., GUNER, A. Solubility profiles of poly(ethylene glycol)/solvent systems, I: Qualitative comparison of solubility parameter approaches. *European Polymer Journal*. 2007, vol. 43, no. 7, pp. 3068–3093.

[62] HONG, P.D., CHOU, C.M., HE, C.H. Solvent effects on aggregation behaviour of polyvinyl alcohol solutions. *Polymer*. 2001, vol. 42, no. 14, pp. 6105-6112.

[63] LUO, C.J., NANGREJO, M., EDIRISINGHE, M. A novel method of selecting solvents for polymer electrospinning. *Polymer*. 2010, vol. 51, no. 7, pp. 1654-1662.

[64] WANNATONG, L., SIRIVAT, A., SUPAPHOL, P. Effects of solvents on electrospun polymeric fibers: preliminary study on polystyrene. *Polymer International*. 2004, vol. 53, no. 11, pp. 1851-1859.

[65] JARUSUWANNAPOOM, T., HONGROJJANAWIWAT, W., JITJAICHAM, S., WANNATONG, L., NITHITANAKUL, M., PATTAMAPROM, C., KOOMBHONGSE, P., RANGKUPAN, R., SUPAPHOL, P. Effect of solvents on electro-spinnability of polystyrene solutions and morphological appearance of resulting electrospun polystyrene fibers. *European Polymer Journal*. 2005, vol. 41, no. 3, pp. 409-421.

[66] PEER, P., STĚNIČKA, M., PAVLÍNEK, V., FILIP, P., KUŘITKA, I., BRUS, J. An electrorheological investigation of PVB solutions in connection with their electrospinning qualities. *Polymer Testing*. 2014, vol. 39, pp. 115-121.

[67] LUBASOVÁ, D., MARTINOVÁ, L. Controlled morphology of porous polyvinyl butyral nanofibers. *Journal of Nanomaterials*. 2011, 6 pp.

[68] LU, P.P., XU, Z.L., YANG, H., WEI, Y.M., XU, H.T. Effects of ethanol and isopropanol on the structures and properties of polyethersulfone/perfluorosulfonic acid nanofibers fabricated via electrospinning. *Journal of Polymer Research*. 2012, vol. 19, no. 4, 10 pp.

[69] YU, X., XIANG, H., LONG, Y., ZHAO, N., ZHANG, X., XU, J. Preparation of porous polyacrylonitrile fibers by electrospinning a ternary system of PAN/DMF/H2O. *Materials Letters*. 2010, vol. 64, no. 22, pp. 2407-2409.

[70] QI, Z., YU, H., CHEN, Y., ZHU, M. Highly porous fibers prepared by electrospinning a ternary system of nonsolvent/solvent/poly(L-lactic acid). *Materials Letters*. 2009, vol. 63 no. 3-4, pp. 415-418.

[71] WANG, H., LIU, Q., YANG, Q., LI, Y., WANG, W., SUN, L., ZHANG, C., LI, Y. Electrospun poly(methyl methacrylate) nanofibers and

microparticles. *Journal of Materials Science.* 2010, vol. 45, no. 4, pp. 1032-1038.

[72] PEER, P., STĚNIČKA, M., FILIP, P., PAVLÍNEK, V. Comparison of electrorheological measurements based on different methods of electric field generation. *Applied Rheology.* 2014, vol. 24, 42875 (4 pp.).

[73] PEER, P., STĚNIČKA, M., FILIP, P., PAVLÍNEK, V. Comparison of electrorheological characteristics obtained for two geometries: parallel plates and concentric cylinders. *Acta Technica.* 2014, vol. 59, pp. 221-235.

[74] HAO, T. *Electrorheological fluids.* The Non-aqueous Suspensions. 1st ed. Amsterdam: Elsevier, 2005. 561 pp. ISBN 0-44452180-1

[75] DAVIS, L.C. Polarization forces and conductivity effects in electrorheological fluids. *Journal of Applied Physics.* 1992, vol. 72, no. 4, pp. 1334-1340.

[76] KIM, S.G., LIM, J.Y., SUNG, J.H., CHOI, H.J., SEO, Y. Emulsion polymerized polyaniline synthesized with dodecylbenzenesulfonic acid and its electrorheological characteristic: temperature effect. *Polymer.* 2007, vol. 48, no. 22, pp. 6622-6631.

[77] SOHN, J.I., SUNG, J.H., CHOI, H.J., JHON, M.S. The effect of particle concentration of poly(*p*-phenylene) on electrorheological response. *Journal of Applied Polymer Science.* 2002, vol. 84, no. 13, pp. 2397-2403.

[78] LENGÁLOVÁ, A., PAVLÍNEK, V., SÁHA, P., QUADRAT, O., STEJSKAL, J. The effect of dispersed particle size and shape on the electrorheological behaviour of suspensions. *Colloids and Surfaces A-Physicochemical and Engineering Aspects.* 2003, vol. 227, no. 1-3, pp. 1-8.

[79] SEDLAČÍK, M., MRLÍK, M., KOŽÁKOVÁ, Z., PAVLÍNEK, V., KUŘITKA, I. Synthesis and electrorheology of rod-like titanium oxide particles prepared via microwave-assisted molten-salt method. *Colloid and Polymer Science.* 2013, vol. 291, no. 5, pp. 1105-1111.

[80] YIN, Y.C., LIU, C.J., WANG, B.X., YU, S.S., CHEN, K.Z. The synthesis and properties of bifunctional and intelligent Fe3O4 titanium oxide core/shell nanoparticles. *Dalton Transactions.* 2013, vol. 42, no. 19, pp. 7233-7240.

[81] PEER, P., STĚNIČKA, M., SEDLAČÍK, M., FILIP, P., PAVLÍNEK, V. Magnetorheological behaviour and electrospinning of PEO suspensions with magnetic nanoparticles. *Journal of Intelligent Material Systems and Structures.* (submitted)

[82] FILIP, P., ŠVRČINOVÁ, P. Measurement of elongational viscosity of polymer melts using SER Universal Testing Platform. *Applied Rheology.* 2012, vol. 22, 14776 (5 pp.).

LIST OF PUBLICATIONS

JOURNALS WITH IMPACT FACTOR

A) related to the Ph.D. thesis

1. PEER, P. (50%), STĚNIČKA, M., SEDLAČIK, M., FILIP, P., PAVLÍNEK, V. Magnetorheological behaviour and electrospinning of PEO suspensions with magnetic nanoparticles. *Journal of Intelligent Material Systems and Structures.* (submitted)

2. PEER, P. (50%), STĚNIČKA, M., PAVLÍNEK, V., FILIP, P., KUŘITKA, I., BRUS, J. An electrorheological investigation of PVB solutions in connection with their electrospinning qualities. *Polymer Testing.* 2014, vol. 39, pp.115-121.

3. PEER, P. (50%), STĚNIČKA, M., FILIP, P., PAVLÍNEK, V. Comparison of electrorheological measurements based on different methods of electric field generation. *Applied Rheology.* 2014, vol. 24, 42875 (4 pp.).

4. PEER, P. (50%), STĚNIČKA, M., PAVLÍNEK, V., FILIP, P. The storage stability of polyvinylbutyral solutions from an electrospinnability standpoint. *Polymer Degradation and Stability.* 2014, vol. 105, pp. 134-139.

5. FILIP, P., ŠVRČINOVÁ, P. (50%) Measurement of elongational viscosity of polymer melts using SER Universal Testing Platform. *Applied Rheology.* 2012, vol. 22, 14776 (5 pp.).

B) non-related to the Ph.D. thesis

6. MRLÍK, M., ILČÍKOVÁ M., SEDLAČÍK, M., MOSNÁČEK, J., PEER, P., FILIP, P. Cholesteryl-coated carbonyl iron particles with improved anti-corrosion stability and their viscoelastic behaviour under magnetic field. *Colloid and Polymer Science.* 2014, vol. 292, no. 9, pp. 2137-2143.

7. SEDLAČÍK, M., PAVLÍNEK, V., PEER, P., FILIP, P. Tailoring the magnetic properties and magnetorheological behavior of spinel nanocrystalline cobalt ferrite by varying annealing temperature. *Dalton Transactions.* 2014, vol. 43, no. 18, pp. 6919-6924.

8. MRLÍK, M., SEDLAČÍK, M., PAVLÍNEK, V., BAŽANT, P., SÁHA, P., ŠVRČINOVÁ, P., FILIP, P. Synthesis and magnetorheological characteristics of ribbon-like, polypyrrole-coated carbonyl iron suspensions

under oscillatory. *Journal of Applied Polymer Science.* 2013, vol. 128, no. 5, pp. 2977-2982.

9. MRLÍK, M., ILČÍKOVÁ, M., PAVLÍNEK, V., MOSNÁČEK, J., PEER, P., FILIP, P. Improved thermooxidation and sedimentation stability of covalently-coated carbonyl iron particles with cholesteryl groups and their influence on magnetorheology. *Journal of Colloid and Interface Science.* 2013, vol. 396, pp. 146-151.

10. SEDLAČÍK, M., PAVLÍNEK, V., VYROUBAL, R., PEER, P., FILIP, P. A dimorphic magnetorheological fluid with improved oxidation and chemical stability under oscillatory shear. *Smart Materials & Structures.* 2013, vol. 22, no. 3, 8 pp.

11. SEDLAČÍK, M., MOUČKA, R., KOŽÁKOVÁ, Z., KAZANTSEVA, N.E., PAVLÍNEK, V., KUŘITKA, I., KAMAN, O., PEER, P. Correlation of structural and magnetic properties of Fe_3O_4 nanoparticles with their calorimetric and magnetorheological performance. *Journal of Magnetism and Magnetic Materials.* 2013, vol. 326, pp. 7-13.

12. SEDLAČÍK, M., PAVLÍNEK, V., SÁHA, P., ŠVRČINOVÁ, P., FILIP, P. The role of particles annealing temperature on magnetorheological effect. *Modern Physics Letters B.* 2012, vol. 26, no. 3, 6 pp.

13. SEDLAČÍK, M., PAVLÍNEK, V., LEHOCKÝ, M., MRÁČEK, A., GRULICH, O., ŠVRČINOVÁ, P., FILIP, P., VESEL, A. Plasma-treated carbonyl iron particles as a dispersed phase in magnetorheological fluids. *Colloids and Surfaces A: Physicochemical and Engineering Aspects.* 2011, vol. 387, no. 1-3, pp. 99-103.

14. SEDLAČÍK, M., PAVLÍNEK, V., SÁHA, P., ŠVRČINOVÁ, P., FILIP, P., STEJSKAL, J. Rheological properties of magnetorheological suspensions based on core–shell structured polyaniline–coated carbonyl iron particles. *Smart Materials & Structures.* 2010, vol. 19, no. 11, 115008.

JOURNALS IN THE SCOPUS DATABASE

15. PEER, P., STĚNIČKA, M., FILIP, P., PAVLÍNEK, V. Comparison of electrorheological characteristics obtained for two geometries: parallel plates and concentric cylinders. *Acta Technica.* 2014, vol 59, pp. 221-235.

16. ŠVRČINOVÁ, P., FILIP, P., LUBASOVÁ, D. On the rheological behaviour of PVB solutions in the process of electrospinning. *Acta Technica.* 2012, vol. 57, pp.197-210.

17. ŠVRČINOVÁ, P., KHARLAMOV, A., FILIP, P. On the measurement of elongational viscosity of polyethylene materials. *Acta Technica.* 2009, vol. 54, pp. 49-57.

OTHER JOURNALS

18. ŠVRČINOVÁ, P., KHARLAMOV, A., FILIP, P. K měření elongační viskozity pomocí 'SER Universal Testing Platform'. *Plasty a kaučuk.* 2009, vol. 46, no. 3-4, pp. 77-79.

19. ŠVRČINOVÁ, P., FILIP, P., LUBASOVÁ, D. Vliv elektroreologického chování polymerních roztoků na elektrostatické zvlákňování. *Plasty a kaučuk.* 2011, vol. 48, no. 1-2, pp. 6-8.

CONFERENCE PROCEEDINGS

A) in the database WoS

1. PEER, P., FILIP, P., STĚNIČKA, M., PAVLÍNEK, V. Comparison of electrorheological characteristics obtained in two geometrical arrangements: parallel plates and concentric cylinders. In Zatloukal, M. *Novel Trends in Rheology VI. Zlín: AIP Conference Proceedings.* 2015 (accepted)

2. PEER, P., FILIP, P. Quality of nanofibrous web in dependence on the preparation of polymer solutions. In Zatloukal, M. *Novel Trends in Rheology V. Zlín: AIP Conference Proceedings.* 2013, vol. 1526, pp. 310-315. ISBN 978-07354-1151-7. ISSN 0094-243X.

3. ZELENKOVÁ, J., PEER, P., FILIP, P. Spinnability of PEO solutions with respect to their aging. In: *NANOCON 2013. 5th International Conference Proceedings.* Ostrava: Tanger Ltd, 2013. ISBN 978-80-87294-44-4.

4. ŠVRČINOVÁ, P., STĚNIČKA, M., FILIP, P., PAVLÍNEK, V. On the comparison of electrorheological measurements with different generation of an electric field. *Journal of Physics: Conference Series.* 2013, vol. 412. ISSN 1742-6596.

5. MRLÍK, M., SEDLAČÍK, M., PAVLÍNEK, V., ŠVRČINOVÁ, P., FILIP, P., SÁHA, P. Magnetorheology of carbonyl iron particles coated with polypyrrole ribbons: The steady shear study. *Journal of Physics: Conference Series.* IOP publishing Ltd, 2013, vol. 412. ISSN 1742-6596.

6. FILIP, P., ŠVRČINOVÁ, P. Invariance of Elongational Viscosity Measurements Using SER Universal Testing Platform with Respect to

Rectangular Shapes of Polymer Samples. In Zatloukal, M. *Novel Trends in Rheology IV. Zlín: AIP Conference Proceedings*. Melville, New York, 2011, vol. 1375, pp. 156-162. ISBN 978-0-7354-0935-4.

7. SEDLAČÍK, M., PAVLÍNEK, V., SÁHA, P., ŠVRČINOVÁ, P., FILIP, P. Core-shell structured polypyrrole-coated magnetic carbonyl iron microparticles and their magnetorheology. In Zatloukal, M. *Novel Trends in Rheology IV. Zlín: AIP Conference Proceedings*. Melville, New York, 2011, vol. 1375, pp. 284-291. ISBN 978-0-7354-0935-4.

8. ŠVRČINOVÁ, P., FILIP, P., LUBASOVÁ, D. On the electrospinning of PVB solutions. In: *Proc. 2nd International Conference NANOCON*. Ostrava, TANGER, 2010, pp. 352-356. ISBN 978-80-87294-19-2.

9. KHARLAMOV, A.A., FILIP, P., ŠVRČINOVÁ, P. A remark to the tube theory. In Zatloukal, M. *Novel Trends in Rheology III*. Melville, AIP, 2009, vol. 1152, pp. 3-15. ISBN 978-0-7354-0689-6.

B) not in the database WoS

10. FILIP, P., PIVOKONSKÝ, R., PEER, P., ZELENKOVÁ. Evaluation of applicability of an SER Universal Testing Platform. In: *10th Annual European Rheology Conference*. Nantes, Groupe Français de Rhéologie, 2015, p. 46.

11. PEER, P., STĚNIČKA, M., SEDLAČÍK, M., PAVLÍNEK, V., FILIP, P. Magnetorheological behaviour of PEO solutions with magnetic nanoparticles. In: *14th Int. Conf. on Electrorheological Fluids and Magnetorheological Suspensions*. Granada, University of Granada, 2014, p. 50.

12. STĚNIČKA, M., PEER, P., PAVLÍNEK, V., FILIP, P. Ageing of polyvinylbutyral solutions with impact on spinnability. In: *Advanced Materials World Congress*. 2013. p. 111. ISBN 978-81-9200068-3-16, 978-81-9200068-3-25.

13. FILIP, P., PEER, P. Process of Electrospinning with an Emphasis to the Rheological Behaviour of PVB Solutions. In: *Proc. 10th IASME/WSEAS Int. Conf. Heat Transfer, Thermal Engineering and Environment*. Istanbul, WSEAS Press, 2012, pp. 159-163. ISBN 978-161804-114-2.

14. ŠVRČINOVÁ, P., STĚNIČKA, M., FILIP, P., PAVLÍNEK, V. A comparison of electrorheological measurements of selected ER suspensions. In: *XVIth International Congress on Rheology*. Lisbon, European Society of Rheology, 2012, p. 143.

15. MRLÍK, M., ILČÍKOVÁ, M., PAVLÍNEK, V., MOSNÁČEK, J., ŠVRČINOVÁ, P., FILIP, P. Viscoelastic characterization of

magnetorheological suspensions consisting of silicone oil and carbonyl iron particles covalently coated with cholesteryl groups. In: *13ᵗʰ Int. Conf. on Electrorheological Fluids and Magnetorheological Suspensions*. Ankara, Gazi University, 2012, pp. 214-215.

16. SEDLAČÍK, M., PAVLÍNEK, V., VYROUBAL, R., ŠVRČINOVÁ, P., FILIP, P., STĚNIČKA, M. Dimorphic magnetorheological fluid with improved oxidation and chemical stability under oscillatory shear. In: *13ᵗʰ Int. Conf. on Electrorheological Fluids and Magnetorheological Suspensions*. Ankara, Gazi University, 2012, pp. 45-46.

17. ŠVRČINOVÁ, P., FILIP, P., LUBASOVÁ, D., MARTINOVÁ, L. Impact of electrorheological behavior of PVB solutions on the process of electrospinning. In Tao, R. *The 12ᵗʰ International Conference on Electrorheological Fluids and Magnetorheological Suspensions*. Singapore: World Scientific Publishing Co. Pte. Ltd., 2011, pp. 363-368. ISBN 13 978-981-4340-22-9, 10 981-4340-22-7.

18. SEDLAČÍK, M., PAVLÍNEK, V., SÁHA, P., ŠVRČINOVÁ, P., FILIP, P. The role of particles annealing temperature on magnetorheological effect. In Tao, R. *The 12ᵗʰ International Conference on Electrorheological Fluids and Magnetorheological Suspensions*. Singapore: World Scientific Publishing Co. Pte. Ltd., 2011, pp. 363-368. ISBN 13 978-981-4340-22-9, 10 981-4340-22-7.

19. SEDLAČÍK, M., PAVLÍNEK, V., SÁHA, P., ŠVRČINOVÁ, P., FILIP, P. Polymer coated carbonyl iron particles and their magnetorheological suspensions. In: *The 4ᵗʰ WSEAS International Conference on Engineering Mechanics, Structures, Engineering Geology*. Athens, WSEAS, 2011, pp. 289-293. ISBN 978-1-61804-022-0.

20. ŠVRČINOVÁ, P., FILIP, P., LUBASOVÁ, D. A relation of electrorheological behaviour of polymer solutions to quality of electrospun fibres. In: *7th Annual European Rheology Conference*. Moscow, Vinogradov Society of Rheology, 2011, p.130. ISBN 978-5-88149-485-8.

21. ŠVRČINOVÁ, P., FILIP, P., LUBASOVÁ, D. Electrospinning of PVB solutions - influence of electrorheological behaviour. In Meyer, J. *Proc. 8th International Conference on Heat Transfer, Fluid Mechanics and Thermodynamics*. Pointe Aux Piments, Mauritius, 2011, pp. 575-579. ISBN 978-1-86854-948-1.

22. ŠVRČINOVÁ, P., FILIP, P., LUBASOVÁ, D. Relation between electrorheological characteristics of PVB solutions and their electrospinnability. In: *Recent Advances in Fluid Mechanics and Heat & Mass Transfer*. Athens, WSEAS Press, 2011, pp. 235-238. ISBN 978-1-61804-026-8.

23. SEDLAČÍK, M., PAVLÍNEK, V., GRULICH, O., MRÁČEK, A., LEHOCKÝ, M., ŠVRČINOVÁ, P., FILIP, P., VESEL, A. On the plasma treatment of carbonyl iron particles and their magnetorheology. In: *3rd International Conference on Advanced Plasma Technologies*. Bohinj, 2010.

24. SEDLAČÍK, M., PAVLÍNEK, V., SÁHA, P., ŠVRČINOVÁ, P., FILIP, P., STEJSKAL, J. The influence of particles synthesis on magnetorheological effect and their sedimentation. In: *Plastko*. Zlín, UTB, 2010.

25. FILIP, P., ŠVRČINOVÁ, P. Extensional viscosity of polymer melts – measurement with a SER Universal Testing Platform. In: *Proc. 5th Pacific Rim Conference on Rheology*. Sapporo, Hokkaido University, 2010, article no. E-4-4.

26. ŠVRČINOVÁ, P., LUBASOVÁ, D., FILIP, P., MARTINOVÁ, L. Influence of viscosity on behaviour of PVB solutions in electrospinning. In: *6th Annual European Rheology Conference 2010*. Göteborg, European Society of Rheology, 2010, p. 283.

27. FILIP, P, ŠVRČINOVÁ, P. On the measurement of extensional viscosity of polymer melts using SER Universal Testing Platform. In Meyer, M. *Proc. 7th Int. Conf. Heat Transfer, Fluid Mechanics, and Thermo-mechanics*. Antalya, HEFAT, 2010. ISBN 978-1-86854-818-7.

28. ŠVRČINOVÁ, P., LUBASOVÁ, D., FILIP, P., MARTINOVÁ, L. On behaviour of PVB solutions in electrospinning. In Zolotarev, I. *Engineering Mechanics 2010*. Prague, Institute of Thermomechanics AS CR, 2010, p. 149-150. ISBN 978-80-87012-26-0.

29. FILIP, P., ŠVRČINOVÁ, P. Choice of polymer samples geometry for measurement of elongational viscosity using SER Universal Testing Platform. In Zolotarev, I. *Engineering Mechanics 2010*. Prague, Institute of Thermomechanics AS CR, 2010. ISBN 978-80-87012-26-0.

30. KHARLAMOV, A.A., ŠVRČINOVÁ, P., FILIP, P. Probabilistic approach to reptation theory. In *5th Annual European Rheology Conference*. Cardiff, Cardiff University, 2009, p. 1.

31. KHARLAMOV, A.A., FILIP, P., ŠVRČINOVÁ, P. A note to the tube theory. In: *Proc. Polymer Processing Society Europe/Africa Regional Meeting*, Larnaca, Polymer Processing Society, 2009.

32. ŠVRČINOVÁ, P., FILIP, P. and KHARLAMOV, A.A. A note to the measurement of extensional viscosity using SER Universal Testing Platform with different shapes of polymer samples. In: *Proc. Polymer Processing Society Europe/Africa Regional Meeting*, Larnaca, Polymer processing Society, 2009.

33. ŠVRČINOVÁ, P., KHARLAMOV, A., FILIP, P. Measurement of elongational viscosity of PE materials. In Naprstek, J., Fischer, C. *Engineering Mechanics 2009*. Prague, UTAM, 2009, pp. 266-267. ISBN 978-80-86246-35-2.

34. KHARLAMOV, A.A., FILIP, P., ŠVRČINOVÁ, P. A remark to the reptation theory. In Naprstek, J., Fischer, C. *Engineering Mechanics 2009*. Prague, UTAM, 2009, pp. 654-650. ISBN 978-80-86246-35-2.

35. ŠVRČINOVÁ, P., KHARLAMOV, A., FILIP, P. On the measurement of elongational viscosity using SER Universal Testing Platform. In Jonáš, P., Uruba, V. *Colloquium Fluid Dynamics*. Prague, Institute of Thermomechanics AS CR, 2008. ISBN 978-80-87012-14-7.

CURRICULUM VITAE

Personal information

Name	Ing. Petra Peer (Švrčinová)
Address	Korýčanská 250, Střílky
Phone	+420 777 274 667
E-mail	peer@ih.cas.cz
Nationality	Czech
Date of birth	13th June 1982
Place of birth	Frýdek-Místek, Czech Republic

Work Experience

Period	2008 – present
Position	Researcher
Name of employer	Institute of Hydrodynamics AS CR, v. v. i.
	Pod Paťankou 5, 166 12 Prague 6

Education

Period	2011 – present
	Ph.D. study
Principal branch	Technology of Macromolecular Substances
Organization	Tomas Bata University in Zlín,
	Faculty of Technology, Polymer Centre

Period	2005 – 2007
Achieved title	Ing.
Study	Nonwoven Textile
Organization	Technical University of Liberec, Faculty of Textile, Department of Nanofibre Nonwoven Textile
Period	2002 – 2005
Achieved title	Bc.
Study	Textile technology
Organization	Technical University of Liberec, Faculty of Textile, Department of Textile Technology

Stays abroad

Period	September 2011
Place	Belgium, Leuven
Type of training	13th European School on Rheology

Projects

2011- 2013	Grant project GA ČR P105/11/2342
	Usage of electrorheological measurements in predictability of the process of electrospinning
	member of the research team

2009-2013	Grant project GA ČR 103/09/2066
	Analysis and development of constitutive equations for description of non-Newtonian fluids
	member of the research team
2008-2012	Grant project GA ČR 103/08/1307
	Rheological modelling of high-pressure polymer flow
	member of the research team
2007-2011	Grant project GA AV ČR A200600703
	Investigation of flow behaviour for a novel class of metallocene-based polymers
	member of the research team
2006-2008	Grant project GA ČR 103/06/1033
	Investigation of unusual flow phenomena of non-Newtonian fluids in complex geometries
	member of the research team

ORIGINAL PAPERS

Comparison of Electrorheological Measurements Based on Different Methods of Electric Field Generation

Petra Peer*[1], Martin Stenicka[2], Petr Filip[1], Vladimir Pavlinek[2]

[1] Institute of Hydrodynamics, Academy of Sciences of the Czech Republic, 166 12 Prague, Czech Republic
[2] Centre of Polymer Systems, University Institute, Tomas Bata University in Zlin, 762 72 Zlin, Czech Republic

*Corresponding author: peer@ih.cas.cz
Fax: x420.233324361

Abstract:

Electrorheological measurements represent a key approach in characterizing the efficiency of electrorheological fluids. The rotational rheometers, the Physica MCR 501 (Anton Paar) equipped with an electrorheological cell and the Bohlin Gemini CVOR 150 (Malvern Instruments) modified for electrorheological experiments generate an electric field in two completely different ways. Each of the two generations has a specific influence on electrorheological measurements. The experimental data were obtained and compared for a suspension of polyaniline powders mixed (10 wt%) in silicone oil. For a concentric-cylinders arrangement, it was shown that the data are fully comparable for both rheometers. However, for a parallel-plate arrangement, the data using the Physica MCR 501 provide higher values in comparison with both the corresponding plate-plate data obtained with the Bohlin Gemini CVOR 150 and with the mutually comparable concentric cylinders data.

Key words:
rheology, electrorheology, rheometry, PANI powder, silicone oil

1 INTRODUCTION

Electrorheological (ER) fluids are suspensions of fine particles in an electrically insulating fluid, usually mineral or silicone oil. When exposed to an electric field their apparent viscosity can increase by several orders, thus shifting their substance from a liquid to almost a solid-like behavior. Hence, their structural and rheological properties can be controlled by electric field strengths. Numerous studies on this topic have been summarized [1–10]. The common factors influencing the measurements of rheological characteristics are, in the case of ER experiments, amplified by the mode of generation of an electric field. Naturally, any mode has, owing to its mechanical effect, an adverse impact on the quality of the measurements. This evokes the question as to whether these negative contributions are comparable for the individual modes. Moreover, this situation is further complicated by the geometrical arrangement used – either a parallel-plate (PP) system or a concentric cylinders (CC) system. As far as the authors are aware, no attention has been paid hitherto to this problem.

The aim of this contribution is to compare the ER characteristics obtained by two rotational rheometers (a Physica MCR 501 (Anton Paar) and a Bohlin Gemini CVOR 150 (Malvern Instruments)) equipped with electrocells generating an electric field in two different ways. Both rheometers are equipped with both geometrical arrangements. Each system is covered with a hood ensuring safety regulations and temperature stability is controlled by either Peltier elements (Physica) or a fluid circulator (Bohlin). The bottom plate for the parallel-plate device and the cup in the CC setup are grounded. In the case of the Physica MCR 501, opening the hood automatically switches off the power supply. The rheometers themselves are fully isolated from the electric current. The substantial difference between the two electrorheologically adapted rheometers consists of the completion of an electric circuit through an upper shaft (described in more detail in the following section).

2 EXPERIMENTAL

2.1 MATERIAL

The ER suspension was prepared by mixing polyaniline (PANI) powder (Sigma Aldrich, USA, base, 50000 g/mol) with silicone oil (Lukosiol M200, Chemical Works Kolin, Czech Republic) in a 10 wt% concentration. The PANI
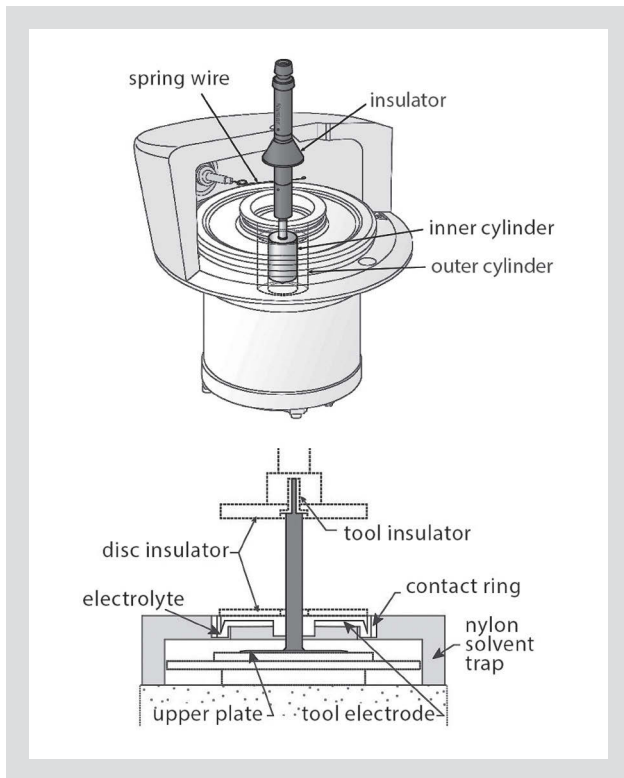
Figure 1: Position of a spring wire in the Physica MCR 501 and the location of an electrolyte in the Gemini 150 device.

Figure 2: Flow curves of a pure silicone oil (without PANI powder, E = 0 kV/mm).

powder was ground, sieved to obtain particle sizes smaller than $45\,\mu m$, and dried at 80 °C in a vacuum oven to a constant weight. The samples were stirred mechanically and consequently placed in an ultrasonic bath for 30 s before each measurement.

2.2 DEVICES AND MEASUREMENT CONDITIONS

The intensity of the electric field in the MCR 501 was varied through an external high-voltage power supply unit HCP 14-12500 (F. u. G. Elektronik GmbH, Rosenheim, Germany) providing an electric field strength of up to 12.5 kV/mm provided that the electric current does not exceed 1 mA (otherwise the voltage is proportionally reduced). The rotational rheometer was equipped with two electrocells: P-PTD200/E parallel plates of 50 mm diameter (gap 0.3 mm) and a C-PTD200/E bob and cup arrangement with inner and outer diameters of 16.6 mm and 18 mm (gap 0.7 mm), respectively.

The intensity of the electric field in the Gemini 150, influenced also by the density of electrolyte, was regulated by a DC high-voltage source TREK (TREK 668B, USA) providing an electric field strength of up to 3 kV/mm with a maximum electric current of 5 mA. The dimensions of the measuring electrocells used were as follows: the diameter of the parallel plates attained 40 mm (gap 0.3 mm) and in the concentric arrangement the inner and outer diameters were 25 mm and 27.5 mm (gap 1.25 mm), respectively.

A Van der Pauw setup was used to measure the DC conductivity using a four-point method. The DC conductivity of the PANI base pressed into pellets (13 mm

in diameter, 1 mm in thickness) attained $7.72 \cdot 10^{-9}$ S/cm. The ER properties (shear viscosity, storage and loss moduli) of polyaniline particles suspended in silicone oil were measured using both devices and both geometrical arrangements. Each point in steady shear flow measurements as well as in small-strain oscillatory tests (dynamic amplitude sweep and frequency sweep) was measured at least three times. All the measurements were carried out at 20 °C.

2.3 DIFFERENCES IN ELECTRIC FIELD GENERATION

Figure 1 depicts the completion of the circuit loops in the individual rheometers enabling the generation of an electric field. The principal difference is in the different mechanical impacts on the ER measurements. In the case of the MCR 501, a circuit loop is completed by a spring wire leaning against an upper shaft and thus producing friction between these two mechanical parts. This implies an increase in viscosity and the oscillatory data and the values representing this increase (e.g. for viscosity roughly comparable with the viscosity of water) have to be subtracted to obtain the correct values of the measured characteristics. Perles et al. [11, Figure 3] found that this devi-

	Mixing	Pause	Pause	Measurement
Steady shear	10 1/s	0 1/s	0 1/s	0.01 - 100 1/s
	30 s	30 s	60 s	
	0 V	0V	xxx V	xxx V
Amplitude sweep	10 1/s	0 1/s	0 1/s	0.0001 - 1 / 0.01
	30 s	30 s	60 s	5 Hz / 3 Hz
	0 V	0V	xxx V	xxx V
Frequency sweep	10 1/s	0 1/s	0 1/s	0.001 / 0.0006
	30 s	30 s	60 s	0.1 - 10 Hz
	0 V	0V	xxx V	xxx V

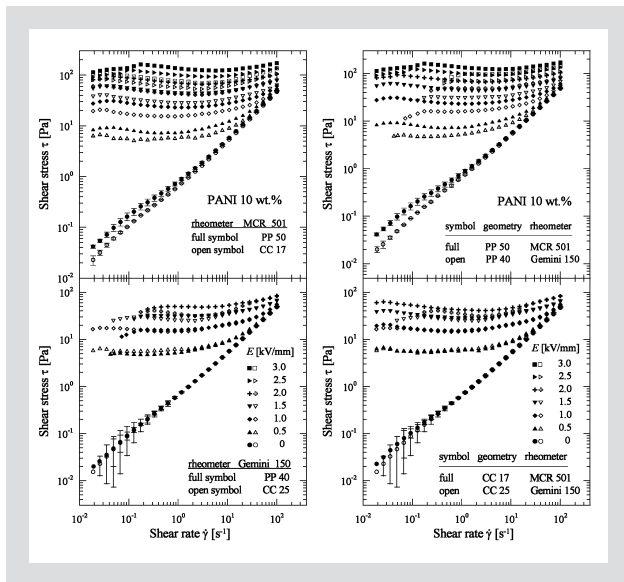Table 1: Entry parameters for all three types of measurements (t = 20 °C).

Figure 3: Shear stress dependent on shear rate: (left) different geometrical arrangements (PP and CC, same rheometer) and (right) same geometrical arrangement (PP or CC, different rheometers).
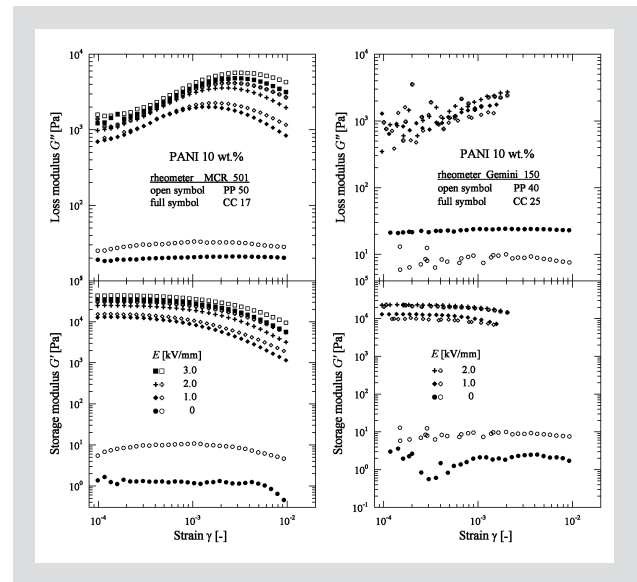

Figure 5: Storage and loss moduli dependent on strain (different geometrical arrangements, same rheometer).
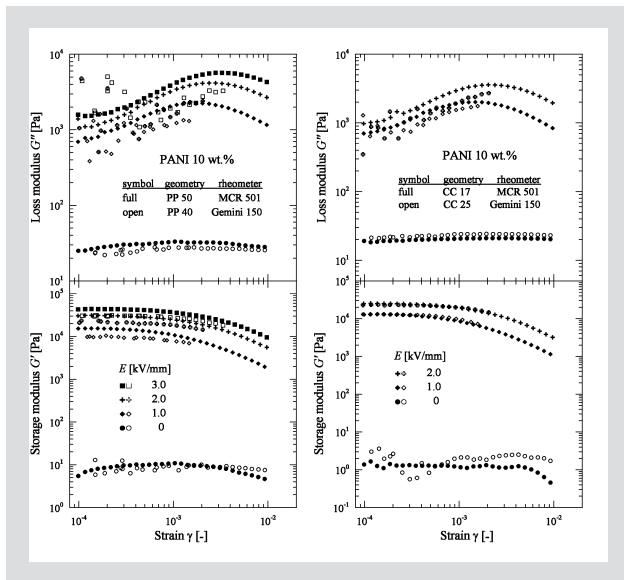

Figure 4: Storage and loss moduli dependent on strain, same geometrical arrangements (PP or CC, different rheometers).

carrier fluid (silicone oil) only, followed by an application of the prepared ER suspensions. As expected, the flow curves of shear rate in the range 1 – 100 1/s corresponding to a pure silicone oil (without PANI powder) are identical (Figure 2). It implies that the differences obtained under the application of an electric field are not influenced by the a priori differences appearing in the classical measurements (absence of electric field).

Three types of measurements were carried out (steady shear, amplitude and frequency sweeps) with the prepared suspensions (10 wt% concentration of PANI powder in silicone oil). The entry parameters of the measurements (time intervals, electric field strength (xxx V stands for the individual values of voltage as indicated in the Figures), ranges of measured points) are summarized in Table 1. Figures 3 – 7 depict the behavior of the flow curves for the same geometry (PP or CC) of both rheometers, and for both geometries of either rheometer. In the case of the MCR 501, the experimental data in these Figures are always reduced by the values obtained for the corresponding measurements with air only.

3   DISCUSSION AND CONCLUSIONS

Non-negligible discrepancies in the measured data are exhibited for different geometrical arrangements of the electrocells and different rheometers. This does not seem to be surprising, since e.g. Rides et al. [12] who compared the shear viscosity results obtained at high shear rates using extrusion rheometers (the same manufacturer) including an instrumented injection moulding machine.

These deviations can be the result for a variety of reasons: differences in construction of both rheometers (in both cases all the parts in contact with the materials are made of stainless steel (1.4571 – MCR 501, 316 – CVOR

ation is negligible for shear rate exceeding 50 1/s. Analogous analysis is valid for the processing of the data obtained with the help of the Gemini 150, for which a circuit loop is completed through an electrolyte housed in the circumferential gutter and resistance is formed between a contact ring and the electrolyte. This adverse phenomenon is reflected by adjusting the parameters used in the data processing by the Gemini software.

2.4   INDIVIDUAL MEASUREMENTS

All the measurements were always carried out for all four electrocells: PP and CC arrangements in either rotational rheometer. Each measurement started with a
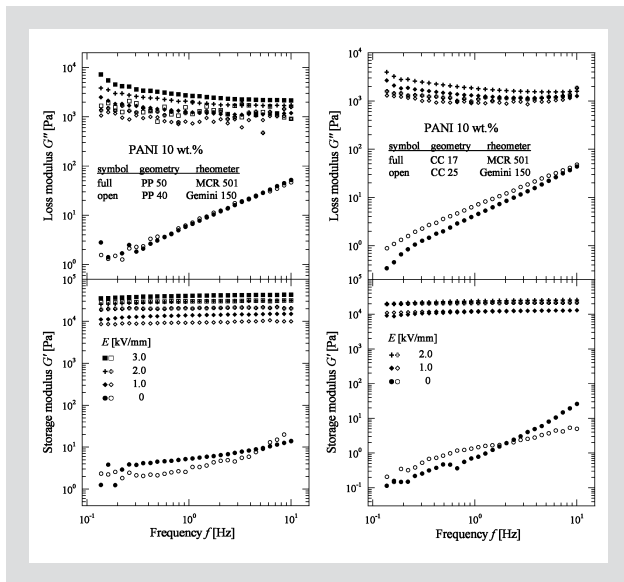
Figure 6: Storage and loss moduli dependent on frequency (same geometrical arrangement (PP or CC), different rheometers).
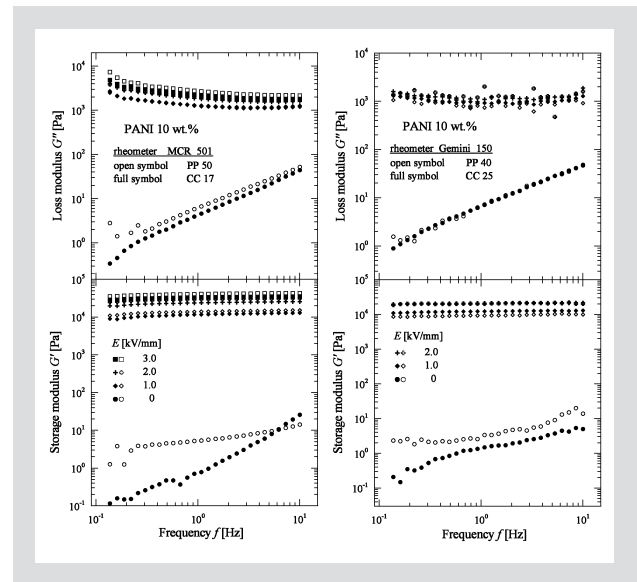

Figure 7: Storage and loss moduli dependent on frequency (different geometrical arrangements, same rheometer).

150)), anti-shock balance precautions in the laboratories, the method of generation of the electric field, the diameters of the corresponding geometrical arrangements (e.g. for a PP arrangement 40 versus 50 mm). Based on Figures 3 – 7 it is possible to come to the conclusions that:

■ The effect of completion of an electric circuit is different, but, loosely speaking, in both cases the values, if mere air only is measured, are comparable to those corresponding, for example, to those obtained for water with no additional mechanical contact. However, these values are negligible in comparison with those for ER fluids.

■ The data from the Physica MCR 501 are smoother and the behavior of the corresponding curves is more continuous (at this point the age difference of the individual devices is probably also a factor).

■ In the case of the Gemini 150, the experimental data are closer for both geometries used.

■ In the Physica MCR 501, usage of parallel-plate geometry provides – on average – higher values in comparison with the CC geometry.

■ When using parallel-plate geometry, the data obtained by the Physica MCR 501 provides higher values (shear viscosity, storage and loss moduli versus strain or frequency) than those obtained by the Gemini 150.

■ When using CC geometry, the data obtained by the Physica MCR 501 and the Gemini 150 are comparable in spite of the difference in corresponding gaps.

ACKNOWLEDGEMENTS

REFERENCES

[1] Block H, Kelly JP: Electro-rheology, J. Phys. D: Appl. Phys. 21 (1988) 1661 – 1677.
[2] Jordan TC, Shaw MT: Electrorheology, IEEE Trans. Electrical Insul. 24 (1989) 849 – 878.
[3] Blackwood KM, Block H: Semi-conducting polymers in electrorheology: a modern approach to smart fluids, Trends Polym. Sci. 14 (1993) 98 – 104.
[4] Parthasarathy M, Klingenberg DJ: Electrorheology: Mechanisms and models, Mater. Sci. Eng. Res. 17 (1996) 57 – 103.
[5] Hao T: Electrorheological fluids, Adv. Mater. 13 (2001) 1847 – 1857.
[6] Hao T: Electrorheological suspensions, Adv. Coll. Interface Sci. 97 (2002) 1 – 35.
[7] Sung JH, Cho MS, Choi HJ, Jhon MS: Electrorheology of semiconducting polymers, J. Ind. Eng. Chem. 10 (2004) 1217 – 1229.
[8] Choi HJ, Jhon MS: Electrorheology of polymers and nanocomposites, Soft Matter 5 (2009) 1562 – 1567.
[9] Liu YD, Choi HJ: Electrorheological fluids: smart soft matter and characteristics, Soft Matter 8 (2012) 11961 – 11978.
[10] Sheng P, Wen W: Electrorheological fluids: Mechanisms, dynamics, and microfluidics applications, Ann. Rev. Fluid Mech. 44 (2012) 143 – 174.
[11] Perles CE, Volpe PLO, Bombard AJF: Study of the cation and salinity effect on electrocoalescence of water/crude oil emulsions, Energy Fuels 26 (2012) 6914 – 6924.
[12] Rides M, Kelly AL, Allen CRG: An investigation of high rate capillary extrusion rheometry of thermoplastics, Polym. Test. 30 (2011) 916 – 924.

Material characterisation

An electrorheological investigation of PVB solutions in connection with their electrospinning qualities

P. Peer [a], [*], M. Stenicka [b], V. Pavlinek [b], P. Filip [a], I. Kuritka [b], J. Brus [c]

[a] Institute of Hydrodynamics, Acad. Sci. Czech Rep., 166 12 Prague 6, Czech Republic
[b] Centre of Polymer Systems, University Institute, Tomas Bata University in Zlin, 760 01 Zlin, Czech Republic
[c] Institute of Macromolecular Chemistry, Acad. Sci. Czech Rep., 162 00 Prague 6, Czech Republic

ARTICLE INFO

ABSTRACT

During the process of electrostatic spinning, the rheological behaviour of polymer solutions is significantly influenced by the presence of an external electric field. The aim of this contribution is to find a correlation between the electrorheological characteristics of polyvinylbutyral (PVB) solutions and their electrostatic spinnability. When exposed to an external electric field, PVB solutions with either poor or good solvents respond in different ways. It was shown that the complex viscosity ratio η_E^*/η_0^* (where η_E^* and η_0^* represent complex viscosities of a solution in the presence and absence of an external electric field, respectively) can serve as an indicator as to whether a chosen material is a potential candidate for acceptable electrospinning. This occurs when the ratio η_E^*/η_0^* increases with increasing electric field strength, i.e., when poor solvents are applied. The possible changes to the physical and chemical properties of PVB solutions were investigated using SEM, FTIR, DSC, ^{13}C- and ^{1}H-NMR techniques.

© 2014 Elsevier Ltd. All rights reserved.

1. Introduction

The process of electrospinning is based on the application of an electrical charge that enables the withdrawal of micro- or nano-fibres from a polymer solution or melt. The high voltage generated between the tip of the pipette and the grounded collector evokes the creation of Taylor cones at the surface of polymer materials placed at the tip. Charged viscoelastic jets emanate from the Taylor cones. Their passage towards the grounded collector is accompanied by a continuous reduction of their diameter caused by the simultaneous stretching of the (non-bifurcating) jets and the evaporation of the solvent. A detailed description of the electrospinning process (sketched in Fig. 1) is presented, e.g., in monographs and reviews [1–4]. The electrospun fibres are characterized by large values of the ratio relating their surface to their volume. This implies their applicability in various areas such as tissue scaffolds, filtration, nanocomposite materials and protective clothing [3,5,6].

In principle, the parameters contributing to the quality of nanofibrous webs can be divided roughly into four basic groups: polymer properties, solvent properties, polymer solution properties and the process parameters. Viscosity represents one of the crucial parameters characterizing the properties of a polymer solution. This parameter in connection with electrospinning has been intensively studied, e.g., in [7–20] and references therein. Both types of viscosity - elongational and shear - were analysed. Although elongational viscosity dominates in the behaviour of viscoelastic jets, a certain portion of shear viscosity is always present.

The shear viscosity of some materials is subject to the presence or absence of an electric field. This dependence is significantly exhibited by so-called electrorheological materials, for which an increase in shear viscosity under the
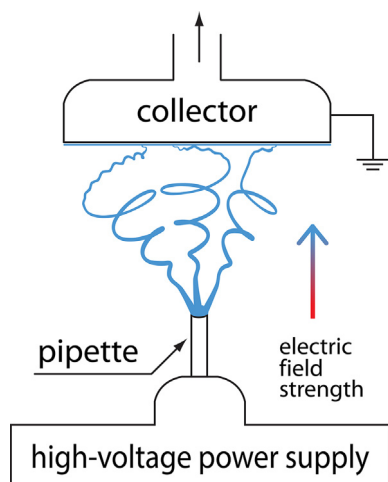
Fig. 1. Sketch of an electrospinning apparatus.

presence of an electric field does not represent mere multiples but several orders. As in the process of electrospinning the viscoelastic jets are exposed to the electric field, attention will be also focused in this direction.

In the following, polyvinylbutyral (PVB) and two pairs of solvents (poor - methanol and ethanol, good - isopropanol and butanol) are taken into account. The applicability and advantages of PVB in the process of electrospinning are summarized in Peer et al. [21]. Unlike good solvents, poor solvents have the potential to contribute to the good electrospinnability of the corresponding PVB solutions. In this case, a combination of the entanglements between chains results in the creation of a physical gel. Presumably these junctions contribute to the stabilization of the viscoelastic jets. Techniques of DSC, FTIR, ^{13}C- and ^{1}H-NMR were applied to the characterization of the possible changes of the physical and chemical properties of PVB materials.

It will be shown that the course of the ratio η_E^*/η_0^* (where η_E^* and η_0^* represent complex viscosities of PVB solutions in the presence and absence of an external electric field, respectively) in dependence on the electric field strength can indicate the suitability of chosen polymer solutions for good electrospinnability. If this ratio is invariant with respect to the electric field strength (PVB in good solvents), then the obtained nanofibrous webs are of poor quality. If this ratio increases with the increase of electric field strength (PVB in poor solvents), then good webs were obtained.

2. Experimental

2.1. Material

Polyvinylbutyral (Mw = 60,000 g/mol; Mowital B 60H, Kuraray Specialities Europe) is a non-toxic, odourless and environmentally friendly polymer. The structure of Mowital B 60H is composed of vinyl butyral, vinyl alcohol and vinyl acetate, in this case 75–81 %, 18–21 % and 1–4 %, respectively. Polyvinylbutyral (PVB) was consecutively dissolved in methanol, ethanol, isopropanol and butanol (quality of p.a., Penta, Czech Republic). For each solvent, the 6, 8, 10, and 12 wt.% solutions (basic characteristics in Table 1) were homogenized using a magnetic stirrer for 72 hours at 250 rpm at 20 °C. The corresponding films were prepared by solution casting on Petri dishes and dried in a fume hood for 5 days at room temperature. During electrorheological (250 V/mm) measurements, the gels were formed in the parallel plate geometry of the rheometer. They were dried in the same way as the films for further investigation. Nanofibrous webs from the PVB solutions were electrospun with the use of a laboratory device (details in Peer et al. [21]) at a voltage of 25 kV and at a distance between the replaceable tip of carbon steel stick (SAE designation 11xx, a diameter 10 mm) and the collector of 10 cm (corresponding to 250 V/mm). The volume of the drop of polymer solution placed onto the stick tip was 0.2 ml. The obtained fibres were analysed using an SEM (Vega 3, Tescan, Czech Republic).

2.2. Characterization of the solutions, gels and nanofibrous webs

The electrorheological measurements were carried out with a Physica MCR 501 rotational rheometer (Anton Paar, Austria) equipped with an electrorheological cell C-PTD200/E (parallel plate arrangement, diameter of plates 50 mm, gap 0.5 mm). The polymer solutions were measured in both steady and oscillatory shear modes in the absence and presence of an external electric field generated by a N5752A DC power supply (Agilent, USA) with the limits 600 V and 1.3 A. The temperature was kept constant at 20 °C during all experiments.

The PVB electrospun nanofibrous webs, films and gels were examined for changes in their functional groups using a Nicolet 6700 (USA) infrared spectrophotometer in ATR mode (attenuated total reflection) with a ZnSe crystal. The webs were scanned from 4,000 to 650 cm^{-1}.

Table 1
Basic characteristics of the solvents and PVB.

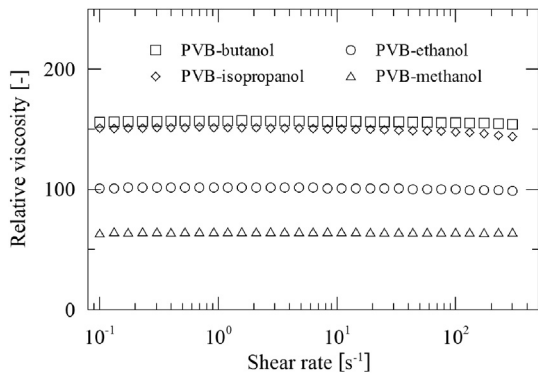|	Relative permittivity [-]	Specific conductivity [S/m]	Surface tension [mN/m]	Density [g/cm^3]	Hansen solubility parameters [MPa$^{1/2}$]		
					δ_D	δ_P	δ_H
Methanol	32.7	$1.5*10^{-7}$	22.12	0.789	15.1	12.3	22.3
Ethanol	24.5	$1.35*10^{-7}$	21.90	0.785	15.8	8.8	19.3
Isopropanol	19.9	$58*10^{-7}$	21.38	0.781	16.0	6.8	17.4
Butanol	17.5	$9.12*10^{-7}$	24.50	0.806	16.0	5.7	15.8
PVB	3.60	$1*10^{-9}$	–	1.090	18.6	4.4	13.0

Fig. 2. Relative viscosity in dependence on shear rate for 10 wt.% PVB solutions.

To measure the glass transition temperature of PVB films and gels, a DSC 1 Mettler Toledo (Switzerland) differential scanning calorimeter was used. The glass transition was determined at a 20 K min^{-1} heating rate over a temperature range of $0 - 250$ °C in an inert nitrogen atmosphere.

Solid-state NMR spectra were measured at 11.7 T using a Bruker Avance III HD 500 US/WB NMR spectrometer (Germany). The following techniques were applied: i) one-dimensional (1D) ^{1}H MAS and ^{13}C CP/MAS NMR experiments and; ii) Torchia's $T_1(^{13}$C) relaxation experiment [22] with a variable delay from 0.1 to 40 s. The spinning frequency was 11 kHz, and the frictional heating of the spinning samples was compensated by active cooling (temperature calibrations were performed with Pb(NO$_3$)$_2$) [23].

3. Results

In general, the rheological behaviour of a solution is subject to polymer chain conformation depending on the quality of the applied solvent. Differences in solution behaviour are reflected by the Hansen solubility parameters [24]: dispersion bonds (δ_D), polar bonds (δ_P) and hydrogen bonds (δ_H) between molecules. Table 1 lists the Hansen solubility parameter values for PVB and the chosen
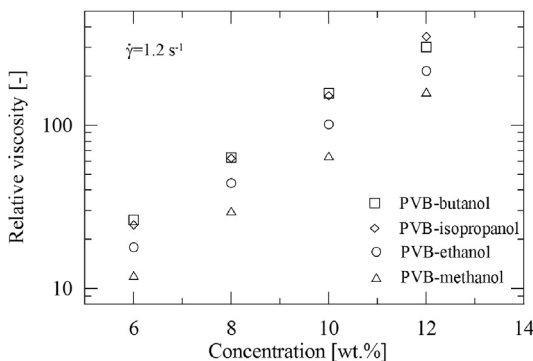
Fig. 3. Relative viscosity in dependence on concentration (the values correspond to the measurements at 1.2 s^{-1}) for all PVB solutions.
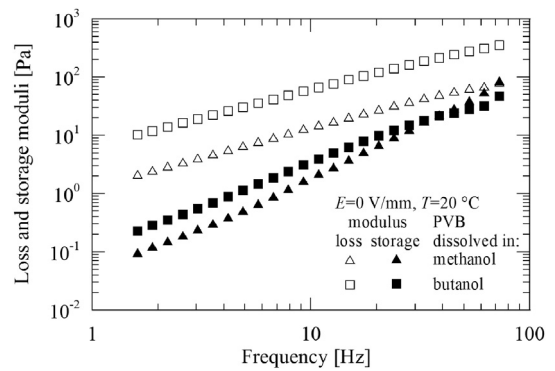
Fig. 4. Loss (open) and storage (solid) moduli in dependence on frequency for 12 wt.% PVB solutions in the absence of an electric field.
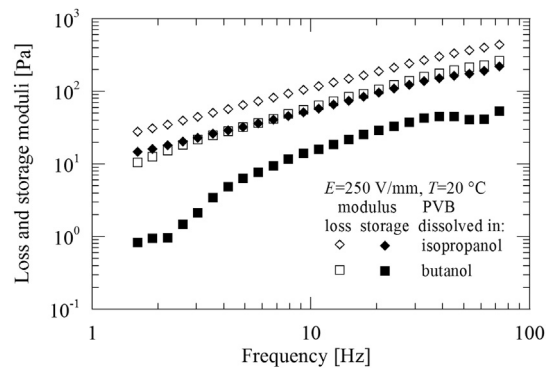
Fig. 5. Loss (open) and storage (solid) moduli in dependence on frequency for 12 wt.% PVB solutions with the good solvents in the presence of an electric field ($E = 250$ V/mm).

solvents. The closer solubility parameters between polymer and solvent represent better miscibility resulting in a larger expansion of the polymer.

Steady shear viscosity was measured for all four PVB solutions, each in 6, 8, 10, and 12 wt.% concentrations. Fig. 2 depicts the measurements for a 10 wt.% concentration where the relative viscosity is expressed as a ratio of the
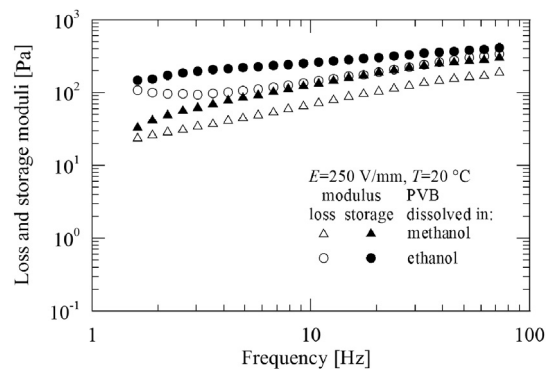

Fig. 6. Loss (open) and storage (solid) moduli in dependence on frequency for 12 wt.% PVB solutions with the poor solvents in the presence of an electric field ($E = 250$ V/mm).
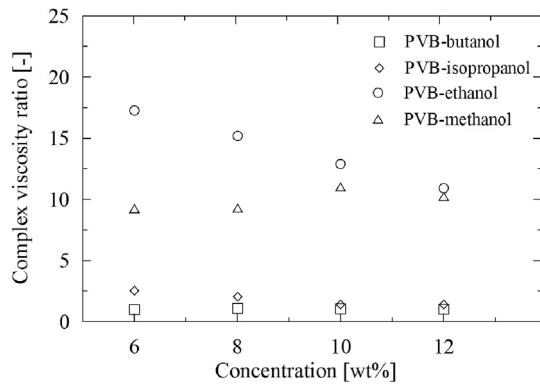
Fig. 7. Complex viscosity ratio as a function of concentration for all PVB solutions.

solution and solvent viscosities. In all cases, the Newtonian character of the individual solutions was observed. This is illustrated in Fig. 3 where the otherwise constant courses of relative viscosities in dependence on shear rate are represented by the respective values at 1.2 s^{-1}. PVB dissolved in the good solvents (butanol, isopropanol) exhibits higher relative viscosities than the PVB solutions with the poor solvents (methanol, ethanol). This means that the PVB chains in methanol and ethanol prefer interactions between segments, and the coils are in the contracted conformations.

The PVB solutions were also examined in oscillatory shear mode to investigate their viscoelastic properties. The viscoelastic characteristics again exhibit higher values for PVB dissolved in the good solvents in comparison with the
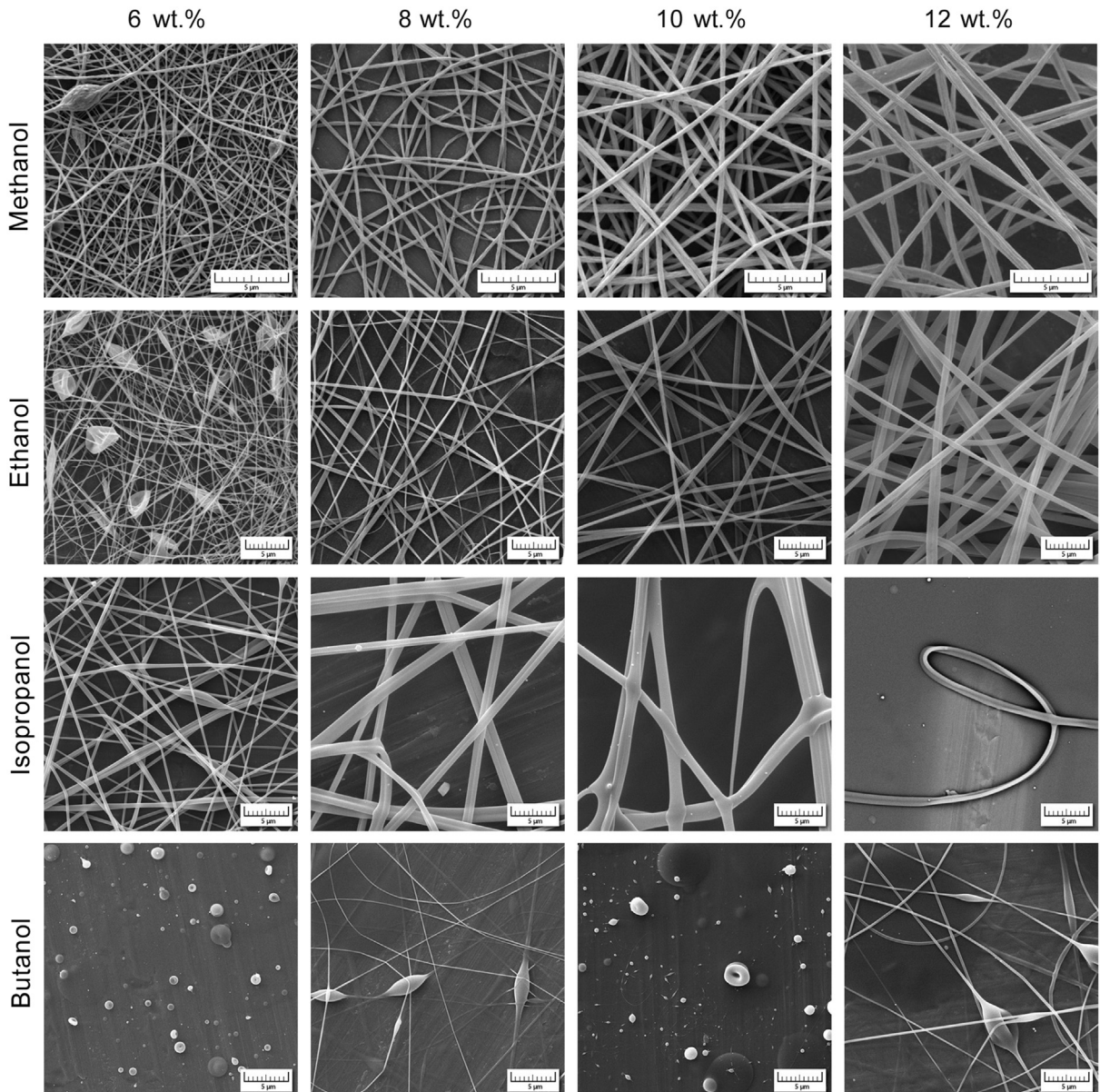
Fig. 8. SEM images of nanofibrous webs electrospun from PVB dissolved in all solvents.

poor solvents, as demonstrated for butanol and methanol in Fig. 4. The dominance of the loss modulus over the storage modulus throughout the frequency range confirms the rather viscous nature of the solutions given by the looser movement of macromolecules.

The preceding experimental data were obtained when no electric field was applied. Qualitatively similar results were obtained in the presence of an electric field; see Figs. 5 and 6. The value for the electric field strength (125 V/0.5 mm, 0.5 mm represents a gap in the parallel plate arrangement in the rotational rheometer) was chosen in such a way that it corresponded to that applied in the electrospinning process (25 kV/10 cm, 10 cm represents a tip-to-collector distance). Due to the external electric field application, the values of the storage modulus significantly increased, particularly for PVB dissolved in the poor solvents (methanol, ethanol), and simultaneously exceeded the values of the loss modulus. In these systems, the presence of the electric field caused the formation of a three-dimensional elastic gel. The poor solvents promote polymer chain intra- and inter-molecular interactions. The chain links may occur due to the formation of hydrogen bonds and chain entanglement.

For each solution, oscillatory experiments were carried out relating the complex viscosity ratio η_E^*/η_0^* to all concentrations (6, 8, 10, and 12 wt.%), where η_E^* and η_0^* represent the complex viscosities of a solution in the presence and absence of an electric field, respectively. Fig. 7 illustrates the behaviour of the complex viscosity ratio at a frequency 10.83 Hz and a constant strain of 1 %. The solutions with the good solvents exhibit no increase in complex
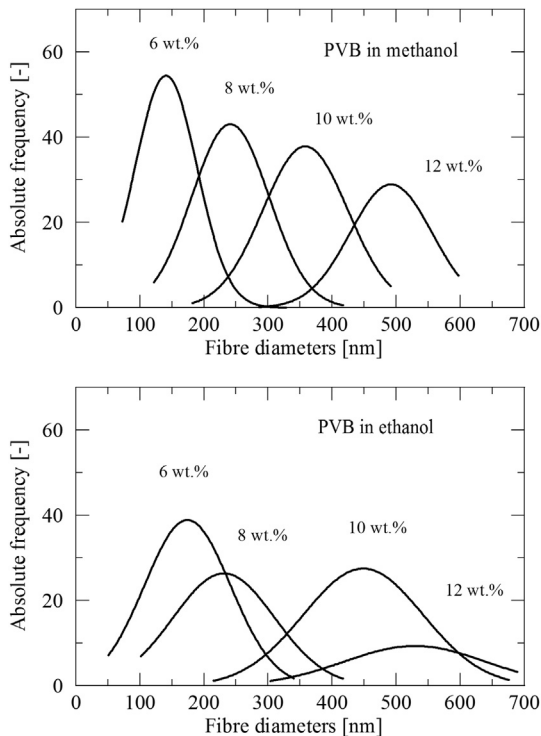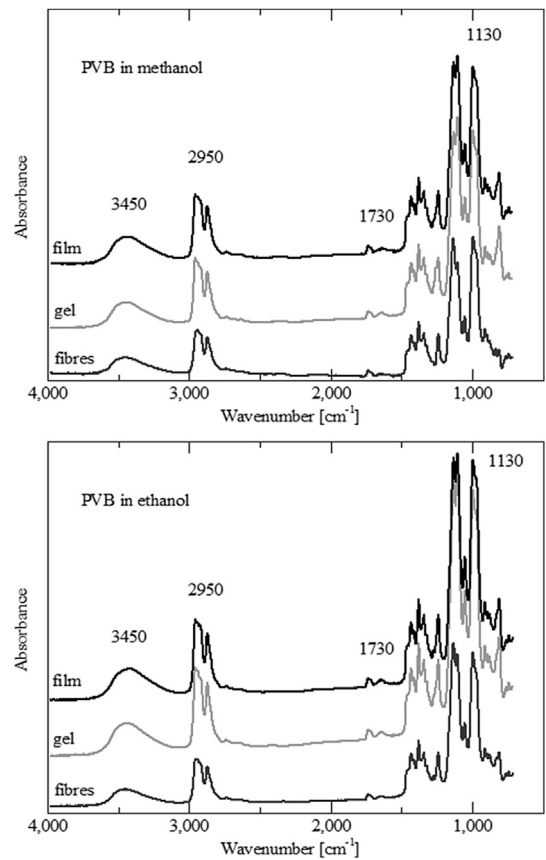
Fig. 10. Infra-red ATR spectra of PVB nanofibres, gel and film created from PVB dissolved in methanol and ethanol.

viscosity in the presence of the electric field, in contrast to the striking enhancement for the poor solvents. The course of the complex viscosity ratio for the PVB-ethanol solution linearly decreases within the concentration range studied. In comparison, the PVB-methanol solution exhibits nearly constant behaviour.

The nanofibrous mats were prepared by the process of electrospinning, and their quality was evaluated using SEM analysis, see Fig. 8. The quality of nanofibres significantly deteriorates if the good solvents are used. Higher quality is achieved with poor solvents. Their solutions achieve higher elasticity (as documented in Figs. 5 and 6) in the presence of the electric field, which contributes to their better electrospinnability. Geometrical characteristics are presented in Fig. 9.

Fig. 9. The histograms of fibre diameters in dependence on concentration.

Table 2
The glass transition temperature (T_g) of the PVB in various forms (film, gel).

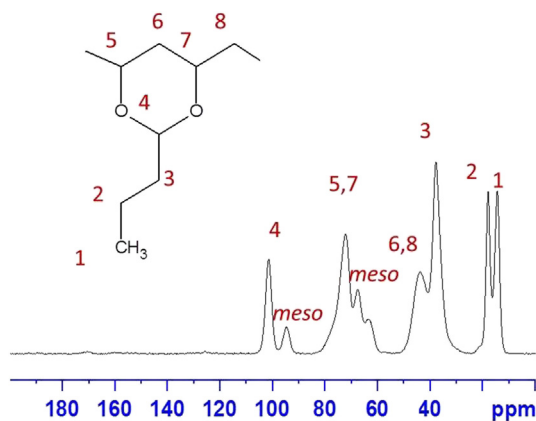| T_g [°C]	Film	Gel
PVB — Methanol	70	60
PVB — Ethanol	69	59
PVB — Butanol	68	70
PVB — Isopropanol	70	69

Fig. 11. ^{13}C CP/MAS NMR spectrum of PVB-ethanol gel with signal assignment.

4. Discussion

A comparison of the chemical and physical properties of three PVB forms (nanofibres, gels, and films) was consecutively carried out.

Possible changes in chemical structure were analysed by FTIR. The infra-red ATR spectra of PVB as nanofibrous web, dried gel and film are plotted in Fig. 10. They are all similar, and no significant changes were observed in the broad band corresponding to the −OH group at 3450 cm^{-1}, together with the stretching modes of C-H in the range 2000−3000 cm^{-1}. The C=O absorption band appearing at 1730 cm^{-1} and C-O-C group band at 1130 cm^{-1} were not altered either. The intensity of the main bonds in different forms of PVB slightly changes. Thus, a comparison of the corresponding peaks showed that there is no significant difference in chemical structure between the PVB nanofibres, gel or film created from all solvents.

One way to analyse thermodynamic properties is through DSC measurements. The glass transition temperature (T_g) is structure sensitive due to steric effects and a formation's intra- or inter-molecular interaction, and it can indicate change in the structure of a polymer chain and also crosslinking. In general, decreasing of T_g means a scission of the polymer chains and increasing leads to the crosslinking of the polymer [25]. The glass transition temperature T_g of PVB in bulk is 63 °C, and dissolving in all solvents increases this value by 5−7 °C; see Table 2. However, the T_g of the gel created in the presence of an electric field is lower by 3−4 °C for poor solvents and higher by 6−7 °C for good solvents when compared with the T_g for PVB in bulk. In the case of films (made in the absence of an electric field), the role of the solvent seems to be negligible.

The last method which was used to reveal the cross-linking or scission of polymer chains is NMR. From the intensities of signals in ^{13}C CP/MAS NMR spectra (Fig. 11), it is clear that the racemic isomer (signals at 73 and 102 ppm) of PVB dominates over the meso isomer (signals at 67 and 95 ppm) in the investigated samples [26]. No differences in signal intensities and resonance frequencies between the analysed samples were found.

To probe local segmental dynamics of PVB systems (PVB-ethanol film and gel), ^{13}C spin-lattice relaxation times $T_1(^{13}$C) were measured. The obtained relaxation times summarized in Table 3 are systematically reduced for the PVB gel. Generally, in solid state the shorter $T_1(^{13}$C) relaxation times indicate released segmental motions. This might suggest increased segmental dynamics in the PVB gel. This finding is in accordance with the DSC measurements that revealed considerably reduced glass transition temperature T_g for the PVB gel if poor solvents are applied. Both these results suggest some decomposition processes reducing the length (molecular weight) of PVB macromolecules in the gel.

As demonstrated in the preceding experimental techniques, the most striking difference between the behaviour of PVB solutions using poor and good solvents is in the dominance of storage modulus over loss modulus in the electric field when poor solvents are used. According to Yu et al. [27], the elastic forces resist the bending of the jet and hinder a jet from breaking up. This confirms that the course (increasing vs. constant) of the complex viscosity ratio indicates the suitability of polymer solutions for the process of electrospinning. Further, Shenoy et al. [28] analysed polymer solutions capable of physical gelation. They found that polymer solutions close to the gelation threshold exhibit a stabilization of the viscoelastic jets, which contributes to the better formation of nanofibrous mats.

5. Conclusions

The electrospinning process is affected by a number of the entry parameters. This contribution focused on the impact of an external electric field on the rheological properties of the polymer solutions. It was shown that an increase in the complex viscosity ratio η_E^*/η_0^* (where η_E^* and η_0^* represent complex viscosities of a solution in the presence and absence of an external electric field, respectively) correlates with good electrospinnability of PVB solutions. This increase is observed for poor solvents, while the complex viscosity ratio is constant for good solvents, for which the quality of nanofibrous web is unacceptable.

Table 3
^{13}C spin-lattice relaxation times $T_1(^{13}$C) of individual structure units measured for the PVB-ethanol film and gel.

Sample	$T_1(^{13}$C) [s]							
	4 (Racem)	4 (Meso)	5,7 (Racem)	5,7 (Meso)	6,8	3	2	1
Film	12.8	16.9	19.8	15.8	12.8	6.7	1.1	1.3
Gel	11.4	12.1	16.8	14.6	10.7	6.1	1.1	1.3

References

[1] S. Ramakrishna, K. Fujihara, W.E. Teo, T.C. Lim, Z. Ma, An Introduction to Electrospinning and Nanofibres, World Scientific Publishing Co, 2005.
[2] A.L. Andrady, Science and Technology of Polymer Nanofibers, John Wiley & Sons, 2008.
[3] Z.M. Huang, Y.Z. Zhang, M. Kotaki, S. Ramakrishna, A review on polymer nanofibers by electrospinning and their applications in nanocomposites, Comp. Sci. Tech. 63 (2003) 2223.
[4] D.H. Reneker, A.L. Yarin, Electrospinning jets and polymer nanofibers, Polymer 49 (2008) 2387.
[5] J. Doshi, D.H. Reneker, Electrospinning process and applications of electrospun fibers, J. Electrostat. 35 (1995) 151.
[6] P. Gibson, H. Schreuder-Gibson, D. Rivin, Transport properties of porous membranes based on electrospun nanofibers, Colloids Surf. A: Physicochem. Eng. Aspects 187–188 (2001) 469.
[7] D.W. Chae, M.H. Kim, B.C. Kim, Temperature dependence of the rheological properties of poly(vinylidene fluoride)/dimethyl acetamide solutions and their electrospinning, Korea-Australia Rheol. J. 22 (2010) 229.
[8] J. Dong, A.D. Asandei, R.S. Parnas, Aqueous electrospinning of wheat gluten fibers with thiolated additives, Polymer 51 (2010) 3164.
[9] S.T. Hemp, M.T. Hunley, S. Cheng, K.C. DeMella, T.E. Long, Synthesis and solution rheology of adenine-containing polyelectrolytes for electrospinning, Polymer 53 (2012) 1437.
[10] M.G. McKee, C.L. Elkins, T.E. Long, Influence of self-complementary hydrogen bonding on solution rheology/electrospinning relationships, Polymer 45 (2004) 8705.
[11] J. Pelipenko, J. Kristl, R. Rosic, S. Baumgartner, P. Kocbek, Interfacial rheology: an overview of measuring techniques and its role in dispersions and electrospinning, Acta Pharm. 62 (2012) 123.
[12] O. Regev, S. Vandebril, E. Zussman, C. Clasen, The role of interfacial viscoelasticity in the stabilization of an electrospun jet, Polymer 51 (2010) 2611.
[13] R. Rosic, J. Pelipenko, P. Kocbek, S. Baumgartner, M. Bester-Rogac, J. Kristl, The role of rheology of polymer solutions in predicting nanofiber formation by electrospinning, Europ. Polym. J. 48 (2012) 1374.
[14] R. Rosic, J. Pelipenko, J. Kristl, P. Kocbek, M. Bester-Rogac, S. Baumgartner, Physical characteristics of poly (vinyl alcohol) solutions in relation to electrospun nanofiber formation, Europ. Polym. J. 49 (2013) 290.
[15] S.P. Rwei, C.C. Huang, Electrospinning PVA solution-rheology and morphology analyses, Fiber. Polym. 13 (2012) 44.
[16] K.M. Schultz, L. Campo-Deano, A.D. Baldwin, K.L. Kiick, C. Clasen, E.M. Furst, Electrospinning covalently cross-linking biocompatible hydrogelators, Polymer 54 (2013) 363.
[17] S.K. Tiwari, S.S. Venkatraman, Importance of viscosity parameters in electrospinning: of monolithic and core-shell fibers, Mater. Sci. Eng. C 32 (2012) 1037.
[18] S.Y. Tsou, H.S. Lin, P.J. Cheng, C.L. Huang, J.Y. Wu, C. Wang, Rheological aspect on electrospinning of polyamide 6 solutions, Europ. Polym. J. 49 (2013) 3619.
[19] C. Wang, J.-H. Jheng, F.-C. Chiu, Electrospun nylon-4,6 nanofibers: solution rheology and Brill transition, Colloid. Polym. Sci. 291 (2013) 23374.
[20] J. Zhao, A. Xu, W.Z. Yuan, J. Gao, J. Tang, L. Wang, F. Ai, Y. Zhang, Evaluation of electrospun nanofiber formation of perfluorosulfonic acid and poly (N-vinylpyrrolidone) through solution rheology, J. Mater. Sci. 46 (2011) 7501.
[21] P. Peer, M. Stenicka, V. Pavlinek, P. Filip, The storage stability of polyvinylbutyral solutions from an electrospinnability standpoint, Polym. Degrad. Stabil. 105 (2014) 134.
[22] D.A. Torchia, Measurement of proton-enhanced C-13 T1 values by a method which suppresses artifacts, J. Magn. Reson. 30 (1978) 613.
[23] J. Brus, Heating of samples induced by fast magic-angle spinning, Solid State Nucl. Magn. Reson. 16 (2000) 151.
[24] C.M. Hansen, Hansen Solubility Parameters: A User's Handbook, second ed., CRC Press, Taylor & Francis Group, USA, 2007.
[25] G.W. Ehreinstein, G. Riedel, P. Trawie, Thermal Analysis of Plastics, Theory and Practice, Hanser Gardner Publications, Germany, 2004.
[26] H. Namgoong, J.-S. Kim, O.H. Han, ^{13}C solid state NMR Study on the dynamics of the poly(vinyl butylal) with various water contents, J. Kor. Magn. Reson. Soc. 6 (2002) 11.
[27] J.H. Yu, S.V. Fridrikh, G.C. Rutledge, The role of elasticity in the formation of electrospun fibers, Polymer 47 (2006) 4789.
[28] S.L. Shenoy, W.D. Bates, H.L. Frisch, G.E. Wnek, Role of chain entanglements on fiber formation during electrospinning of polymer solutions: good solvent, non-specific polymer-polymer interaction limit, Polymer 46 (2005) 3372.
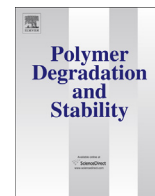
The storage stability of polyvinylbutyral solutions from an electrospinnability standpoint

Petra Peer [a],*, Martin Stenicka [b], Vladimir Pavlinek [b], Petr Filip [a]

[a] Institute of Hydrodynamics, Academy of Sciences of The Czech Republic, Pod Patankou 5, 166 12 Prague 6, Czech Republic
[b] Centre of Polymer Systems, University Institute, Tomas Bata University in Zlin, Nad Ovcirnou 3685, 760 01 Zlin, Czech Republic

A B S T R A C T

The quality of electrospun fibres is subject to many factors ranging from the characteristics of the materials used to processing conditions. Although an important parameter for applicability, less attention has been paid to the storage stability of applied polymer solutions and its impact on the quality of electrospun webs. The aim of this study is to analyse the storage stability of polyvinylbutyral solutions in methanol and ethanol for the formation of undisturbed nanofibres. The quality of nanofibrous mats produced over a period of 197 days, during which the solutions were stored under constant conditions, was investigated. Using rheological measurements, SEM, FTIR, and DSC techniques, it was shown that the storage period for the solutions used had almost no influence on the quality of electrospun fibres, which is a positive result for practical use.

© 2014 Elsevier Ltd. All rights reserved.

1. Introduction

The quality of nanofibrous webs created by an electrospinning process plays a crucial role for their application in various fields such as filters, nanocomposite materials, membranes, and in medical areas [1–5]. In the electrospinning process, single jets are ejected from the apices of Taylor cones created at the surface of a drop of polymer solution (Fig. 1). Jet forming is initialised by an electric field generated by a high-voltage power supply between the tip of the stick where the drop is stored and the grounded collector. In principle, the charged polymer jets are, during their passage from the tip onto the collector, simultaneously exposed to two basic factors reducing their diameters: high extension rate, the magnitude of which should not result in a jet disruption, and the rate of solvent evaporation optimally corresponding to the situation in which the solvent is completely evaporated at the moment of reaching the collector.

Polyvinylbutyral (PVB) is a useful material in the electrospinning process. PVB is frequently added to increase the spinnability of the prepared solutions. This procedure was applied to the production of boron nitride nanofibres [6]. Mullite nanofibres were obtained through an optimal dosage of PVB [7]. PVB was used as a spinnable carrier for manufacturing luminescent ceramic fibres [8]. Mesoporous silica nanofibres were prepared with the assistance of PVB during the process of electrospinning [9]. Composite nanofibres were fabricated from PVB/silica [10] as well as multiwalled carbon nanotube/PVB [11]. The addition of PVB proved crucial in the preparation of bead-free resol fabrics [12] as well as in the production of composite fibres containing yttrium and cerium [13,14]. Using a PVB/inorganic salt solution, it is also possible to prepare well-aligned and highly-ordered nanofibrous architecture [15]. PVB in combination with polyaniline and polyethylene oxide was used in the construction of humidity sensors [16,17]. However, in this case the formation of beads in nanofibres was beneficial, as it enabled good adhesion to the electrode.

Polyvinylbutyral also plays an important role if used separately. For example, it is possible to introduce interlayers connecting glass plies in laminated glass. The properties of the interlayers were improved by using electrospun nanofibres composed of PVB and carbon nanotubes [18]. Recently, pure commercial polyvinylbutyrals were also analysed [19]. Analyses of electrospinning processes, when only pure PVB (+solvents) was used, are discussed, e.g., in Refs. [20–24].

Practically all studies on electrospinning have focused on four basic groups of factors participating in the creation and affecting the quality of nanofibrous webs. These include the polymer (molecular weight, molecular weight distribution, topology of macromolecules), solvent (surface tension, solubility parameters, relative

---

* Corresponding author. Tel.: +420 233109029; fax: +420 233324361.
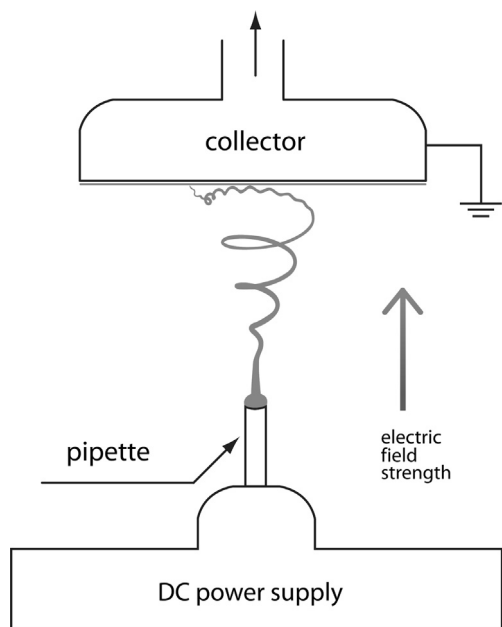E-mail address: peer@ih.cas.cz (P. Peer).

Fig. 1. Schematic sketch of an electrospinning apparatus.

Table 1
Characteristics of PVB and solvents used.

Property		PVB	Ethanol	Methanol
Relative permittivity		3.6	24.5	32.7
Specific conductivity [S/m]		1.0×10^{-9}	1.4×10^{-7}	1.5×10^{-7}
Surface tension [mN/m]		–	21.9	22.1
Density [kg/m^3]		1090	785	789
HSP [MPa$^{1/2}$]	δ_D	18.6	15.8	15.1
	δ_P	4.4	8.8	12.3
	δ_H	13.0	19.3	22.3

permittivity), solution (viscosity, concentration, specific conductivity), and process parameters (electric field strength, tip-to-collector distance, temperature, humidity).

As far as the authors are aware and in spite of the fact that PVB exhibits various forms of degradability, no attention has been paid to the possible time degradation of the polymer solutions in connection with the corresponding quality of electrospun nanofibres [25–31]. The aim of this study is to analyse and qualitatively compare nanofibrous mats prepared by electrospinning from PVB solutions with methanol and ethanol within a period of almost 7 months, simulating the durability of these solutions in practical applications. During this time, the PVB solutions were kept under constant storage conditions. Methanol and ethanol, although poor solvents of PVB, contribute to higher quality of the electrospun nanofibres in comparison to a situation when good solvents are used, e.g. [21].

2. Experimental

For a qualitative comparison of the solutions of PVB in methanol and ethanol and corresponding nanofibrous mats over a period of almost 7 months (1, 8, 15, 29, 57, 87, 113, 141, 169, and 197 days), the following characterisation techniques were used: conductivity and rheological measurements, a scanning electron microscopic (SEM) analysis of electrospun nanofibres, infra-red spectroscopy, and differential scanning calorimetry (DSC) measurements.

2.1. Materials

Polyvinylbutyral (Mw = 60,000 g/mol; Mowital B 60H, Kuraray Specialities Europe) was dissolved in methanol and ethanol (quality of p.a., Penta, Czech Republic) at 10 wt.% concentration. The structure of Mowital B 60H is composed of vinyl butyral, vinyl alcohol and vinyl acetate, in this case 75–81, 18–21 and 1–4%, respectively. Basic characteristics of the entry components are summarised in Table 1, including the Hansen solubility parameters (HSP). To homogenise both solutions, a magnetic stirrer was used at 150 rpm at 20 °C over 5 days. Afterwards, the solutions were poured into flasks, which were placed into a tempered dark box (20 °C) and taken out just before each measurement.

A choice of 10 wt.% concentration was based on the trend relating concentration vs. quality of electrospun nanofibres. For 6 wt.% concentration, the electrospun webs exhibit a quantity of non-fibrous formations (beads, etc. – their appearance attained approximately 90 pcs/50 × 50 square micrometres) for both polymer solutions (PVB in methanol and PVB in ethanol). These imperfections disappear with an increasing concentration. The quality of webs corresponding to 10 wt.% concentration is very good as documented in the next section.

2.2. Conductivity measurements

The conductivity of both solutions (Table 2) was measured using a Conductivity Meter Lab 960 (SCHOTT Instruments, Germany) before each rheological measurement. As the maximal experimental deviation of the device used is approximately 0.5%, the deviation of conductivity for both solutions was approximately 1% during the whole testing period.

2.3. Rheological measurements

The rheological measurements, carried out with a Bohlin Gemini rotational rheometer (Malvern, U.K.) equipped with a bob and cup (25 mm and 27.4 mm in diameter) arrangement, included both steady shear and oscillatory modes. The temperature was kept constant at 20 °C during all experiments.

2.4. Electrospinning

The prepared PVB solutions were electrospun using a proposed laboratory device (see Fig. 2) at a voltage of 25 kV with a tip-to-collector distance of 100 mm. The laboratory device is assembled with the materials exhibiting very low conductivity to ensure that an electric field is not affected by the device itself. The basic construction is formed by aluminium rods, the lower (1 × 1.16 m) and upper (0.5 × 1.16 m) mm thick tables are made of fibre-glass reinforced thermoset polyester material Glastic UTR (Röchling Glastic Composites, USA; insulation resistance 3.1×10^{12} Ohm) as well as the nuts and bolts fixing a draw with a collector to the upper plate. The pieces forming the draw are only glued. A distance between a replaceable tip of carbon steel stick (SAE designation 11xx, a diameter 10 mm) and the collector is handled manually with a linear guidance preserving perpendicularity between a stick axis

Table 2
Conductivity of prepared PVB solutions.

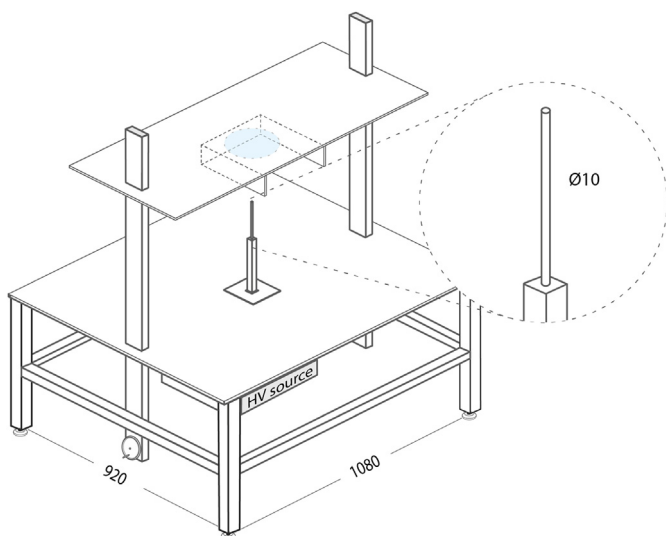| Time [days]	Conductivity PVB-ethanol [mS/m]	Conductivity PVB-methanol [mS/m]	Temperature [°C]
1	1.26	3.62	21.7
113	1.29	3.64	22.9
197	1.28	3.60	23.0

Fig. 2. Schematic sketch of the proposed electrospinning device.

and the upper plate. A volume of the drop of polymer solution placed into the stick tip was 0.2 ml. An electric field was generated by a high-voltage power supply Spellman SL70PN150 (Spellman, USA). The obtained fibres were analysed using the SEM technique (Vega 3, Tescan, Czech Republic).

2.5. Infra-red spectroscopy measurements

The PVB electrospun nanofibrous webs were examined for any changes in their functional groups using a Nicolet iS50 FTIR spectrometer in the ATR mode (attenuated total reflection) with a ZnSe crystal. The nanofibrous webs were scanned from 4000 to 650 cm^{-1}.

2.6. DSC measurements

A Mettler Toledo DSC-4 differential scanning calorimeter was used to measure the glass transition temperature of the PVB nanofibrous webs. The glass transition was determined at a 20 K min^{-1} heating rate over a temperature range of 0–250 °C under nitrogen atmosphere.

3. Results and discussion

The development of measured characteristics over the 197-day period as documented by the measurements obtained with the
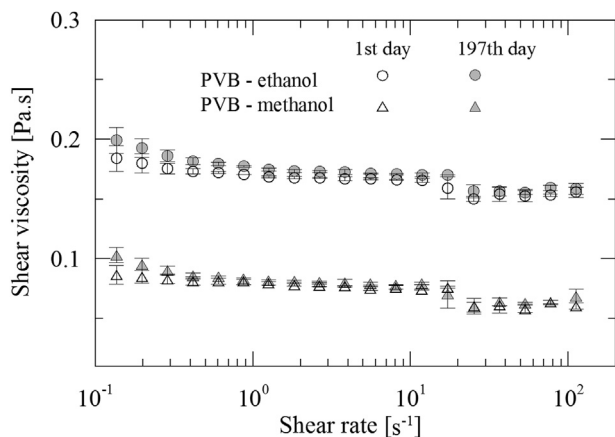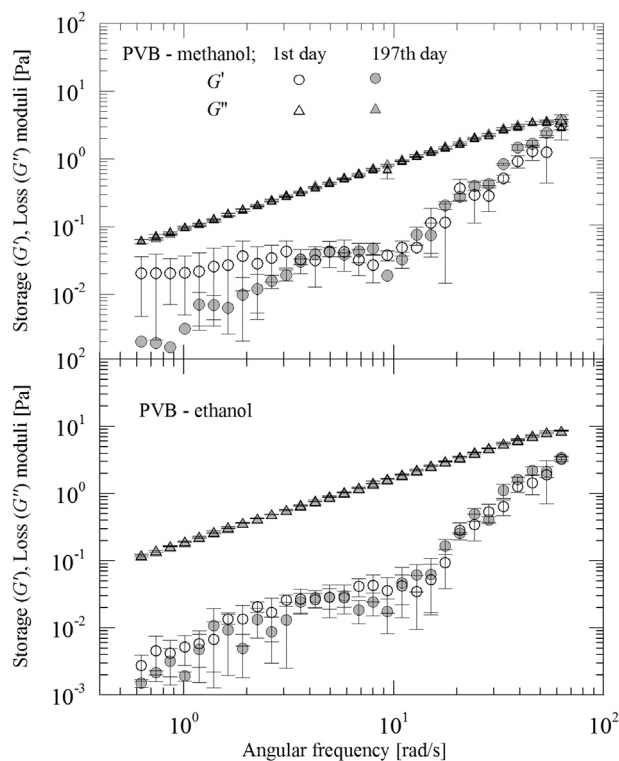
Fig. 4. Storage and loss moduli in dependence on angular frequency.

above introduced characterisation methods is consecutively presented.

The rheological behaviour of both solutions is subject to a polymer chain conformation reflecting a mutual relationship between PVB and the individual solvents that is characterised by the Hansen solubility parameters [32]: dispersion bonds (δ_D), polar bonds (δ_P), and hydrogen bonds (δ_H) between molecules, see Table 1. Closer solubility parameters between PVB and the solvent imply better miscibility.

3.1. Steady shear properties

Fig. 3 presents the dependence of the shear viscosity of PVB solutions on shear rate. Both PVB solutions exhibit nearly Newtonian behaviour. As indicated by the Hansen solubility parameters
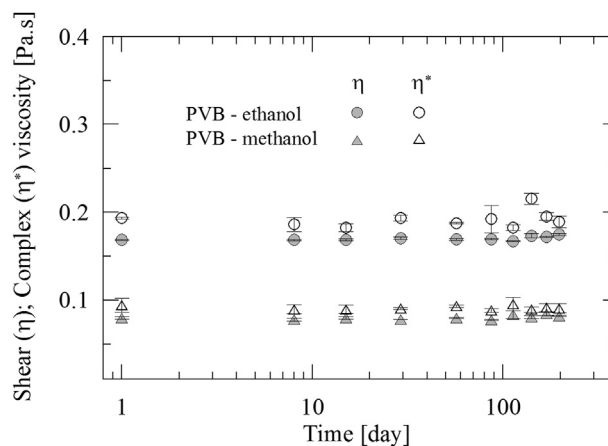

Fig. 3. Shear viscosity of PVB solutions.

Fig. 5. Shear viscosity (at shear rate 1.26 s^{-1}) and complex viscosity (at angular frequency 1.18 rad/s) in dependence on elapsed days.
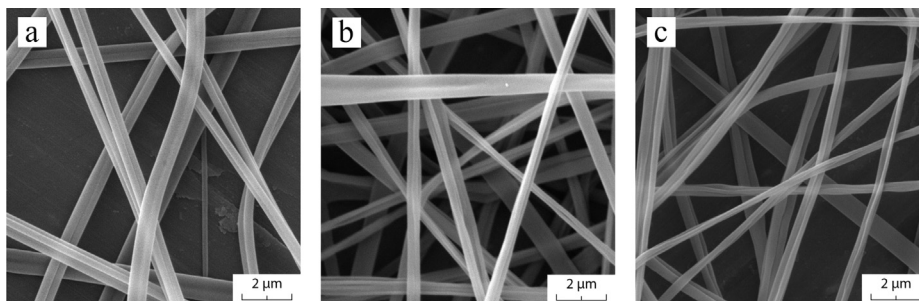
Fig. 6. SEM images of nanofibrous webs, PVB in ethanol a) 1st day; b) 113th day; c) 197 day-old solution samples.
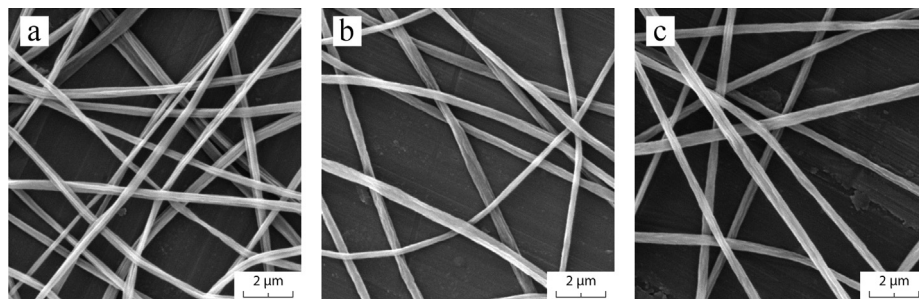

Fig. 7. SEM images of nanofibrous webs, PVB in methanol a) 1st day; b) 113th day; c) 197 day-old solution samples.
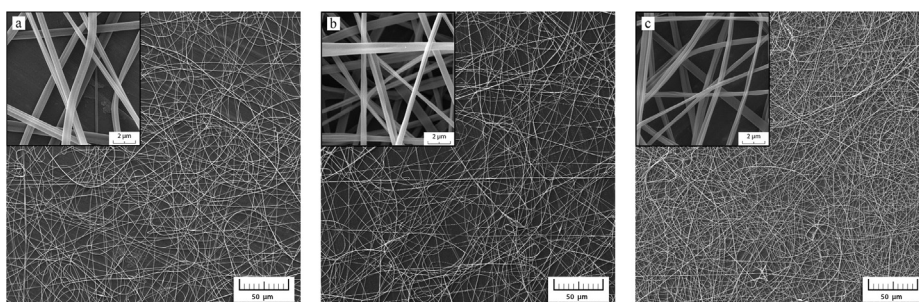

Fig. 8. SEM images (larger area) of nanofibrous webs (PVB in ethanol) electrospun from: a) 1 day-; b) 113 day-; c) 197 day-old solution samples.

(Table 1), PVB-ethanol attains a higher viscosity due to the better solubility of PVB in ethanol than in methanol. All the measurements taken in between the two limiting time cases (1st day and 197th day) attain more or less identical values showing the long term stability of solution properties under storage conditions. For simplicity and clarity, only data corresponding to those two limiting time cases (and occasionally to the 113th day) are graphically presented in the following.

3.2. Oscillatory flow

PVB solutions were also tested in oscillatory mode. As in the case of the steady shear measurements, the oscillatory characteristics exhibit identical behaviour through the whole time period (Fig. 4). The dominance of the loss modulus over the storage one in the frequency range confirms the rather viscous nature of the solutions given by the free movement of macromolecules.
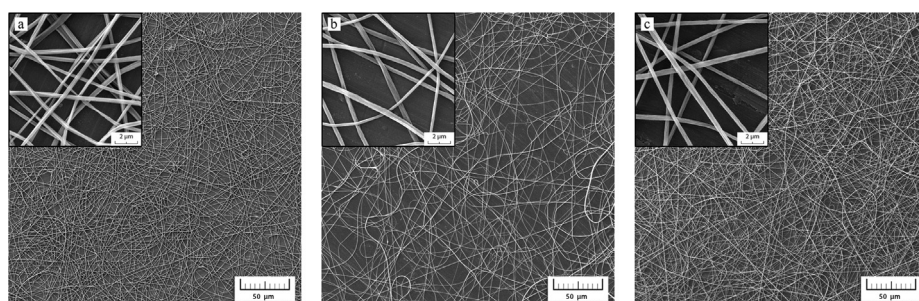

Fig. 9. SEM images (larger area) of nanofibrous webs (PVB in methanol) electrospun from: a) 1 day-; b) 113 day-; c) 197 day-old solution samples.

Obviously, no dramatic changes in the viscoelastic behaviour were identified for the whole monitoring period. Neither of the solvents has a negative influence on polymer chains; in addition, the lower affinity of the solvents does not result in phase separation over time. Both shear and complex viscosities exhibit near constant values at the corresponding shear rate or angular frequency (Fig. 5), which proves the long term stability of the solutions.

3.3. SEM analysis of fibres

Both PVB solutions are suitable for electrostatic spinning [21]. The quality of electrospun fibres was evaluated by SEM analysis (Figs. 6–9). More complex pictures (Figs. 8 and 9) document almost beadless formation of electrospun webs. The electrospun fibres were arranged on the sheets in a circular shape (diameter of 13 cm) in a relatively homogeneous and thick layer.

Due to lower viscosity, the fibres electrospun from PVB-methanol are slightly smaller in diameter than those spun from PVB-ethanol (Fig. 10). In the initial days, the fibre diameters of both samples seem to be more uniform compared to the situation after 60 days of storage. However, on average the diameters did not vary significantly.

Ambient parameters during the electrospinning process such as relative humidity and temperature can significantly influence fibre diameter. A higher temperature causes a decrease in viscosity resulting in a reduction of the mean fibre diameter [33]. With an increase of relative humidity, the evaporation of the solvent decelerates which also leads to a reduction of mean fibre diameter [34–36]. Based on this fact, slight fluctuations in mean fibre diameters without any noticeable impact on their quality can be observed (Fig. 11).

3.4. FTIR analysis of nanofibrous webs

The infra-red spectra of PVB nanofibrous webs in time dependence are presented in Fig. 12. The infra-red spectra of both fresh nanofibrous webs show very similar behaviour generated by the presence of a broad band corresponding to the −OH group at 3450 cm^{-1}, together with the C−H stretching bond at 2950 cm^{-1}. The C=O bond appears at 1730 cm^{-1} and C−O−C group at 1130 cm^{-1}. The intensity of the main bonds increases for PVB nanofibrous electrospun from older solutions. Nevertheless, a comparison of the different peaks showed no significant change in the functional groups among the PVB nanofibres created from both solutions.

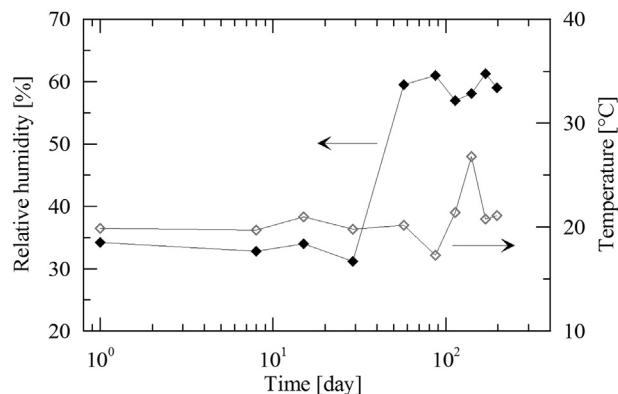The glass transition temperature (T_g) is extremely structure-sensitive due to steric effects and the formation of intra- and inter-molecular interactions. The structure of a polymer in bulk is affected by the prior polymer chain shape in a solution. The glass transition temperature of original PVB in bulk is 63 °C and dissolved in solvents is increased by almost 7 °C. During the time period under investigation, the values of T_g changed negligibly in both cases; see Table 3. Hence, regardless of the kind of solvent and the age of the solution, stable properties of PVB nanofibres were observed.

4. Conclusions

No impact of ageing on the rheological properties of PVB-based solutions kept dark and at constant temperature was monitored
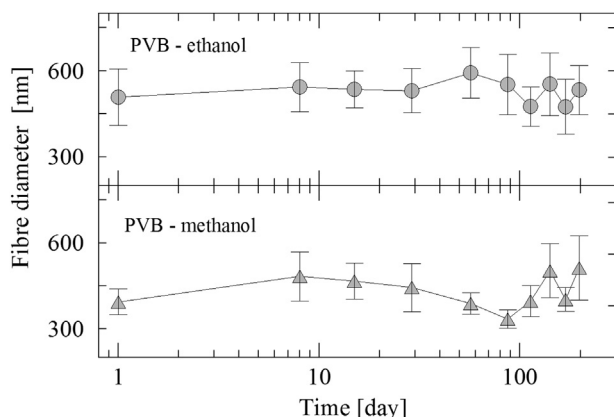

Fig. 11. Time dependence of relative humidity and temperature.

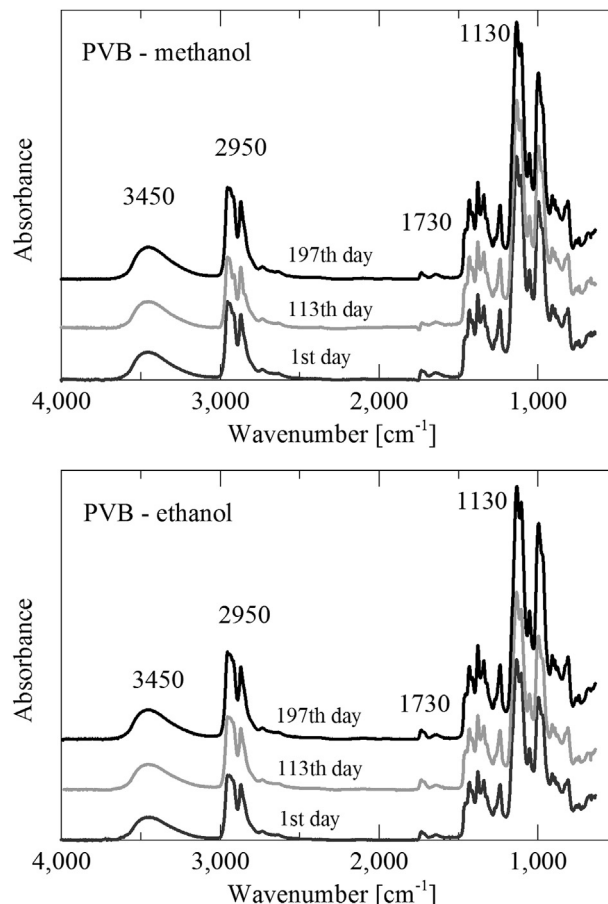**Fig. 10.** Time dependence of mean fibre diameters.

Fig. 12. Infra-red spectra of PVB nanofibrous electrospun from older solutions.

Table 3
Glass transition temperature of prepared PVB solutions.

Time [days]	T_g [°C] PVB-ethanol	T_g [°C] PVB-methanol
1	69	70
113	69	69
197	70	69

during the long-term study. Only small changes in mean fibre diameters and the morphology of electrospun fibres were documented. However, these changes are rather a consequence of processing conditions (mainly relative humidity) than the effect of solutions ageing. Both solutions exhibited storage stability as shown by various characterisation methods. The chemical structure of polymer nanofibres did not change over time. The long-term stability is highly beneficial from the industrial point of view.

Stability analysis of more complicated cases (other entry materials) will be the topic of next work.

Acknowledgements

References

[1] Ramakrishna S, Fujihara K, Teo WE, Lim TC, Ma Z. An introduction to electrospinning and nanofibres. Singapore: World Scientific Publishing Co.; 2005. pp. 90–152.

[2] Andrady AL. Science and technology of polymer nanofibers. New Jersey: John Wiley & Sons; 2008. pp. 81–109.

[3] Huang ZM, Zhang YZ, Kotaki M, Ramakrishna S. A review on polymer nanofibers by electrospinning and their applications in nanocomposites. Compos Sci Technol 2003;63:2223.

[4] Reneker DH, Yarin AL. Electrospinning jets and polymer nanofibers. Polymer 2008;49:2387.

[5] Rosic R, Pelipenko J, Kocbek P, Baumgartner S, Bester-Rogac M, Kristl J. The role of rheology of polymer solutions in predicting nanofiber formation by electrospinning. Eur Polym J 2012;48:1374.

[6] Qiu Y, Yu J, Rafique J, Yin J, Bai X, Wang E. Large-scale production of aligned long boron nitride nanofibers by multijet/multicollector electrospinning. J Phys Chem C 2009;113:11228.

[7] Mohammad Ali Zadeh M, Keyanpour-Rad M, Ebadzadeh T. Synthesis of mullite nanofibres by electrospinning of solutions containing different proportions of polyvinyl butyral. Ceram Int 2013;39:9079.

[8] Lu Q, Liu G, Wei Q, Liu G, Zhuang J. Preparation and characterization of $Lu_2SiO_5:Ce^{3+}$ luminescent ceramic fibers via electrospinning. Ceram Int 2013;39:8159.

[9] Chuang YJ, Liao JD, Chen LJ. Polyvinylbutyral-assisted synthesis and characterization of mesoporous silica nanofibers by electrospinning route. J Compos Mater 2012;46:227.

[10] Chen LJ, Liao JD, Lin SJ, Chuang YJ, Fu YS. Synthesis and characterization of PVB/silica nanofibers by electrospinning process. Polymer 2009;50:3516.

[11] Imaizumi S, Matsumoto H, Konosu Y, Tsuboi K, Minagawa M, Tanioka A, et al. Top-down process based on electrospinning, twisting, and heating for producing one-dimensional carbon nanotube assembly. ACS Appl Mater Interfaces 2011;3:469.

[12] Wang L, Huang ZH, Yue M, Li M, Wang M, Kang F. Preparation of flexible phenolic resin-based porous carbon fabrics by electrospinning. Chem Eng J 2013;218:232.

[13] Berutti FA, Alves AK, Bergmann CP, Clemens FJ, Graule T. Synthesis of CeO_2 and Y_2O_3-doped CeO_2 composite fibers by electrospinning. Particul Sci Technol 2009;27:203.

[14] Alves AK, Berutti FA, Clemens F, Graule T, Bergmann CP. The effect of heat treatment temperature on CeO_2 and Y_2O_3 doped CeO_2 electrospun fibres. Rev Adv Mater Sci 2009;21:200.

[15] Song B, Cui W, Chang J. Study on the effect of inorganic salts on the alignment of electrospun fiber. J Appl Polym Sci 2011;122:1047.

[16] Lin Q, Li Y, Yang M. Polyaniline nanofiber humidity sensor prepared by electrospinning. Sens Actuators B Chem 2012;161:967.

[17] Lin Q, Li Y, Yang M. Highly sensitive and ultrafast response surface acoustic wave humidity sensor based on electrospun polyaniline/poly(vinyl butyral) nanofibers. Anal Chim Acta 2012;748:73.

[18] Alhazov D, Zussman E. Study of the energy absorption capabilities of laminated glass using carbon nanotubes. Compos Sci Technol 2012;72:681.

[19] Corroyer E, Brochier-Salon MC, Chaussy D, Wery S, Belgacem MN. Characterization of commercial polyvinylbutyrals. Int J Polym Anal Charact 2013;18:346.

[20] Lubasova D, Martinova L. Controlled morphology of porous polyvinyl butyral nanofibers. J Nanomater; 2011. Article ID 292516.

[21] Peer P, Filip P, Lubasova D. On the rheological behaviour of PVB solutions in the process of electrospinning. Acta Technica 2012;57:197.

[22] Yener F, Jirsak O. Comparison between the needle and roller electrospinning of polyvinylbutyral. J Nanomater; 2012. Article ID 839317.

[23] Yener F, Jirsak O, Gemci R. Using a range of PVB spinning solution to acquire diverse morphology for electrospun nanofibres. Iran J Chem Chem Eng 2012;31:49.

[24] Yener F, Yalcinkaya B. Electrospinning of polyvinyl butyral in different solvents. e-Polymers 2013;13:229.

[25] Liu R, He B, Chen X. Degradation of poly(vinyl butyral) and its stabilization by bases. Polym Degrad Stab 2008;93:846.

[26] Feller RL, Curran M, Colaluca V, Bogaard J, Bailie C. Photochemical deterioration of poly(vinylbutyral) in the range of wavelengths from middle ultraviolet to the visible. Polym Degrad Stab 2007;92:920.

[27] Liau LCK, Hsieh YP. Kinetic analysis of poly(vinyl butyral)/glass ceramic thermal degradation using non-linear heating functions. Polym Degrad Stab 2005;89:545.

[28] Liau LCK, Chien YC. Kinetic investigation of ZrO_2, Y_2O_3, and Ni on poly(vinyl butyral) thermal degradation using nonlinear heating functions. J Appl Polym Sci 2006;102:2552.

[29] Liau LCK, Tung MT. Kinetic investigation of photocatalytic effects on poly(vinyl butyral) photodegradation. Ind Eng Chem Res 2006;45:2199.

[30] Safy El-Din NM, Sabaa MW. Thermal degradation of poly(vinyl butyral) laminated safety glass. Polym Degrad Stab 1995;47:283.

[31] Merinska D, Tupy M, Kasparkova V, Popelkova J, Zvonicek J, Pistek D, et al. Degradation of plasticized PVB during reprocessing by kneading. Macromol Symp 2009;286:107.

[32] Hansen CM. Hansen solubility parameters: a user's handbook. 2nd ed. New York: CRC Press, Taylor and Francis Group; 2007. p. 347.

[33] Wang C, Chien HS, Hsu CH, Wang YC, Wang CT, Lu HA. Electrospinning of polyacrylonitrile solutions at elevated temperatures. Macromolecules 2007;40:7973.

[34] De Vrieze S, Van Camp T, Nelvig A, Hagstrom B, Westbroek P, De Clerck KJ. The effect of temperature and humidity on electrospinning. J Mater Sci 2009;44:1357.

[35] Tripatanasuwan S, Zhong ZX, Reneker DH. Effect of evaporation and solidification of the charged jet in electrospinning of poly(ethylene oxide) aqueous solution. Polymer 2007;48:5742.

[36] Pelipenko J, Kristl J, Jankovic B, Baumgartner S, Kocbek P. The impact of relative humidity during electrospinning on the morphology and mechanical properties of nanofibers. Int J Pharm 2013;456:125.

Magnetorheological behaviour and electrospinning of PEO suspensions with magnetic nanoparticles

Petra Peer[1], Martin Stenicka[2], Michal Sedlacik[2], Petr Filip[1] and Vladimir Pavlinek[2]

[1] Institute of Hydrodynamics, Academy of Sciences of the Czech Republic, Pod Patankou 5, 166 12 Prague, Czech Republic

[2] Centre of Polymer Systems, University Institute, Tomas Bata University in Zlin, Nad Ovcirnou 3685, 760 01 Zlin, Czech Republic

Corresponding author:

Martin Stenicka, Centre of Polymer Systems, University Institute, Tomas Bata University in Zlin, Nad Ovcirnou 3685, 760 01 Zlin, Czech Republic

E-mail: stenicka@ft.utb.cz

Abstract

The properties of poly(ethylene oxide) (PEO) aqueous suspensions with magnetic nanoparticles (MNPs) synthesized under microwave assisted radiation are studied. The MNPs are formed by iron (III) chloride hexahydrate ($FeCl_3 \cdot 6H_2O$) dissolved in ethylene glycol ($C_2H_4(OH)_2$) and subsequently in aqueous ammonia solution (approx. 25 wt.% aq.). The polymer suspension exhibits substantial advantages over a suspension when 'classical' carrier fluids (water and silicone oil) are used. First, a presence of PEO significantly contributes to a fabrication of nanofibrous webs the morphology of which is documented by SEM technique. Second, better sedimentation stability of the processed suspension during electrospinning reflects in a uniform distribution of MNPs along the nanofibres thus ensuring even magnetic performance of the resulting membranes.

Introduction

Electrospinning (*e.g.* Agarwal et al. (2013)) represents a relatively cost-effective, simple and versatile method by means of which nanofibrous webs can be prepared. With the development of their applications, as for instance in tissue engineering, protective clothing and membrane-based

separation - to mention a few, still more advanced controlled and tailored properties are required. One of them is represented by magnetic behaviour of the resulting products. This behaviour can be significantly generated by the applied magnetorheological (MR) fluids (de Vicente et al. (2011)).

Originally, these MR fluids consisted of metal particles dispersed in non-magnetic Newtonian carrier liquid such as water (Miao et al. (2011)) or various oils (Bell et al. (2012)). An advantage of these liquids is a notable difference in viscosity if an external magnetic field is applied or not. This results in solid-like and liquid-like behaviour of the studied suspensions. However, this favourable property can seriously deteriorate in time due to sedimentation and agglomerative instability. This adverse process can be to some extent suppressed by using thixotropic agents (fumed silica or clay particles (de Vicente et al. (2003); Lim et al. (2004); Ulicny et al. (2005); Lopez-Lopez et al. (2008)), iron nanoparticles (Ginder et al. (1996); Rosenfeld et al. (2002); Wereley et al. (2006); Gomez-Ramirez et al. (2009)), plastic-like carrier fluids, elongated particles, two different diameters of particles and core / shell structured magnetic particles (Choi et al. (2014)). An application of these precautions is always accompanied by a reduction of difference between viscosities when no-field and magnetic field is applied. Nevertheless, from the practical point of view, this reduction is not significant and is more than balanced by improved stability of the MR fluids.

At present, there are in principle two immediate basic ways how to improve preparation and MR properties of suspension. First, the 'classical' carrier liquids such as Newtonian oils are substituted by various polymers, and second, magnetic particles are coated (core-shell structures) by materials contributing to reduced sedimentation under service of the corresponding suspensions (Guo et al. (2009); Cavaliere et al. (2010); Kannarkat et al. (2010); Sung et al. (2012); Hong et al. (2013); Kim et al. (2013); Li et al. (2013); Khalil et al. (2013); Mrlik et al. (2013); Sim et al. (2013); Bagheri et al. (2014); Ger et al. (2014); Kim et al. (2014); Savva et al. (2014); Singh et al. (2014); Shahrivar and de Vicente (2014); Ziyadi et al. (2014)).

Poly(ethylene oxide) (PEO) represents a non-toxic biocompatible polymer exhibiting favourite attributes to the process of electrospinning. Even a small participation of this carrier component can significantly contribute to quality of electrospinning process (for reference see Peer et al. (2014)). PEO alone or in a combination with other polymer carrier liquids for MNPs was used by Wang et al. (2004), Faridi-Majidi and Sharifi-Sanjani (2007) and Hyun et al. (2013). It is also hypothesized that with high molecular weight PEO (such as 600 to 2 000

kg/mol) metal salts can be reduced at shorter times and under ambient conditions (Saquing et al. (2009)). Morphology of the electrospun nanofibres containing MNPs can be tailored, e.g. aligned fibrous arrays are produced by so-called magnetic electrospinning (Yang et al. (2007), Hu et al. (2013)). The PEO nanofibres with MNPs are applied in a variety of fields such as bioengineering, magnetic targeting drug delivery, magnetic fluids intracellular hyperthermia or magnetic resonance imaging.

In this paper, behaviour of a novel MR fluid is compared with that in which 'classical' carrier fluids are used. This is carried out by detailed MR measurements and by the sedimentation tests. In our case these tests are important only in their initial stages as they serve for an evaluation of homogeneity of the MR fluid with MNPs directly applied to an electrospinning process under no magnetic field. The resulting effect consists in more uniform distribution of MNPs in nanofibrous webs thus ensuring homogeneous magnetic properties of the resulting membranes. The preferred application of MR fluids exhibits the following advantages resulting from the development of this branch in the past decades: excellent efficiency of the MNPs concerning magnetic properties (application of nanofibrous mats in practice), sophisticated core-shell structures ensuring very good sedimentation stability (and

consequently an even distribution of MNPs in the process of electrospinning as mentioned above) and resistance against mechanical disturbances caused by presence of MNPs (tearing, cutting, scissoring) in electrospun mats due to smooth surface of MNPs.

Experimental

Materials

MNPs were prepared under microwave assisted radiation ensuring homogeneous conditions during the synthesis. Iron(III) chloride hexahydrate ($FeCl_3 \cdot 6H_2O$) was dissolved in ethylene glycol ($C_2H_4(OH)_2$) and subsequently in aqueous ammonia solution (approx. 25 wt.% aq.). Size of the prepared MNPs is approximately 20 nm, for more details see Sedlacik et al. (2013). All chemicals used were in reagent grade (Penta, Czech Republic).

Prepared MNPs were subsequently dispersed (5 wt.%, 10 wt.% and 15 wt.%) in traditional carrier liquids (distilled water and silicone oil ($\eta = 100$ mPa.s), Dow Corning, USA) and prepared PEO aqueous solutions.

PEO (300 kg/mol, Sigma-Aldrich, USA) was dissolved in distilled water at two various concentrations, namely 4 wt.% aq. and 8 wt.% aq. Polymer solutions were magnetically stirred for 48 hrs at 25 °C; afterwards MNPs were mixed with polymer solution and placed in an ultrasonic bath for 5 min.

Rheological characterization

The rheological measurements were carried out with a rotational rheometer Physica MCR 501 (Anton Paar, Austria) equipped with the concentric cylinders (inner/outer diameter 26.6 / 28.9 mm) and MR cell 180 / 1T (parallel plates 20 mm in diameter; gap 0.5 mm).

MR fluids were measured at steady shear in the absence / presence of an external magnetic field and temperature was kept constant at 25 °C during all experiments. True magnetic flux density was measured using a Hall probe.

Electrospinning of PEO suspension with MNPs

Nanofibrous webs from PEO suspensions containing MNPs were electrospun using a laboratory device (details in Peer et al. (2014)) at the voltage of 25 kV. The distance between the replaceable tip and the collector was 200 mm. The volume of polymer solution placed onto the tip attained 0.2 ml. The obtained fibres were analysed via SEM technique (Vega 3, Tescan, Czech Republic). The iron content in electrospun fibres was confirmed by energy dispersive X-ray fluorescence spectroscopy (EDX-XRF, ARL QUANT´X, Thermo Scientific, USA).

Results and discussion

Rheological properties

As well known (*e.g.* Sung et al. (2004); Gupta et al. (2005)), shear viscosity increases with concentration of MNPs. These differences for all three types of the carrier liquids are depicted in Figure 1, where concentration of MNPs attains 15 wt.%. The non-Newtonian character of the PEO solutions is also apparent. More pronounced sedimentation rate in the case of distilled water as a carrier liquid rather questions trustworthiness of measured data (discussed later). A more detailed development in shear viscosity for different concentration of MNPs for the case of the PEO solutions is presented in Figure 2.
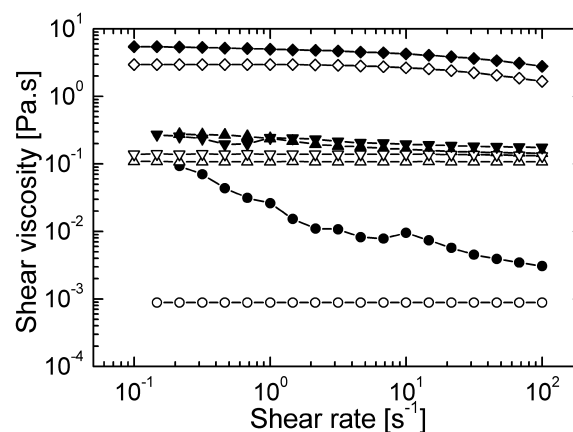

Figure 1. Dependence of shear viscosity on shear rate for different carrier liquids (no MNPs – open symbols, 15 wt.% MNPs – solid symbols): ($\bigcirc\,\bullet$) distilled water, ($\triangle\,\blacktriangle$) silicone oil, ($\bigtriangledown\,\blacktriangledown$) PEO (4 wt.% aq.), ($\diamondsuit\,\blacklozenge$) PEO (8 wt.% aq.). Tabulated value 0.890 mPa.s was used for neat distilled water (at $T = 25$ °C).
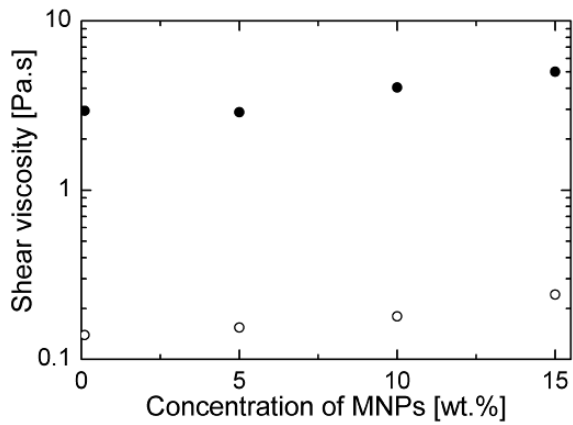
Figure 2. Dependence of shear viscosity (for shear rate 1 s^{-1}) on concentration of MNPs for carrier liquid based on PEO: PEO (4 wt.% aq.) (○), PEO (8 wt.% aq.) (●).

Magnetorheological properties

The differences in rheological behaviour of MR fluids with 'classical' carrier liquids (water, silicone oil) and based on PEO solutions in the presence and the absence of magnetic field are shown in Figures 3 and 4.
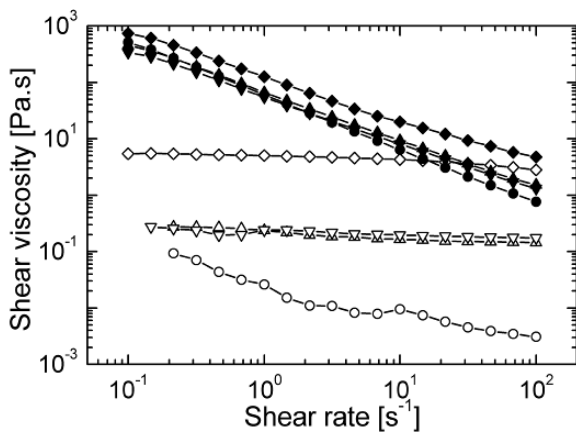

Figure 3. Dependence of shear viscosity on shear rate for MR fluids containing different carrier liquids with dispersed MNPs (15 wt.%). Magnetic field B [mT]: 0 (open) and 254 (solid), (○●) distilled water, (△▲)

silicone oil, (▽▼) PEO (4 wt.% aq.), (◇◆) PEO (8 wt.% aq.).
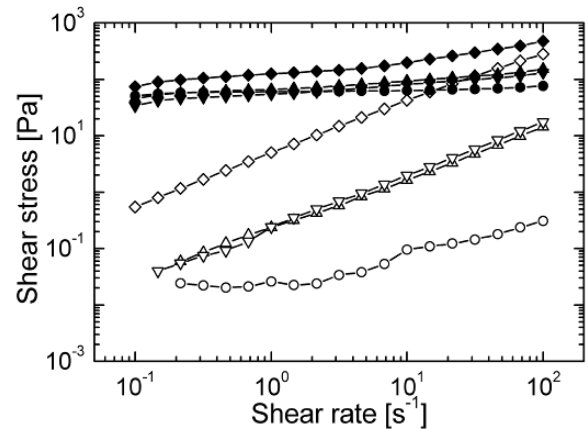
Figure 4. Dependence of shear stress on shear rate for MR fluids containing different carrier liquids with dispersed MNPs (15 wt.%) at presence and absence of the magnetic field. Symbols as in Figure 3.

In field-on state, all MNPs suspensions present significant increase in shear viscosity caused by chaining of the MNPs. The obtained field-on viscosities are roughly comparable for all suspensions. However, the differences in MR efficiency (defined as a ratio of the field-on viscosity to the field-off viscosity) are evident (Figure 5). The water based system demonstrates the highest MR performance; however this result is again nonnegligibly influenced by sedimentation of MNPs in the absence of magnetic field. Therefore, more stable MR behaviour of suspensions containing PEO as a carrier liquid exhibits higher benefits from a practical point of view. The higher concentration of MNPs in suspensions

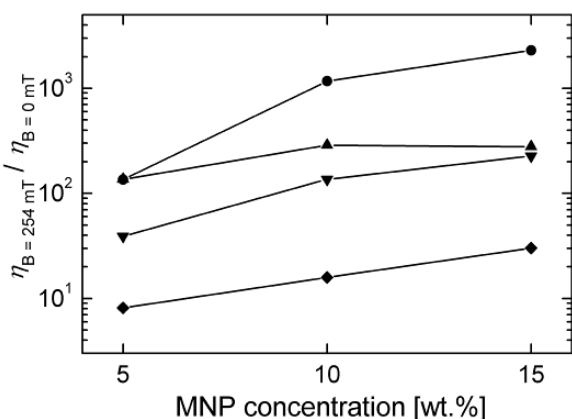positively influences the MR efficiency irrespectively which carrier fluid is employed (Figure 5).

Figure 5. MR efficiency (compared at the shear rate of $1\,\mathrm{s}^{-1}$) of MNPs dispersed in various carrier fluids. Symbols as in Figure 3.

Sedimentation stability

The rheological behaviour of all suspensions was confronted with their sedimentation stability which belongs to the key factors in practical applications. The obtained results (the sedimentation ratio is defined as the height of suspension with dispersed MNPs in time to the initial height) are depicted in Figure 6. From our viewpoint (applicability of the prepared materials to the electrospinning process), only an initial stage of the sedimentation curves is significant, as the materials are processed in hours not in days. The experimental results depicted in Figure 5 indicate uniform distribution of MNPs in PEO solution when used for electrospinning.
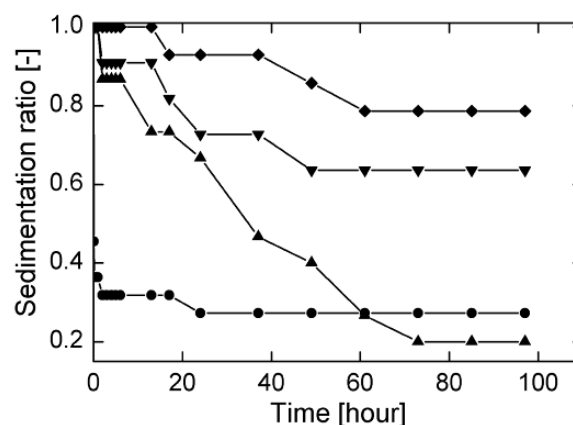
Figure 6. Sedimentation ratio *vs.* time of MNPs (5 wt.%) dispersed in various carrier fluids. Symbols as in Figure 3.

Electrospinning

Besides the improved sedimentation stability, the presence of PEO in suspension allows to prepare the nanofibres with magnetic properties via electrospinning which extends the application field.

To obtain the high-quality fibres, the viscosity of spinnable solution plays an important role (*e.g.* Sung et al. (2004)). In our case, the viscosity was influenced both by a concentration of MNPs in the carrier liquid and by a concentration of PEO in a solution. As PEO represents an excellent material for electrospinning, relatively higher values of viscosity of the carrier liquid (Figure 3) in comparison with some other liquids has no adverse effect on quality of electrospinning. No fibres are created when the concentration of PEO is too low (4 wt.% aq.) (Figure 7). However with an increasing concentration (8 wt.% aq.), a good quality of fibres is obtained (Figure 8). The presence of

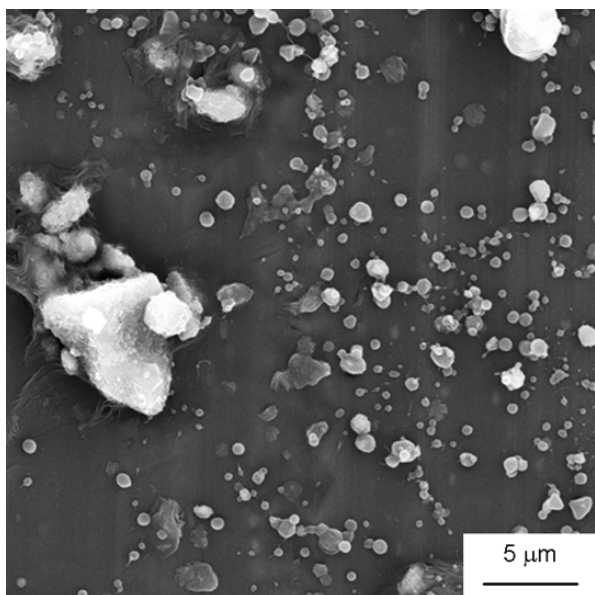MNPs within nanofibres was confirmed via EDX-XRF.

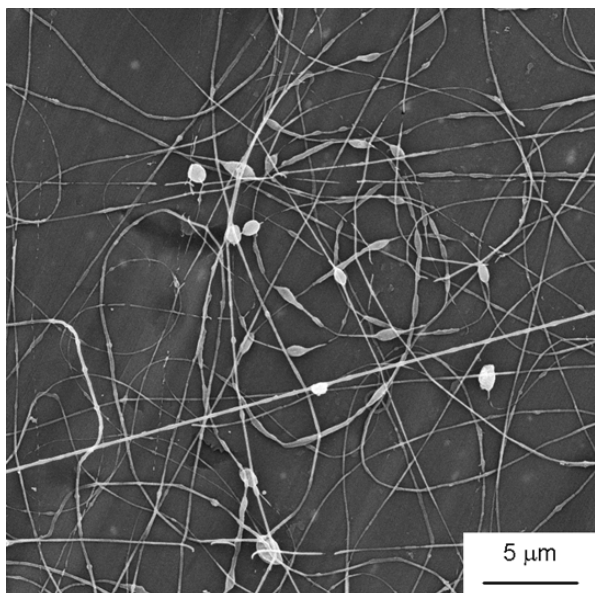**Figure 7.** SEM picture of the disintegrated material made of PEO solution (4 wt.% aq.) containing MNPs (15 wt.%).

Figure 8. SEM picture of fibres made of PEO solution (8 wt.% aq.) containing MNPs (15 wt.%), a mean diameter of nanofibres attained 174 nm.

Conclusions

MNPs were synthesized under microwave assisted radiation and subsequently dispersed in 'classical' and PEO based carrier fluids to compare their MR efficiency. As shown, a presence of polymer in the carrier fluid has a positive impact on the stability of MR fluid without an apparent reduction of MR performance. Consequently, the nanofibres produced by an electrospinning method exhibit more homogeneous distribution of MNPs that reflects in uniform magnetic properties of the corresponding membranes.

References

Agarwal S, Greiner A and Wendorff JH (2013) Functional materials by electrospinning of polymers. *Progress in Polymer Science* 38: 963–991.

Bagheri H, Roostaie A and Daliri R (2014) An electrospun magnetic nanocomposite for a facile micro-scaled analysis approach. *Analytical Methods* 6: 5838–5846.

Bell RC, Karli JO, Vavreck AN et al. (2008) Magnetorheology of submicron diameter iron microwires dispersed in silicone oil. *Smart Material & Structures* 17: 015028.

Cavaliere S, Salles V, Brioude A et al. (2010) Elaboration and characterization of magnetic nanocomposite fibers by electrospinning. *Journal of Nanoparticle Research* 12: 2735–2740.

Choi HJ, Zhang WL, Kim S et al. (2014) Core-shell structured electro- and magneto-responsive materials: Fabrication and characteristics. *Materials* 7: 7460–7471.

de Vicente J, Lopez-Lopez MT, Gonzalez-Caballero F et al. (2003) Rheological study of the stabilization of magnetizable colloidal suspensions by addition of silica nanoparticles. *Journal of Rheology* 47: 1093-1109.

de Vicente J, Klingenberg DJ and Hidalgo-Alvarez R (2011) Magnetorheological fluids: A review. *Soft Matter* 7: 3701–3710.

Faridi-Majidi R and Sharifi-Sanjani N (2007) In situ synthesis of iron oxide nanoparticles on poly(ethylene oxide) nanofibres through an electrospinning process. *Journal of Applied Polymer Science* 105: 1351–1355.

Ger TR, Huang HT, Huang CY et al. (2014) Study of polyvinyl alcohol nanofibrous membrane by electrospinning as a magnetic nanoparticle delivery approach. *Journal of Applied Physics* 115: 17B908.

Ginder JM, Davis LC and Elie LD (1996) Rheology of magnetorheological fluids: models and measurements. *International Journal of Modern Physics B* 10: 3293-3303.

Gomez-Ramirez A, Lopez-Lopez MT, Duran JDG et al. (2009) Influence of particle shape on the magnetic and magnetorheological properties of nanoparticle suspensions. *Soft Matter* 5: 3888–3895.

Guo J, Ye X, Liu W et al. (2009) Preparation and characterization of poly(acrylonitrile-co-acrylic acid) nanofibrous composites with Fe_3O_4 magnetic nanoparticles. *Materials Letters* 63: 1326–1328.

Gupta P, Elskin CL, Long TE et al. (2005) Electrospinning of linear homopolymers of poly(methyl methacrylate): Exploring relationships between fibre formation, viscosity, molecular weight and concentration in a good solvent. *Polymer* 46: 4799–4810.

Hong CH, Liu YD and Choi HJ (2013) Carbonyl iron suspension with halloysite additive and its magnetorheology. *Applied Clay Science* 80–81: 366–371.

Hu H, Jiang W, Lan F et al. (2013) Synergic effect of magnetic nanoparticles on the electrospun aligned superparamagnetic nanofibers as a potential tissue engineering scaffold. *RSC Advances* 3: 879–886.

Hyun DC, Jo E, Park CJ et al. (2013) Ultrasonic breaking of fibers and microparticles into mesoporous particles with high loading of magnetic nanoparticles. *Macromolecular Materials and Engineering* 298: 575–582.

Kannarkat JT, Battogtokh J, Philip J et al. (2010) Embedding of magnetic nanoparticles in polycaprolactone nanofiber scaffolds to facilitate bone healing and regeneration. *Journal of Applied Physics* 107: 09B307.

Khalil A, Lalia BS, Hashaikeh R et al. (2013) Electrospun metallic nanowires: Synthesis, characterization, and applications. *Journal of Applied Physics* 114: 171301.

Kim SY, Kwon SH, Liu YD et al. (2014) Core-shell structured cross-linked poly(glycidyl methacrylate)-coated carbonyl iron microspheres and their magnetorheology. *Journal of Materials Science* 49: 1345–1352.

Kim YJ, Ebara M and Aoyagi T (2013) A smart hyperthermia nanofiber with switchable drug release for inducing cancer apoptosis. *Advanced Functional Materials* 23: 5753–5761.

Li P, Liu C, Song Y, Niu X et al. (2013) Influence of Fe_3O_4 nanoparticles on the preparation of aligned PLGA electrospun fibers induced by magnetic field. *Journal of Nanomaterials*: Article ID 483569.

Lim ST, Cho MS, Jang IB et al. (2004) Magnetorheological characterization of carbonyl iron based suspension stabilized by fumed silica. *Journal of Magnetism and Magnetic Materials* 282: 170–173.

Lopez-Lopez MT, Kuzhir P, Bossis G et al. (2008) Preparation of well-dispersed magnetorheological fluids and effect of dispersion on their magnetorheological properties. *Rheologica Acta* 47: 787–96.

Miao C, Shen R, Wang M et al. (2011) Rheology of aqueous magnetorheological fluid using dual oxide-coated carbonyl iron particles. *Journal of the American Ceramic Society* 94: 2386–2392.

Mrlik M, Ilcikova M, Pavlinek V et al. (2013) Improved thermooxidation and sedimentation stability of covalently-coated carbonyl iron particles with cholesteryl groups and their influence on magnetorheology. *Journal of Colloid and Interface Science* 396: 146–151.

Peer P, Stenicka M, Pavlinek V et al. (2014) The storage stability of polyvinylbutyral

solutions from an electrospinnability standpoint. *Polymer Degradation and Stability* 105: 134–139.

Rosenfeld N, Wereley NM, Radhakrishnan R et al. (2002) Behavior of magnetorheological fluids utilizing nanopowder iron. *International Journal of Modern Physics B* 16: 2392-2398.

Saquing CD, Manasco JL and Khan SA (2009) Electrospun nanoparticle–nanofiber composites via a one-step synthesis. *Small* 5: 944–951.

Savva I, Constantinou D, Marinica O et al. (2014) Fabrication and characterization of superparamagnetic poly(vinyl pyrrolidone)/poly(L-lactide)/Fe_3O_4 electrospun membranes. *Journal of Magnetism and Magnetic Materials* 352: 30–35.

Sedlacik M, Moucka R, Kozakova Z et al. (2013) Correlation of structural and magnetic properties of Fe_3O_4 nanoparticles with their calorimetric and magnetorheological performance. *Journal of Magnetism and Magnetic Materials* 326: 7–13.

Shahrivar K and de Vicente J (2014) Thermogelling magnetorheological fluids. *Smart Materials and Structures* 23: 025012.

Sim HH, Kwon SH and Choi HJ (2013) Xanthan gum-coated soft magnetic carbonyl iron composite particles and their magnetorheology. *Colloid and Polymer Science* 291: 963–969.

Singh RK, Patel KD, Lee JH et al. (2014) Potential of magnetic nanofiber scaffolds with mechanical and biological properties applicable for bone regeneration. *PLOS ONE* 9: e91584.

Sung JH, Kim HS, Jin HJ, et al. (2004) Nanofibrous membranes prepared by multiwalled carbon nanotube / poly(methyl methacrylate composites. *Macromolecules* 37: 9899–9902.

Sung YK, Ahn BW and Kang TJ (2012) Magnetic nanofibers with core (Fe_3O_4 nanoparticle suspension) / sheath (poly ethylene terephthalate) structure fabricated by coaxial electrospinning. *Journal of Magnetism and Magnetic Materials* 324: 916–922.

Ulicny JC, Golden MA, Namuduri CS et al. (2005) Transient response of magnetorheological fluids: Shear flow between concentric cylinders. *Journal of Rheology* 49: 87-104.

Wang M, Singh H, Hatton TA et al. (2004) Field-responsive superparamagnetic composite nanofibers by electrospinning. *Polymer* 45: 5505–5514.

Wereley NM, Chaudhuri A, Yoo JH et al. (2006) Bidisperse Magnetorheological fluids using Fe particles at nanometer and micron scale. *Journal of Intelligent*

Material Systems and Structures 17: 393-401.

Yang D, Lu B, Zhao Y et al. (2007) Fabrication of aligned fibrous arrays by magnetic electrospinning. *Advanced Materials* 19: 1702–1706.

Ziyadi H, Heydari A and Rezayat SM (2014) Preparation and characterization of magnetic $\alpha\text{-}Fe_2O_3$ nanofibres coated with uniform layers of silica. *Ceramics International* 40: 5913–5919.

Measurement of Elongational Viscosity of Polymer Melts Using SER Universal Testing Platform

P. Filip*, P. Svrcinova

Institute of Hydrodynamics, Academy of Science of the Czech Republic, Pod Patankou 5, 166 12 Prague 6, Czech Republic

*Corresponding author: filip@ih.cas.cz
Fax: x420.233324361

Abstract:

The measurement of elongational viscosity still evokes a series of problems in comparison with the relatively well-established measurement of shear viscosity. Recently new techniques have appeared enabling measurement of elongational viscosity with the samples for which the aspect ratios of their geometrical shapes (i.e. length vs. width (diameter)) can attain moderate values, i.e. not necessarily of a longitudinal character as in the case of earlier techniques. The aim of this contribution is to experimentally demonstrate the invariantness of transient uniaxial elongational viscosity measured with respect to a rectangular shape and thickness of LDPE samples using a SER Universal Testing Platform fixed in an Anton Paar MCR 501 host system. The width of the samples was varied within the range 2.1-12.7 mm and thickness altered within 0.1-1 mm. An advantage of fixing polymer samples directly to both drums (if possible) over the application of clamps is documented.

Zusammenfassung:

Die Messung der Dehnviskosität ist weiterhin mit einer Reihe von Fragestellungen verbunden im Vergleich mit den sehr gut etablierten Messungen der Scherviskosität. Mit Hilfe von kürzlich entwickelten neuen Methoden kann die Dehnviskosität ermittelt werden, bei denen das Aspektverhältnis (Länge zu Breite bzw. Durchmesser) der Probe moderate Werte annehmen kann, d. h. bei denen nicht notwendigerweise sehr lange Proben verwendet werden müssen. In dieser Arbeit wird die Unabhängigkeit der transienten Dehnviskosität von Proben mit einem rechteckigen Querschnitt in einfacher Dehnung mit dem SER in Kombination mit dem MCR 501 gemessen. Die Breite der Probe wurde variiert und lag im Bereich von 2.1 bis 12.7 mm. Ihre Dicke variierte zwischen 0.1 und 1.0 mm. Der Vorteil der Befestigung der Polymerprobe direkt auf den Trommeln im Gegensatz zu der Verwendung von Klemmen wird gezeigt.

Résumé:

Mesurer la viscosité extensionnelle présente encore une série de problèmes qui contrastent avec la mesure relativement bien établie de la viscosité de cisaillement. Récemment, de nouvelles techniques ont vu le jour, permettant la mesure de la viscosité extensionnelle d'échantillons dont les formats géométriques (c-à-d longueur sur largeur (ou diamètre)) peuvent atteindre des valeurs modérées, c-à-d ne présentant pas un caractère longitudinal, comme dans le cas des techniques précédentes. Le but de cette contribution est de démontrer expérimentalement l'invariance de la viscosité extensionnelle uniaxiale transitoire d'échantillons de LDPE par rapport à leur forme rectangulaire et à leur épaisseur, en utilisant une Plateforme de Test Universel SER fixée à un Anton Paar MCR 501. La largeur des échantillons varie entre 2.1 et 12.7 mm et l'épaisseur entre 0.1 et 1 mm. L'avantage de fixer les échantillons polymères directement sur les deux tambours (si possible) relativement à l'utilisation de clips de fixation est démontré.

1   INTRODUCTION

When using the 'classical' devices for measurement of elongational viscosity of polymer melts (Meissner [1], Meissner and Hostettler [2], Münstedt [3]) it is necessary to prepare longitudinal samples (length considerably exceeds width (diameter)) of polymeric materials. Necessity of this requirement has been eliminated with the appearance of novel experimental devices such as the filament stretching rheometer (McKinley and Sridhar [4], modification for high-temperature measurements of polymer melts Bach et al. [5], Chellamuthu et al. [6]) or
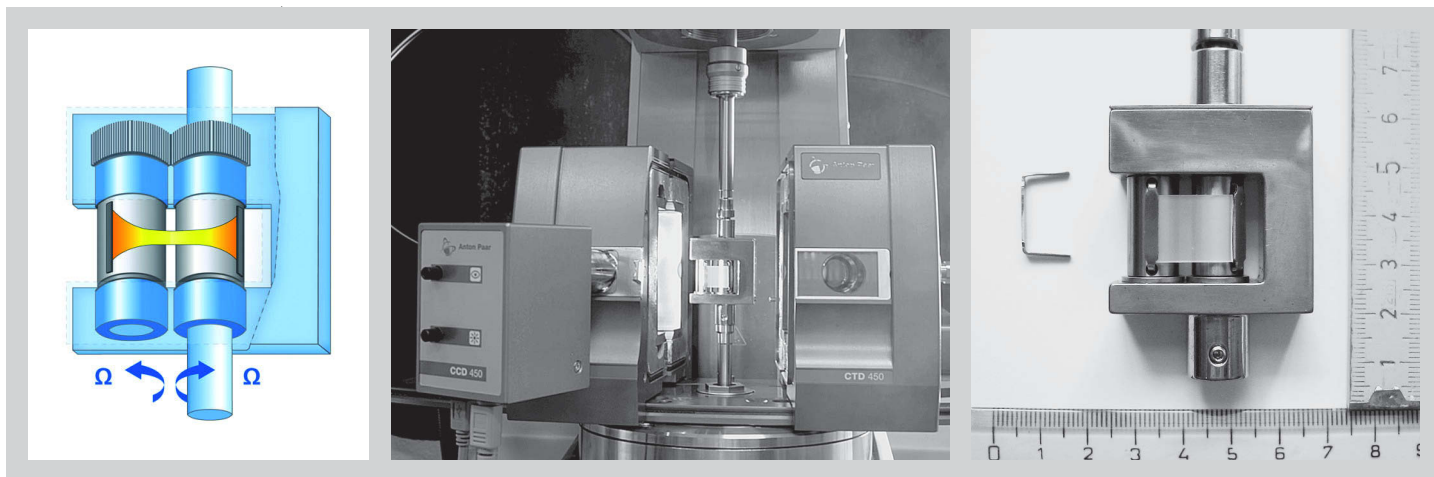
the SER Universal Testing Platform (Sentmanat [7, 8], Sentmanat and Hatzikiriakos [9], Sentmanat et al. [10]) for which an application of the samples with comparable length and width (diameter) is possible. A detailed analysis of various experimental devices was recently given in Tropea et al. [11] and with the emphasis to a semi-hyperbolic die in Baird et al. [12].

The SER Universal Testing Platform (Figure 1) is formed by two counter-rotating drums (10.3 mm in diameter each) that stretch a rectangular sample that is fixed by clamps to the drums. This Platform has been implanted in the rotational rheometers of various commercial producers. The basic difference with regard to the geometric arrangement of the SER U.T.P. in the ovens of the individual host systems is related to the various temperature fields generated in the respective ovens. The distribution substantially differs from one oven to another and it is really difficult to say that a temperature indicated by a device corresponds to the true temperature at the location of the rectangular sample. Such correspondence improves remarkably with the symmetrical input and output of heated air; nevertheless the best method of checking temperature requires the use of thermocouples (type K due to their characteristics). This situation contrasts with the temperature conditions in the 'traditional' oil bath (Münstedt [3]) in which inaccuracies do not exceed 0.1°C. Appropriately selected oil can also substantially reduce the difficulties caused by possible gravitational or buoyancy effects. The possibilities for compensating the potential appearance of sagging if the SER U.T.P. is used will be discussed later as well as the problems connected with the presence of the clamps used to fix the samples (i.e. if more than one revolution of the drums seems to be necessary).

The aim of this contribution is to analyse the measurement of elongational viscosity using SER U.T.P. with the emphasis on the use of fixing clamps and a variety of rectangular shapes of LDPE material.
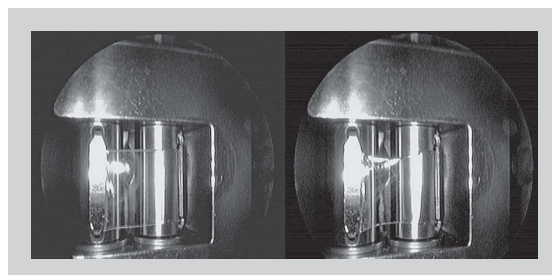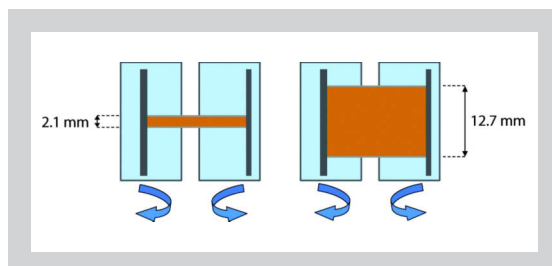
2 EXPERIMENTAL

Measurements were carried out using an SER Universal Testing Platform from Xpansion Instruments. The model SER-HV-P01 was used with an Anton Paar MCR501 rotational rheometer host system. For the measurement of the rheological properties of polymer melts a convection-heated measuring chamber CTD450 equipped with a camera system was used (Figures 2 and 3).

The low-density polyethylene (LDPE) Escorene used in the experiments was produced by Exxon, USA (MFI = 0.33 g/10 min, density 0.992 g/cm^3, M_w = 366300 g/mol, M_n = 30280 g/mol). Rectangular samples of this polymer were prepared from the pellets, flat sheets hot pressed and cooled under weight with the emphasis on air bubbles elimination. Only centre parts of the sheets were used with respect to uneven flatness at the margins. The width of the samples prepared consecutively was 12.7, 11.0, 9.3, 7.4, 6.5, 4.2 and 2.1 mm (Figure 4), their thickness varied within an interval of 0.3 – 1.0 mm, the case at which the thickness reached 0.1 mm is also presented. The fixed active length (12.7 mm = 1/2") is given by the geometric arrangement of the SER unit.

Transient uniaxial extensional viscosity was measured in the temperature range of 180–200°C under the extensional strain rates 0.0316, 0.1, 0.316, 1.0, 3.16, and 10 s⁻¹. As the material used enables the rectangular samples to be fixed directly to the pre-heated drums without use of the clamps, a comparison was made between the measurements carried out with and without the clamps.

3 RESULTS AND DISCUSSION

The presence of a digital camera enabling continuous screening of the whole experiment has the following advantages:

- the proper fixing of both sample ends to the drums can be checked
- the volume of a rectangular sample should be equally distributed between both drums
- the sample colour can be observed as a basic indication of possible material degradation
- possible sagging of polymeric material and its development over time can be observed (Figure 5)

On the other hand, an angle between the camera and fixed sample does not allow an analysis of the true strain rate.

There are roughly speaking three ways how to deal with material sagging. One consists of the permanent revolving of both drums using a very low pre-tension step of 20 μNm (Aho et al. [13, 14]). Under this applied torque the material is still stretched and sagging is suppressed. Simultaneously the reduced cross-sectional area of a sample is re-calculated including temperature-dependent material density. The second approach – which was used in this work – involves time shifting using a digital camera recording, in which the time interval that elapsed between the start of the experiment and the point at which the material was stretched (and thus gravitational force was eliminated) is subtracted prior to data processing (Table 1). The third approach competing the preceding ways due to their shortcomings (possible change of material structure, difference between real and used cross-sectional area) is a simple acceptance of sagging (in a responsible measure).

Figures 6 to 8 document the invariantness of the measurement of transient elongational viscosity within a broad range of sample widths (4.2–12.7 mm) and thicknesses (0.3–1.0 mm) at temperatures of 180, 190, and 200°C (for more detail see Table 2). Figure 9 illustrates the difference with Figure 8 (sample width 7.4 mm) if no time shifting factors (Table 1) are applied. Each experiment on the
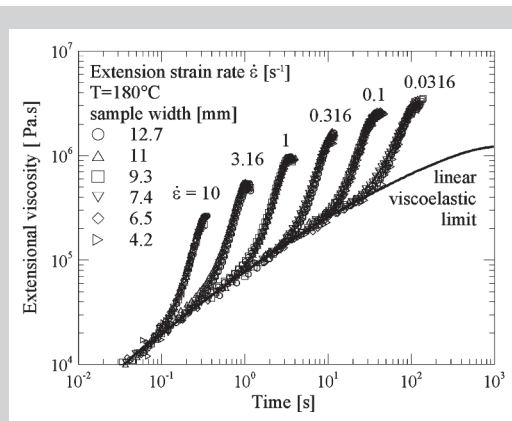

Figure 6 (above):
Comparison of uniaxial extensional viscosity measured with the samples of various widths and thicknesses at a temperature of 180°C.
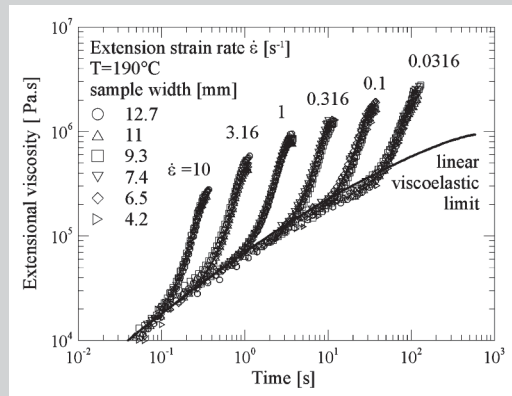
Figure 7 (middle):
Comparison of uniaxial extensional viscosity measured with the samples of various widths and thicknesses at a temperature of 190°C.
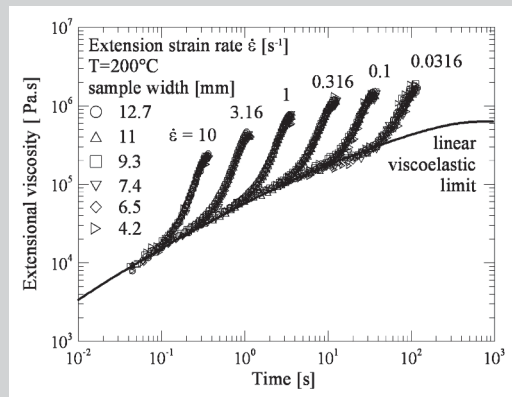
Figure 8 (below):
Comparison of uniaxial extensional viscosity measured with the samples of various widths and thicknesses at a temperature of 200°C.

Table 1 (above):
Time shifting factors applied to evaluation of transient elongational viscosity in Figures 6 to 8.

Table 2 (below):
Width and thickness of the individual samples used in Figures 6 to 8.

T [°C]	Width [mm]	$\dot{\varepsilon} = 0.316 \, s^{-1}$	$\dot{\varepsilon} = 0.1 \, s^{-1}$	$\dot{\varepsilon} = 0.0316 \, s^{-1}$
180	12.7	-	-	4.5 s
	4.2	-	-	4 s
190	12.7	-	-	0.15 s
	11	-	-	3.5 s
200	12.7	0.3 s	-	-
	7.4	0.5 s	2 s	3 s
	6.5	0.5 s	0.8 s	1 s

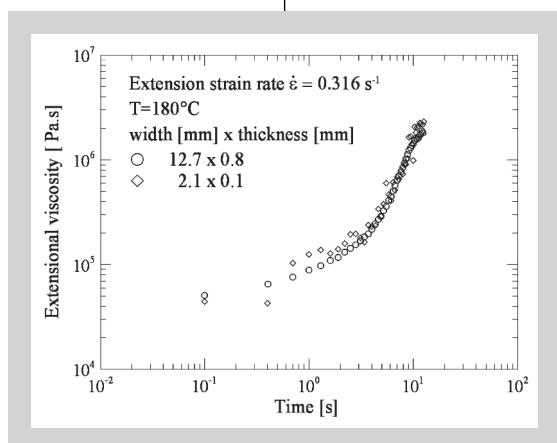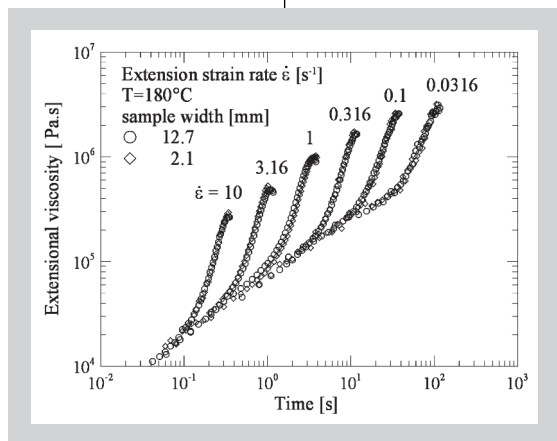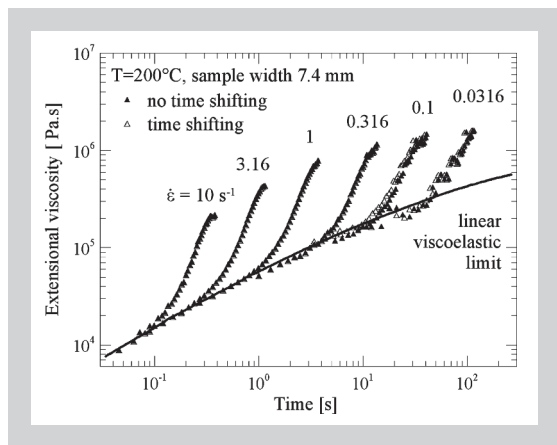| Width [mm]	Thickness [μm]																	
	$\dot{\varepsilon}=10\,s^{-1}$			$\dot{\varepsilon}=3.16\,s^{-1}$			$\dot{\varepsilon}=1\,s^{-1}$			$\dot{\varepsilon}=0.316\,s^{-1}$			$\dot{\varepsilon}=0.1\,s^{-1}$			$\dot{\varepsilon}=0.0316\,s^{-1}$		
	180°	190°	200°	180°	190°	200°	180°	190°	200°	180°	190°	200°	180°	190°	200°	180°	190°	200°
12.7	550	817	747	691	779	766	769	769	783	801	731	757	1042	787	789	582	768	816
	695	515	812	751	788	833	769	769	993	774	783	701	556	752	743	542	529	852
	772	1026	913	683	964	584	751	929	616	759	881	631	807	822	1015	832	1057	899
11.0	749	657	476	834	616	542	772	614	490	811	607	521	788	853	490	779	596	455
	768	590	607	839	550	592	771	686	508	820	757	539	766	578	522	849	643	489
	765	625	673	835	821	465	780	659	506	806	667	541	781	639	511	854	616	462
9.3	601	599	864	638	608	496	611	607	886	628	552	490	655	579	872	597	598	549
	587	601	833	613	592	866	606	592	471	622	583	845	621	566	511	606	611	465
	594	605	497	633	593	611	609	608	491	643	597	883	595	580	544	648	599	462
7.4	664	611	626	572	591	602	614	549	616	644	589	607	665	607	618	601	583	621
	634	589	613	631	553	645	631	592	591	588	581	584	644	565	623	645	670	609
	629	564	634	617	566	559	622	553	592	593	603	601	660	564	611	593	625	604
6.5	543	554	532	519	531	560	629	523	610	637	592	557	638	556	559	629	599	553
	503	524	524	527	527	512	491	547	525	538	594	579	654	564	555	567	605	559
	542	535	519	562	533	543	491	661	560	608	625	556	526	552	557	565	632	510
4.2	368	399	412	362	397	322	393	397	379	410	397	398	404	413	357	402	402	402
	350	373	316	412	409	414	398	409	370	397	409	409	411	340	341	394	394	394
	391	401	354	360	372	318	382	372	367	391	372	370	336	361	370	407	407	407

Figure 9:
Comparison of uniaxial extensional viscosity with and without time shifting at a temperature of 200°C.

Figure 10:
Comparison of uniaxial extensional viscosity measured with the samples of two widths (2.1 and 12.7 mm) at a temperature of 180°C.

Figure 11:
Comparison of uniaxial extensional viscosity measured with the samples of two distinctive dimensions at a temperature of 180 °C.

individual parameters (strain rate, temperature, sample width) was carried out at least three times, prior to each temperature run the oven was pre-heated for at least 1 hour. The temperature of each sample after fixing was approached from below to prevent the material from possible degradation and more pronounced sagging.

The same conclusion is valid even for distinctly different widths of rectangular samples, i.e. 2.1 and 12.7 mm (the respective widths differ by a multiplicative factor of 6) as depicted in Figure 10. Figure 11 presents the result obtained for two samples that were remarkably different not only in width (2.1 versus 12.7 mm) but also in thickness (0.1 versus 0.8 mm). These experimental results varies from the theoretical conclusions by Yu et al. [16] in which they restricted the dimensions of the samples applicable for measurements using the SER U.T.P.

The homogeneity of the samples to be measured always plays a crucial role. For the Münstedt-type rheometer this issue has recently been discussed in Burghelea et al. [15]. For the SER unit adequate homogeneity of the material itself and also the more or less constant thickness of the sample are very important. In our experience accurate and reproducible measurements can be achieved if the thickness across the whole prepared sample only varies by up to 3 % (i.e. not ±3 %, but up to 3 %).

Sometimes the material being measured ruptures during passage over a clamp. The exact location of rupture can easily be determined with

the help of the camera system. Based on the results reported above this singularity can be removed by changing the dimensions of the rectangular sample. The use of a thinner sample also leads to more rapid heating of the whole sample to the temperature required, and thus reduces the time during which the sample is in the oven at rest, and consequently the degree of sagging.

Sagging is also very much influenced by the time interval during which a sample is fixed to both drums, as longer fixing means a higher decrease in the temperature in the oven. For some materials there is the possibility of eliminating the use of clamps for fixing the rectangular samples. This results not only in a substantial time reduction during sample fixing but also in the elimination of possible singularities accompanying the presence of the clamps. For better passage of the material that has been stretched after one revolution it is possible to fix both sample ends to the drums in such a way that their thickness reduces 'continuously to zero' at both lateral ends [17] (Figure 12). Figure 13 depicts and compares both possibilities of fixing (when no rupture appears during passage over a clamp) and justifies the measurements made without the clamps. Impossibility of using the Sentmanat U.T.P. when samples rupture during passage over a clamp is documented in Figure 14. This substantiates the measurement with the samples directly fixed to both drums.

4 CONCLUSIONS

Measurements of the extensional viscosity of LDPE Escorene were carried out using a broad range of widths and thicknesses of rectangular polymer samples in the SER Universal Testing Platform using the Anton Paar MCR501 rotational rheometer host system. The measurements were carried out at three different temperatures: 180, 190, and 200°C. Based on the experimental results the following statements about LDPE can be made:

■ the measurement of elongational viscosity is invariant with respect to the dimensions of rectangular samples
■ the use of thinner and narrower samples leads to better heating and less sagging
■ in the absence of skilled personnel (carrying out regular experimental work), the use of wider samples facilitates their horizontal fixing
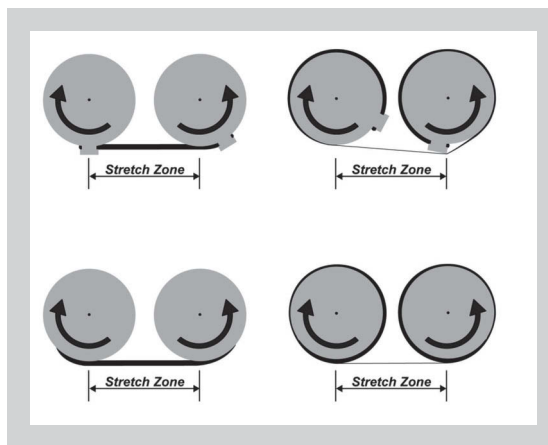
■ possible singularities caused by the presence of the fixing clamps can be removed by choosing rectangular samples of different dimensions or removing the clamps, i.e. fixing the samples directly to the drums

ACKNOWLEDGMENTS

REFERENCES

[1] Meissner J: Stress and recovery maxima in LDPE melt elongation, Polym. Bull. 1 (1979) 397-402.

[2] Meissner J, Hostettler J: A new elongational rheometer for polymer melts and other highly viscous liquids, Rheol. Acta 33 (1994) 1-21.

[3] Münstedt H: New universal extensional rheometer for polymer melts. Measurements on a polystyrene sample, J. Rheol. 23 (1979) 421-436.

[4] McKinley GH, Sridhar T: Filament-stretching rheometry of complex fluids, Ann. Rev. Fluid Mech. 34 (2002) 375-415.

[5] Bach A, Rasmussen HK, Hassager O: Extensional viscosity for polymer melts measured in the filament stretching rheometer, J. Rheol. 47 (2003) 429-441.

[6] Chellamuthu M, Arora D, Winter HH, Rothstein JP: Extensional flow-induced crystallization of isotactic poly-1-butene using a filament stretching rheometer, J. Rheol. 55 (2011) 901-920.

[7] Sentmanat ML: Dual wind up extensional rheometer, US Patent No. 6578413.

[8] Sentmanat ML: Miniature universal testing platform: From extensional melt trheology to solid-state deformation behavior, Rheol Acta 43 (2004) 657-669.

[9] Sentmanat ML, Hatzikiriakos SG: Mechanism of gross melt fracture elimination in the extrusion of polyethylenes in the presence of boron nitride, Rheol. Acta 43 (2004) 624-633.

[10] Sentmanat ML, Wang BN, McKinley GH: Measurement the transient extensional rheology of polymer melts using the SER universal testing platform, J. Rheol. 49 (2005) 585-606.

[11] Tropea C, Yarin AL, Foss JS: Handbook of experimental fluid dynamics, Springer Verlag, Berlin, Heidelberg (2007).

[12] Baird DG, Chan TW, McGrady C, Mazahir SM: Evaluation of the use of a semi-hyperbolic die for measuring elongational viscosity of polymer melts, Appl. Rheol. 20 (2010) 34900.

[13] Aho J, Rolón-Garrido VH, Syrjälä S, Wagner MH: Extensional viscosity in uniaxial extension and contraction flow - Comparison of experimental methods and application of the molecular stress function model, J. Non-Newt. Fluid Mech. 165 (2010) 212-218.

[14] Aho J, Rolón-Garrido VH, Syrjälä S, Wagner MH: Measurement technique and data analysis of extensional viscosity for polymer melts by Sentmanat Extensional Rheometer (SER), Rheol. Acta 49 (2010) 359-370.

[15] Burghelea TL, Stary Z, Münstedt H: Local versus integral measurements of the extensional viscosity of polymer melts, J. Rheol. 53 (2009) 1363-1377.

[16] Yu K, Marín JMR, Rasmussen HK, Hassager O: 3D modeling of dual wind-up extensional rheometers, J. Non-Newt. Fluid Mech. 165 (2010) 14–23.

[17] Svrcinova P., Kharlamov A, Filip P: On the measurement of elongational viscosity of polyethylene materials, Acta Technica 54 (2009) 49-57.

Figure 12:
Comparison of geometries of stretched samples fixed with clamps or directly to the drums.

Figure 13:
Comparison of uniaxial extensional viscosity measured with and without the clamps at a temperature of 180°C (sample width 12.7 mm).
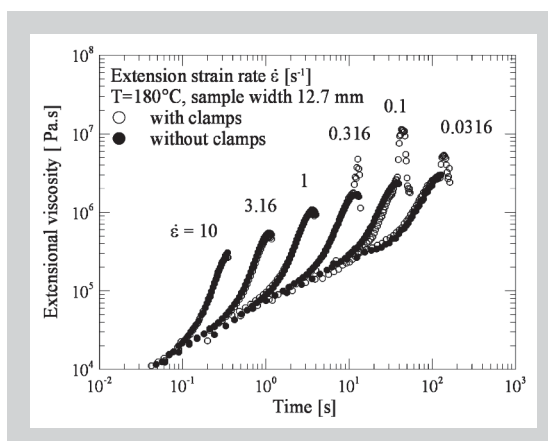
Figure 14:
Comparison of uniaxial extensional viscosity measured with and without the clamps at a temperature of 180°C (sample width 12.7 mm, with ruptures during passage over a clamp for lower values of extension strain rates).